DEVELOPMENT AND CHARACTERIZATION OF INNOVATIVE FIBER REINFORCED PREPREGS AND THEIR COMPOSITES CONTAINING FUNCTIONAL FILLERS

A Thesis Submitted to
the Graduate School of
İzmir Institute of Technology
in Partial Fulfillment of the Requirements for the Degree of

DOCTOR OF PHILOSOPHY

in Mechanical Engineering

by
Yusuf Can UZ

July 2021
İZMİR

Dedicated to my mother and father:
Naide UZ Sait Ali UZ

ACKNOWLEDGEMENTS

First, I would like to thank my advisor Prof. Metin TANOĞLU for his mentorship, patience, valuable suggestions, and guidance in my dissertation during my Ph.D. I feel honored to be supervised by him. I would also like to thank my Ph.D. thesis committee members Prof. H. Seçil ARTEM and Assoc. Prof. Dr. Engin for their support and valuable suggestions. Thanks to valuable community members, the thesis has emerged.

Thanks to Tanoğlu Research Group, who helped and supported throughout my Ph.D. study, Osman KARTAV, Mehmet Deniz GÜNEŞ, Seçkin MARTİN, Ceren TÜRKDOĞAN, Gözde ESENOĞLU, Mustafa AYDIN, Zeynep AY SOLAK, Bertan BEYLERGİL, Hikmet Sinan ÜSTÜN, and Hatice SANDALLI.

I am grateful to Çisem ÖZSAVAŞ. All illustrations in the presented thesis were designed and drawn by her. Thanks to the motivation and support she gave in this journey, both scientifically and aesthetically.

Finally, I dedicate this dissertation to my mother Naide UZ, and father Sait Ali UZ, who are my biggest supporters and lovers in my life. Thank you for raising me as a free individual.

ABSTRACT

DEVELOPMENT AND CHARACTERIZATION OF INNOVATIVE FIBER REINFORCED PREPREGS AND THEIR COMPOSITES CONTAINING FUNCTIONAL FILLERS

This Ph.D. thesis aims to prepare laboratory-scale carbon fiber reinforced prepregs and improve the performance of their composites by incorporating functionalized single-wall carbon nanotubes (SWCNTs). The effect of nano-scale functional fillers on the characterization of prepregs and their composites was investigated to develop innovative materials for primary structures. To affect dispersion characteristics, SWCNTs were functionalized by oxidizing their surface with the carboxyl (-COOH) group using acid treatment. The modified resin system containing 0.05, 0.1, and 0.2 wt. % F-SWCNTs were developed with novel multi-step dispersion techniques. FTIR spectroscopy was performed to identify new bonding groups formed after the covalent functionalization. Unidirectional carbon fiber reinforced prepregs with/without F-SWCNTs were prepared using a drum-type winding technique by utilizing the solvent-dip (solution impregnation) process. The effect of F-SWCNTs on the curing process and kinetic parameters of the carbon fiber/epoxy-based prepregs were investigated using non-isothermal DSC. The activation energy of the curing reaction was calculated by the isoconversional methods. Also, the new numerical approach called GMN was developed to determine the activation energy of the thermosetting materials. For the fabrication of prepreg-based composite laminates, the vacuum bag-only (VBO) method was performed. The fiber volume fractions of the CFRP samples changed between 55.3% and 50.16%. The mechanical and thermomechanical properties of prepreg-based CFRP composites with/without F-SWCNTs were investigated. The optimum mechanical properties of F-SWCNTs filled CFRP composite was achieved at 0.05 wt.% of F-SWCNTs. However, mechanical properties were decreased due to the addition of higher content of F-SWCNTs, in comparison with neat CFRP.

ÖZET

FONSİYONEL DOLGULAR İÇEREN YENİLİKÇİ FİBER TAKVİYELİ PREPREGLERİN VE ONLARIN KOMPOZİTLERİNİN GELİŞTİRİLMESİ VE KARAKTERİZASYONU

Bu doktora tezinin amacı, laboratuvar ölçeğinde karbon fiber takviyeli prepregler hazırlamak ve işlevselleştirilmiş tek duvarlı karbon nanotüpler (SWCNT'ler) dahil ederek onların kompozitlerinin performansını iyileştirmektir. Nano ölçekli fonksiyonel dolgu maddelerinin prepreglerin ve bunların kompozitlerinin karakterizasyonu üzerindeki etkisi, birincil yapılar için yenilikçi malzemeler geliştirmek için araştırıldı. Dağılım özelliklerini etkilemek için, SWCNT'ler, bir asit muamelesi kullanılarak yüzeylerini karboksil (-COOH) grubu ile oksitleyerek işlevselleştirildi. Ağırlıkça %0.05, 0.1 ve 0.2 F-SWCNT'ler içeren modifiye reçine sistemi özgün çok adımlı dispersiyon teknikleriyle geliştirilmiştir. Kovalent işlevselleştirmeden sonra oluşan yeni bağlanma gruplarını belirlemek için FTIR spektroskopisi yapıldı. F-SWCNT'li / F-SWCNT'siz tek yönlü karbon fiber takviyeli prepregler, solvent daldırma (çözelti emdirme) işlemi ile tambur tipi sarma tekniği kullanılarak hazırlandı. F-SWCNT'lerin karbon fiber/epoksi bazlı prepreglerin kürleme süreci ve kinetik parametreleri üzerindeki etkisi, izotermal olmayan DSC kullanılarak araştırıldı. Kürleme reaksiyonunun aktivasyon enerjisi izokonversiyonel yöntemlerle hesaplandı. Ayrıca, termoset malzemelerin aktivasyon enerjisini belirlemek için GMN adı verilen yeni sayısal yaklaşım geliştirilmiştir. Prepreg bazlı kompozit laminatların üretimi için sadece vakum torbası (VBO) yöntemi uygulandı. CFRP numunelerinin lif hacim fraksiyonları %55.3 ile %50.16 arasında değişmiştir. F-SWCNT'leri olan/olmayan prepreg bazlı CFRP kompozitlerin mekanik ve termomekanik özellikleri araştırıldı. F-SWCNT'lerle doldurulmuş CFRP kompozitinin optimum mekanik özellikleri, F-SWCNT'lerin ağırlıkça %0.05'inde elde edildi. Bununla birlikte, saf CFRP ile karşılaştırıldığında, daha yüksek F-SWCNT içeriğinin eklenmesi ile mekanik özellikler azalmıştır.

TABLE OF CONTENTS

LIST OF TABLES

Table **Page**

Table **Page**

LIST OF FIGURES

Figure **Page**

Figure **Page**

Figure **Page**

Figure **Page**

Figure **Page**

Figure **Page**

CHAPTER 1

INTRODUCTION

1.1. History of Composite Materials

Composite materials can be defined as new and artificial materials created by combining the components at a macro level to protect their boundaries to gather the properties of two or more same or different types of materials in new and single materials for a specific purpose. Composite materials generally consist of a low-strength matrix main phase and the reinforcement phase dispersed in this phase. With the development of technology, composite materials containing three or more phases are designed.

The history of using composite materials as a construction material is very old. Many civilizations in history have used composites by developing building materials by combining the basic elements of the surrounding environment. For example, bricks were made by mixing mud and straw in certain proportions. In the 12th century AD, the Mongols made use of composite materials science to make lighter and stronger archery bows. They made bows using bamboo, silk, cattle tendons and horns, and pine resin. Research at a museum has tested some springs that are about 1000 years old, and it has been shown that these springs are almost as durable as the new generation springs. In the late 1800s, canoe manufacturers used paper and resin to make lighter laminates. The papers made of sawdust were bonded with shellac and turned into a layered structure. However, successful results could not be obtained since the resin system did not harden. The first synthetic resins that were obtained using the polymerization process and could be converted from liquid to solid were developed between 1870 and 1890.

Although the composite has been used since mudbrick, asphalt, and reinforced concrete, it has made a rapid development after the "Condensation Reaction" was invented in the 1930s. The first composite plastic samples used for military purposes during World War II, only after 1946 could reach commercial size all over the world. So, it is still a new material all over the world. Since the first applications, many innovations have been made in both reinforcement materials and matrix materials, and new composite materials with

much higher performance values have been made by applying new combinations. In short, composite materials have shown very rapid development and have the quality of a material that continues to continue this development rapidly, exceeding the quality of being a contemporary material and reaching the quality of the material of the future. It is seen those composite materials, which theoretically have an infinite life and an almost infinite usage area, have a great potential thanks to these properties. In composite materials, matrix resin properties, type of reinforcement material, and the type of placement can increase the mechanical, chemical, and thermal properties of the composite, and this carries the composites to a very different dimension compared to other conventional manufacturing materials. While manufacturing with conventional materials, only the material is shaped, but in composite product manufacturing, the material itself is also produced while shaping. Thus, composites, which have become a serious competitor to conventional engineering materials, have the feature of being new, thanks to their superior qualities. With the use of carbon fiber for polymeric composite materials in the 1960s, the industry has gained great momentum. With the replacement of steel with polymeric fiber-reinforced composites, 60-80% weight gain was possible, and 20-50% weight gain was possible when replacing aluminum. Today, these structures have a wide range of applications from the energy sector to the aviation industry. The beginning of composites in Turkey was with polyester water tanks and the bodywork of the "Anadol" brand automobile.

In summary, there are many advantages provided by fiber-reinforced polymeric composite structures:

• Increasing the strength value of parameters such as tensile, bending, compressive, and impact strength of the structures it is used in,

• Providing higher strength values in unit area weight compared to both unreinforced plastics and metals,

• Maintaining their shape and functionality by providing dimensional stability under various mechanical and environmental forces,

• High corrosion resistance,

• Low costs,

• High fracture toughness,

• Providing convenience in design and application.

Since the early 2000s, the development of nanotechnology together with composite structures has provided innovations in many engineering fields. Named as the

composite structures of the future, nanoengineered composites are open to very remarkable developments in both commercial and academic fields.

1.2. Future: Nanoengineered Composite Materials

Nowadays, nanotechnology is one of the most innovative application areas for researchers. Numerous developments have been made for this area of interest, with trending applications in material technology. Nanoparticles are particles with a size between 1 and 100 nm. This difference in size provides different properties at the atomic level. This change in the properties of nanoparticles is very beneficial for many uses, especially in the aerospace and composite industries [1, 2]. Composite materials are widely used and are also being affected by the addition of nanotechnology to production processes. Nanocomposites can be designed by using nanoparticles, as well as found in nature, for example, in the structure of the abalone shell and bone.

Mechanically, nanocomposites have provided superior properties to conventional composite materials due to the very high surface/volume ratio and/or the exceptionally high aspect ratio (length/diameter) of the reinforcements. The reinforcing filler material may consist of particles (e.g., metals), layers (e.g., clay piles), or fibers (e.g., carbon nanotubes or electrospun fibers). The interface area between the matrix and the nanoscale reinforcement phase is typically much greater than the interface area of conventional composite materials. This expanded surface area in combination with nanoscale reinforcements means that a relatively small amount of nanoscale reinforcement can have a significant effect on the macro-scale properties of the composite. For example, the addition of carbon nanotubes can improve electrical and thermal conductivity, while other types of nanoparticles can result in improved optical properties, dielectric properties, heat resistance, or mechanical properties such as hardness, strength, and resistance to wear and damage. Nano reinforcement is usually dispersed into the matrix during processing, and for the most common non-spherical, high aspect fillers, the percentage by weight (mass fraction) may remain very low (0.5% to 5%) due to the low infill filtration threshold. Four different types of nanocomposites can be created: ceramic, metal, polymeric and magnetic. The presented research is focused on polymeric nanocomposites.

The addition of nanoparticles to a polymer matrix can dramatically improve its performance simply by taking advantage of the nanoscale filler [19]. This method is particularly effective in fabricating composites when uniform dispersion of the filler, whose properties of the nanoscale filler are significantly better than the matrix, is achieved. The homogeneous distribution of these nanoparticles in the polymer matrix at low concentrations by weight leads to significant improvements in many mechanical properties of the designed structure, such as compression and bending. On the other hand, the agglomeration of nanoscale fillers produces clusters that function as structural defects and result in failure. Carbon nanotube or graphene-based polymer nanocomposites are used to develop innovative solutions for a wide variety of high value-added applications in areas such as the energy, aerospace, and defense industries.

1.3. What is Prepreg?

Advanced composite materials based on carbon fiber-reinforced thermoset polymers have become common in primary aerospace structures, as well as high-performance sporting goods, and marine and wind energy areas. Most high-performance structural composites for aerospace applications begin as layers of prepreg, or carbon fiber beds pre-impregnated with a catalyzed but uncured resin. A prepreg is a fiber-reinforced resin system that cures under heat and pressure to fabricate lightweight structures with high strength. Prepreg is used in the design of application-specific structures with the use of anisotropic mechanical properties throughout the fibers and the polymer matrix providing filling properties by keeping the fibers in one system. Prepregs achieve very impressive performances, especially in the field of aerospace & defense industry. The main usage areas are civil aircraft, primary structures, interiors, aero-engines, defense aircraft, helicopters, and spaces in aerospace. For example, the mass fraction of carbon fiber prepregs is about 50% for the Airbus A350XWB. Moreover, carbon fiber prepregs have been fabricated to form the airfoils of the Airbus fleet since 2000. Many fiber types can be used for preparing pre-impregnated fibers, such as glass, basalt, aramid, and carbon fibers. They provide composites with mechanical performances: high strength/weight ratio, as well as good thermal, electrical, and chemical properties. Also, there are three matrix types: epoxy, phenolic, and

bismaleimide. Each of them has different advantages depending on the area of use. Epoxy has excellent mechanical performance, providing good environmental resistance, high toughness, and easy processing. The matrix is partially cured which is also known as B-stage during the prepreg process. Prepregs are kept ready for further processing by stopping the curing reaction through the freezer.

The most common technique is to form a laminate with prepreg layers, sequentially: prepregs are stacked on the tool, sealed in a vacuum bag assembly, and placed in a pressurized oven. The oven temperature is then raised and the air in the bag is drawn and the ambient is pressurized. Consolidation pressure provides to tighten the fiber bed, allowing the structure to take the form of a mold and in some cases removes excess resin. The applied pressure also eliminates porosity, which is the main manufacturing defect in prepreg-based composites, by directing the resin to dry areas and precipitating the bubbles of trapped air and/or volatiles. The elevated temperature reduces the resin viscosity, providing ease to flow and wet the fiber reinforcement before curing is completed. Finally, prepreg-based composite laminates are fabricated under heat and pressure.

Autoclave processing remains a benchmark for the production of robust and high-performance structures that are widely used within the composite industry. In addition to its superior performance features, it includes high purchasing, operating, and tooling costs. In an industry where price performance is increasingly important, autoclaves used to produce large parts impose a relatively inflexible production environment. Part designs must be designed according to the existing pressurized vessel dimensions. In addition, the production carried out in a nitrogen environment has both health hazards and operational difficulties. The anticipated market growth for composites and the disadvantages of the autoclave process necessitated the development of alternative methods. Out-of-Autoclave (OoA) manufacturing techniques and materials have been developed to manufacture autoclave quality parts. Instead of the high curing temperatures required for the autoclave process, OoA prepregs that can be cured at low temperatures have been introduced. OoA prepregs produced by impregnating the resin into reinforcement fibers at the appropriate temperature have demonstrated that it is possible to produce autoclave quality parts using vacuum-bag-only (VBO) consolidation. Thanks to these developed materials and production methods, purchasing and operating costs have been significantly reduced. In addition, the VBO technique has eliminated the constraints in part designs since it can work in harmony with conventional furnaces and vacuum pumps. In addition, the low

curing pressure provided by the consolidation at atmospheric pressure (27 inHg vacuum pressure) has eliminated autoclave-induced defects such as honeycomb core crushing and paved the way to produce lighter materials.

1.4. Objectives

The motivation of the presented study is finding innovative solutions in engineering applications by preparing OoA prepregs. There has been a growing demand for high-performance composites (CFRPs with higher mechanical properties) on the market. This thesis aims to provide a comprehensive investigation on the preparation and characterization of prepregs and their hybrid composites containing functionalized SWCNTs and to build up knowledge of processing-structure-property relationships. This thesis has focused on the incorporation of the nano-sized fillers within the matrix (Bisphenol-A epoxy), then adapts the nano-sized filled matrix to carbon fiber reinforced OoA prepregs produced with the laboratory-scale drum-type winding machine. Then, laminated composites structures were manufactured with performance-enhanced prepregs using the VBO method. The objectives are as follows.

- Functionalization of the single-wall carbon nanotubes (SWCNTs) to improve dispersion characteristics within the epoxy matrix.
- Dispersion of functionalized SWCNTs (F-SWCNTs) within the resin system to manufacture nanoengineered prepregs.
- Characterize the rheological behavior of the resin systems structure to adjust optimal prepregging parameters.
- Preparation of the nanoengineered OoA prepregs using drum-type prepregging machine for carbon fiber-reinforced polymeric (CFRP) composite production.
- Investigate the thermal behavior of prepregs containing various amounts of F-SWCNTs to reveal the effect on the cure kinetics.
- Fabrication of the functional CFRP composites with/without F-SWCNTs using the VBO method.

- Determine the mechanical, chemical, and thermomechanical properties of the reference and nano-sized filler reinforced CFRPCs.

The goals of the presented thesis are identified as follows:

- The volume fraction of the carbon fiber is higher than 45%.
- The void content of laminate is lower than 5%.
- High mechanical properties as much as commercial prepregs.
- Achieve uniform fiber volume fraction throughout the part.

1.5. Problem Statement

In recent years, the essential reason for the growing popularity of CNTs as nano-scale reinforcements is not only excellent mechanical and thermal properties but also CNTs can provide improving both interlaminar and intralaminar properties. Due to their superior properties such as high modulus, high fracture toughness and electrical and thermal conductivity carbon nanotubes (CNTs) attracted great attention for various applications such as structural components, functional composites, sensor technology, electronics, aerospace & defense technologies.

Although CNTs have impressive properties, the incorporation of CNTs as a reinforcement constituent in composites is still limited due to poor interfacial interactions between CNT and polymer matrix surfaces, and difficulties in dispersing interfering CNTs during processing. Therefore, the biggest challenge in the improvement of functional performance by incorporating CNTs depends on the homogeneity and stability of the CNT dispersion in the resin system, and the bonding quality between the CNT and polymer surfaces. This can be called as agglomeration problem of CNTs. Also, viscosity is the most important parameter for preparing prepregs to achieve good wetting of fibers. The other challenge in the resin impregnation for nanoengineered prepreg preparation is to obtain an appropriate range of viscosity with adding CNTs. One of the most important problems is the excessive increase in viscosity with the addition of CNTs to the resin system.

Surface modification of the CNTs is the proposed solution for the agglomeration problem. The proposed solution to keep the viscosity value in the desired range is to

impregnate the fibers at the appropriate temperature by performing rheological characterization.

1.6. Contributions

The presented thesis is based on the idea of improving the performance of materials used in the production of laminated prepreg-based CFRP composites by incorporating nano-sized fillers within the epoxy matrix. Referring to this idea, the aim is taken to develop and characterize the performance of the carbon fiber (CF) prepregs and their laminated composites by incorporation of SWCNTs. Based on our knowledge, there are only a few studies reported in the literature on the investigation of the effect of the nanoengineered prepregs on the performance of CFRP composites. The presented thesis is one of the most comprehensive studies on the development and characterization of nanoengineered prepregs and their composites. Although CNT-reinforced commercial prepregs have been extensively examined in the literature, there are few studies on the preparation and characterization of nanoengineered prepregs with laboratory-scale machines. Therefore, there is a need for laboratory-scale prepreg manufacturing lines to develop and characterize the innovative resin system for various applications. According to the literature review, this thesis has an important place as the first study on the development and characterization of laboratory-scale OoA prepregs containing SWCNTs in Turkey. Significant results have been obtained with the composites produced by the VBO method obtaining results close to the autoclave quality. Thanks to the thermal characterization of the produced prepregs, information about the curing kinetics was obtained and successful laminates were fabricated.

The desired improvement could not be obtained with the inability to transfer the superior properties of CNTs to composite structures. The biggest challenge in the development of nanoengineered composites by incorporating the outstanding properties of CNTs into the polymer is to achieve a homogeneous and stable dispersion. Therefore, it has been observed that the functionalization process was applied in most of the studies performed to overcome the problem. With the functionalization process, the performance of the CNT / polymer nanocomposite is improved by its positive effect on the distribution of CNTs in the matrix and the interfacial interactions between the CNT and the polymer.

By changing the surface properties of CNTs with functionalization, the possibility of bonding with the medium in which it will be dispersed is increased. In the presented thesis, a unique multi-step dispersion flow chart has been created by blending the dispersion techniques that have been successful in the literature and suitable for the conditions of this study.

One of the most important contributions of the presented thesis to the literature is the new mathematical approach to curing kinetics. This thesis has improved the mechanical and thermal performances of prepreg-based composite structures by achieving the goals set in the beginning.

1.7. Thesis Outline

Chapter 1 starts with the historical information and future of the composite materials. After mentioning the importance of nanotechnology for composite materials, the definition of prepreg, which is the main material of the thesis, has been made. Then, the main objectives, problem statement, and the contributions of this thesis to the literature have been presented.

Chapter 2 is the part where fundamentals of prepregs and their composites are given. After mentioning the advantages of prepregs and their importance for the market, manufacturing methods are summarized. In particular, the importance of carbon fiber prepregs in the market and literature has been mentioned. Rheological and thermal characterization of prepregs is very crucial to produce high-quality prepreg-based composites. This chapter, which includes literature research on the mechanical and chemical characterization of the manufactured composites, has been concluded by mentioning the general structure of hybrid composites.

In Chapter 3, detailed information about CNTs is given. The dispersion techniques required to transfer the extraordinary properties of CNTs to composite structures have been introduced. The functionalization methods of CNTs used to establish stronger bonds with the polymer matrix that will be dispersed are mentioned. Information is given on how to prepare unidirectional (UD) prepregs using the filament winding technique of these nano-scale filler materials. Literature studies on this subject are included at the end of Chapter 3.

Chapter 4 provides fundamentals of cure kinetics for thermosetting materials. A brief overview of differential scanning calorimetry (DSC) is given. While the theory of cure kinetics is introducing, a new mathematical approach for determining activation energy is presented. Literature studies on this subject are included at the end of Chapter 4.

Chapter 5 includes the basics of OoA processing. Achieving advanced composite material has taken major steps with the use of OoA prepreg. One of the outlines that the presented chapter emphasizes is the processing of OoA prepregs. The basics of air permeability, void mitigation, resin impregnation, and curing process are presented in this part. The main processing steps of the VBO method are listed. Literature studies on this subject are included at the end of Chapter 5.

The methodology applied in this thesis is presented in Chapter 6, consisting of the details of the materials, sample preparation, experimental and characterization techniques.

Chapter 7 introduce the experimental results for the fabricated prepreg-based CFRP composites with/without F-SWCNTs. The effect of the nano-sized fillers on the structural and functional performance of the CF prepregs and their composites is reported. Chapter 7 started with a visual examination of the dispersion of F- SWCNTs in different mediums. FTIR spectrometry was used to detect the presence of functional groups in the walls of F-SWCNTs. The rheological characterization of the epoxy system to be used for the prepreg was made and it was checked whether it was in the appropriate range for the prepregging machine. Thermal characterization of UD prepregs with/without F-SWCNTs produced using a drum-type prepreg machine was performed and a detailed study was obtained about the curing kinetics. Laminates were manufactured using the VBO method in line with this information. Finally, mechanical, chemical, and thermo-mechanical characterizations were applied to prepreg-based composites. The fractured surface of the composites was examined under SEM. All the experimental results are discussed according to the results obtained from the literature.

Conclusions and suggestions for future work are provided in Chapter 8.

The processing chain of the presented study is summarized in Figure 1.1.

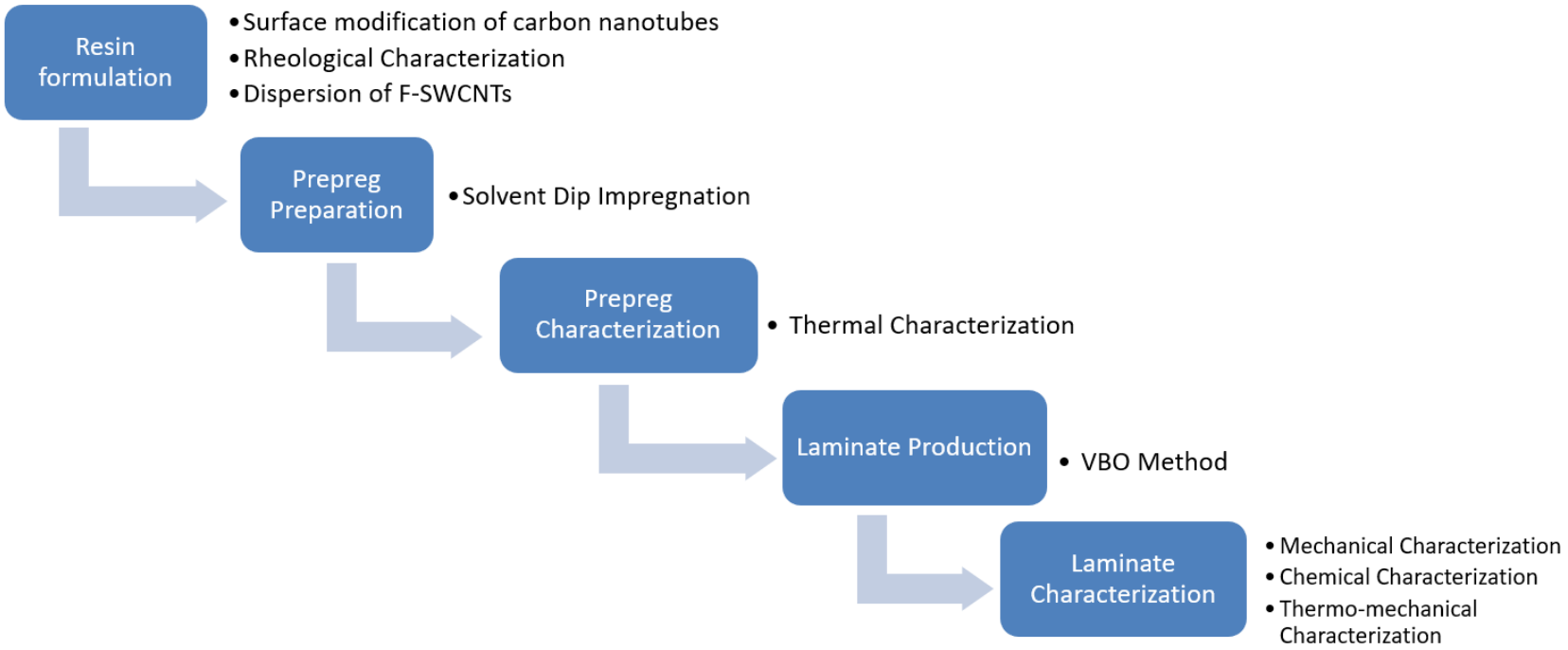

Figure 1.1. The processing chain of the nanoengineered prepregs and their composites

CHAPTER 2

FUNDAMENTALS OF PREPREGS THEIR COMPOSITES

2.1. Advantages of Prepregs

Prepreg takes a superior place as a high value-added composite material when the main technologies are compared in terms of performance and production volumes (Figure 2.1). The resin generally cures at elevated temperature and undergoes a chemical reaction that transforms the prepreg into a solid structural material that is a high strength, capable of operating at high temperatures, extremely stiff, and lightweight as much. Prepregs make a significant impact in many industries that require advanced material properties. For instance, the aerospace industry works on purpose-developed parts for a wide variety of aircraft components such as aircraft flooring, interiors, cargo liners, and much more, thanks to the superior properties of prepregs. Prepregs could be designed with materials that have a very low thermal expansion to work well with extreme temperatures [1].

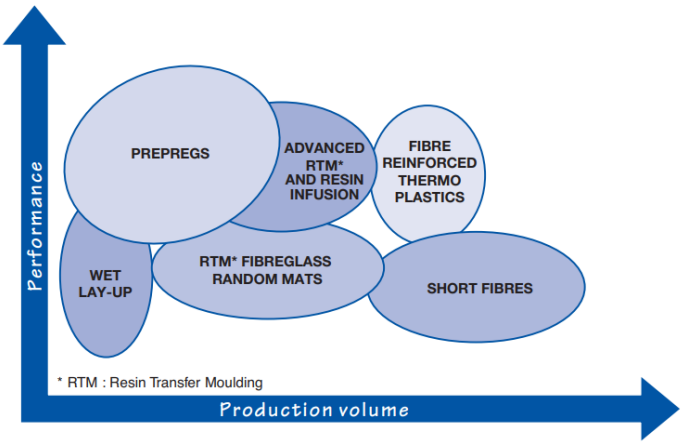

Figure 2.1. The position of prepreg technology in terms of performance and production volumes (Source: HexPly Prepreg Technology)

Research in the aerospace industry must consider the large changes in temperature that most aircraft materials will experience during flight. In the interior of the aircraft, prepregs are utilized for ideal comfort levels of passengers, reducing the effects of vibration. Moreover, prepregs offer high resistance to environmental corrosion. Aerospace manufacturers need materials that will be least affected by extreme environmental conditions. This growth in the use of prepreg composites instead of metal has been provided by the design potential of higher strength/weight ratio, better fatigue strength, and anisotropic properties.

Manufacturing defects that are mostly observed during traditional composite fabrication include incomplete filling, dry spots, non-uniform resin dispersion, void formation, uneven curing, and a low degree of curing [2]. The most serious problem is the formation of voids which take generally their source from air entrapped during lay-up, volatiles in the resin mixture. Since the prepregs are cured under pressure and temperature, the adhesion between the layers is very strong and the void content is minimized. Also, fibers are kept partially cured in which the resin/fiber ratio can be tightly controlled. Therefore, fiber volume content can be obtained in prepreg can be very high. For instance, high fiber volume content is about 65% with void content less than 0.5% in laminate produced using Out-of-Autoclave (OoA) prepreg. [3-5]. The high fiber content volume is very important for the composite structure, as the excess resin will reduce the general mechanical properties. Commonly used thermoset resins such as epoxy and hardeners such as amide contain hazards for human health. Therefore, keeping the resin system separate from the composite part production floor contributes significantly to the solution of health problems. For this reason, prepregs are safer for human health than other fabrication processes. Prepregs stored under the storage conditions are kept ready for production and are easy to use. The wet layup procedure in composite manufacturing is a labor-intensive method that can be affected by human error such as controlling fiber direction and resin distribution. The mechanical properties of a composite structure whose fibers are not properly aligned will decrease significantly. On the other hand, misalignment of fibers during the vacuum-forced infusion of the resin can create similar problems.

2.2. Prepreg Market Forecast

There has been a pronounced increase in global demand for prepreg-based composites from several industry segmentations, especially aerospace and automotive. In terms of revenue, the global prepreg market was valued at USD 7 billion in 2019 and is projected to reach USD 11.5 billion by 2024, at a CAGR of 10.5% between 2019 and 2024 [6]. The main factors behind the growth of the prepreg market are increased use of prepreg in aerospace & defense, increased demand from the automotive industry, ease of use, and increased use of prepreg in wind energy. The aerospace & defense applications had the largest share of over 40% in prepreg use in 2019. This trend is predicted to continue with a strong CAGR from 2020 to 2027 [7]. Replacing traditional materials with lightweight, prepreg-based composites has been an important implementation in manufacturing light aircraft to increase fuel efficiency with reducing emissions and material usage. In the automotive industry, manufacturers have driven increasingly to explore the use of prepreg to reduce vehicle weight. These in turn support carbon and other polymeric fiber reinforcements to produce lighter and stronger materials. Furthermore, the increasing use of a lightweight blade, which is necessary to increase the potential of renewable energy, is an important driving force for the continuity of the market. Figure 2.2 shows the prepreg types which are available in the market for many usage segmentation. The segmentations of the global prepreg market and top companies are given in Table 2.1.

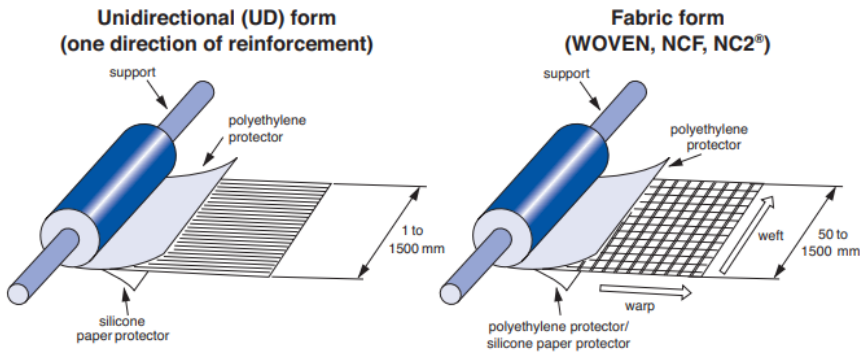

Figure 2.2. Prepreg types which are available in the market
(Source: Hexcel Prepreg Technology)

Table 2.1. The segmentations of the global prepreg market

Major parameter	Description
Market Segments by Manufacturing Technology	Solvent Dip, Hot Melt
Market Segments by Weave Type	UD Prepreg, Fabric Prepreg
Market Segments by Resin	Epoxy, Phenolic, BMI, Thermoplastics
Market Segments by Fiber	Carbon fiber, Glass fiber, Aramid fiber
Market Segments by End-Use Industry	Commercial Aerospace, Military/Defense, General Aviation, Space/Satellite, Sporting Goods, Marine, Wind Energy, Automotive, Civil Engineering, and others
Market Segments by Region	North America, Europe, Asia Pacific, and others.
Top Companies Name	Hexcel, Cytec Solvay Group, Toray, TenCate, Gurit, Mitsubishi Rayon Corporation, and others
CAGR	~10%

2.3. Carbon Fiber Reinforced Prepregs

Leading industries in the use of carbon fiber prepreg include aerospace & defense, automotive, sports & recreation, and wind energy [8,9]. When measured in terms of value and volume, the aerospace & defense industry takes a large share of the cake (e.g., Figure 2.3). The most important factor is the use of carbon fiber prepreg by giant companies such as Boeing and Airbus. Boeing and Airbus are preparing to produce approximately 10 thousand new wide-body aircraft in the next 20 years. According to The Teal Group, aircraft production will increase 5.8% annually from an estimated market size of $ 164 billion in 2017 to $ 218 billion in 2022. With mentioned growth rate, carbon fiber prepreg, which has 58% of its market share in 2019, continues to develop with the fastest growth rate by using both the superior properties of carbon fiber and the advantages of prepreg

material [10]. Carbon fiber prepregs, which can reach high fiber volume content with the amount of resin kept under control, have excellent structural and mechanical properties. It gives high tensile strength and elasticity to composites produced together with the use of carbon fiber with prepreg technology. For example, there are many studies showings that carbon fibers have a tensile strength about 10 times higher than that of iron.

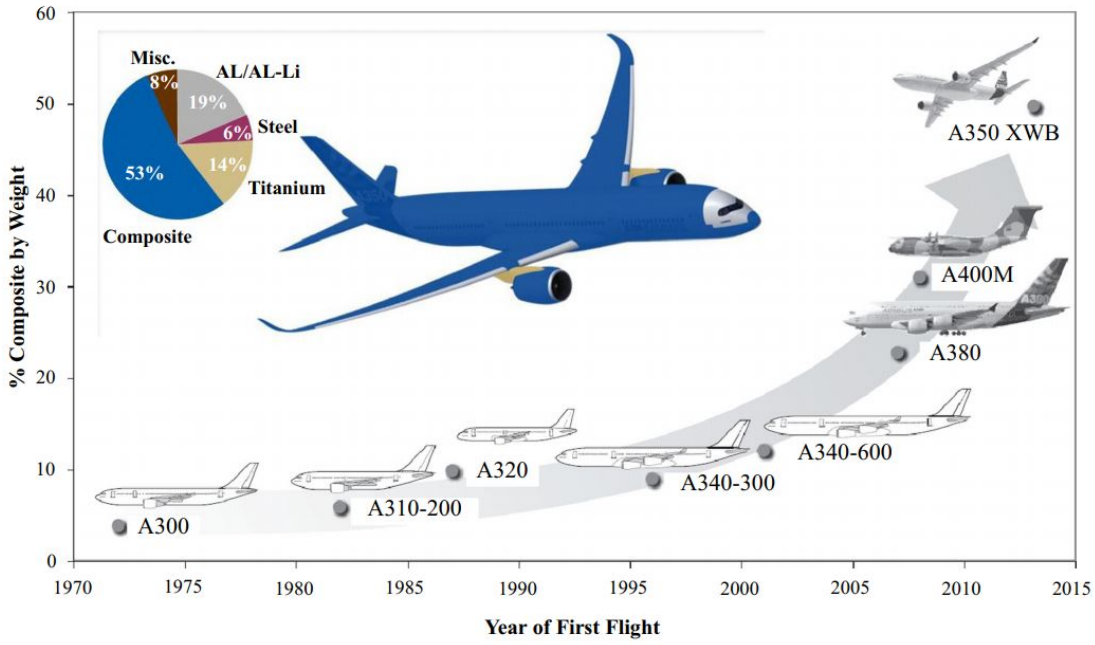

Figure 2.3. The increase in weight ratios of composites used in various aircraft over the years (Source: Xu, Y et al., 2018)

2.4. Prepreg Manufacturing Methods

There are mainly four types of manufacturing methods for prepregs: solution dip, solution spray, holt melt, and film calendaring. Solvent dip and hot melt methods are widely used for practical applications. Both methods are based on the same principle, reducing the viscosity of the resin to impregnate properly the fiber bed [11]

The hot-melt manufacturing process had the largest market with a share of 74% in 2019. It is widely used with its advantages such as easy handling, resin content control, and product quality. In the hot-melt method, the resin is brought to high temperatures to

cover the fiber as a thin film. Resin control is achieved using doctoring blades. The heated resin is first coated on the backing film before passing through the doctoring blades (see Figure 2.4). Then, a fiber reinforcement is clamped between two layers of a resin film. Next, heated compaction rollers are used to press the films by forcing the resin into the fabric. Finally, a cooling mechanism is performed to reduce resin viscosity before rolling [12]. In addition, the geometry of the fiber tows, resin film thickness, type of impregnation rollers, fiber tension and release action of the coating paper are the other parameters that affect the quality of the prepregs [13, 14].

The solvent dip manufacturing process uses a resin bath in which the fiber reinforcement is passed through. The process involves the use of a solvent to dissolve the resin system. The principle of this process is based on dipping the fiber reinforcements into the resin solution at a controlled fiber tension and rate (see Figure 2.5). Next, the impregnated fibers pass through a heated oven to evaporate the solvent before rolled into a core. Finally, lamination lay-up of thermoset prepreg at this B-stage point can be performed easily with good tack [15]. Theoretical research for the solution immersion method has been done by Liu et al. [16]. Resin, volatile contents, and coated resin thickness are defined as a function of impregnation rate. The main aim of the investigation is to find optimum resin content for a given condition.

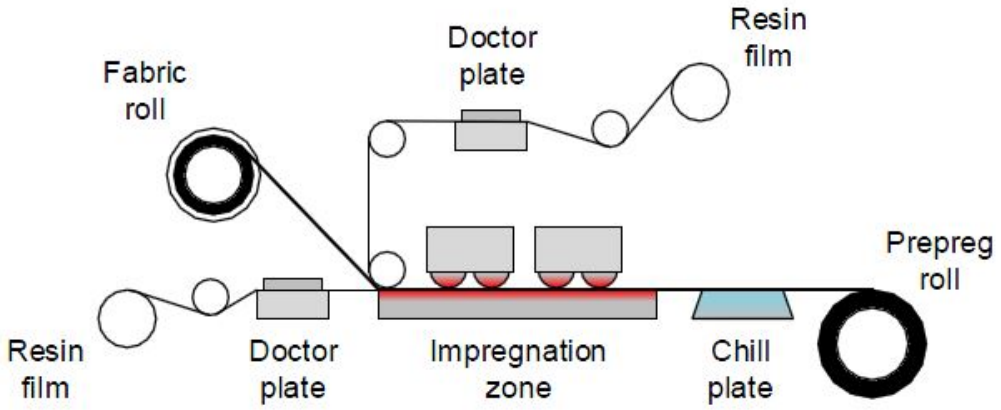

Figure 2.3. Schematic of the hot-melt manufacturing process
(Source: Palardy-Sim, M., 2016)

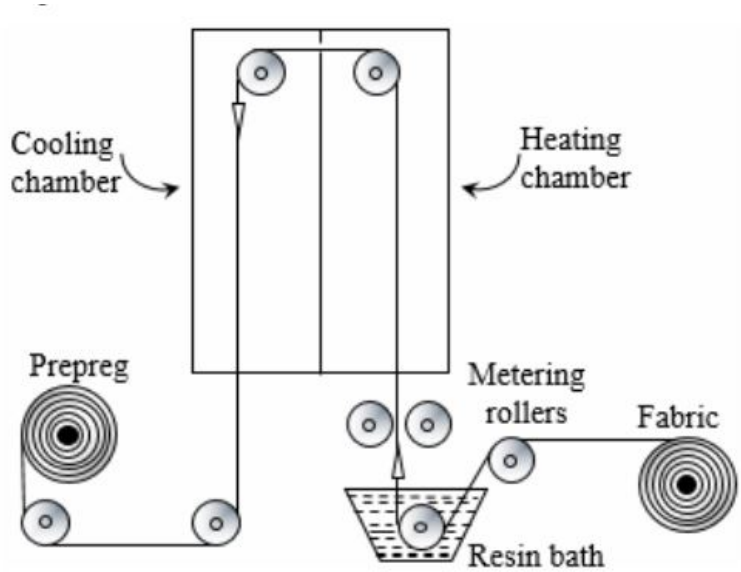

Figure 2.4. Schematic of the solvent dip manufacturing process
(Source: Dimeski, D., & Srebrenkoska, V., 2014)

The investment cost of the hot-melt manufacturing process is much higher than the solvent dip process. However, it weakens the overall strength of the final composite material because of the solvent used in the process being trapped inside the prepreg sequence. In addition, it affects product quality as the solvent evaporates, changing the moisture content of the prepreg system. On the other hand, it is widely used in product development and laboratory studies due to its advantages such as ease of installation and investment cost.

2.5. Characterization of Prepregs and their Composites

Prepregs have several benefits that are readiness to use without any treatment, ease of handling, uniform fiber alignment, control of the resin content, applicability to complex mold geometries, and very low void contents in their composites. Therefore, the most suitable structures for applications requiring high performance are obtained with prepreg-based manufacturing processes. The quality of reinforced polymer composite structures depends on two main factors, high fiber volume fraction (~65%) and low void content (<2%) [16]. It is possible to obtain a high fiber volume fraction with minimal

voids in the laminated composite structure by characterizing the production process and materials [17]. Otherwise, high void content occurs in laminates produced because of insufficient impregnation of the fibers. This situation affects the mechanical integrity and functional properties of composite materials [18]. Prepregs are designed to tackle one of the most challenging aspects of composite manufacturing – uniform resin impregnation through the fibers. Dealing with resin impregnation and determining the curing schedule is more challenging while working with high viscosity resin. Consequently, the prepregs and their composites must be analyzed in more detail, particularly to optimize the processing properties of the prepreg materials [19,20].

The increasing interest in rheological characterization has demonstrated its importance for composite resins in recent years. Developing new resin systems for innovative materials is linked to information about flow, gel temperature, and minimum viscosity [21,22]. Polymer prepregs contain both viscous and elastic properties. Superior properties can be provided to composite structures with the rheological characterization of prepregs by optimizing their tack properties and curing cycle. These studies also help to optimize prepreg processing parameters. At this point, the most critical parameter for processing prepregs is viscosity. The viscosity must be within certain limits (1.5-2.4 Pa s) to wet the fibers well with the proper handling characteristics [23]. Many important parameters such as mixing speed, epoxy type, and content of filler material, if any, affect the resin curing.

Well, understanding resin curing mechanics is an important step in the production of fiber-reinforced thermoset composites. Curing cycle parameters such as temperature, time and pressure directly affect the quality of composites. During the composite production, the curing schedule offered by the resin supplier or prepreg manufacturer is performed. This schedule is often set in an ideal situation and may not be a good representative for actual curing in a composite manufacturing process. Therefore, the curing behavior of prepregs has to be examined before fabricating their composites [24-26]. Thermal analysis techniques can be used to investigate the effect of curing mechanisms on material properties Moreover, thermal characterization plays a significant role in composite material properties, providing safe operating temperatures, process control characteristics, and quality assurance of these materials [27].

The mechanical and thermal properties of prepreg-based composites are linked to cross-linking reactions that occur during the epoxy curing process [28]. Epoxy resin is a thermosetting material that can form a three-dimensional network when it reacts with the

hardener. Since it is an exothermic process, the heat of the reaction is released during the curing reaction. The curing mechanism is quite complicated as epoxy resin is subjected to many physical and chemical reactions during crosslinking [29-30]. These chemical reactions play an important role in resin morphology, which determines the properties of fiber volume contents for prepreg-based composites. Since crosslinking continues after production, prepregs should be stored in a cold environment. In this way, it may be possible to extend the shelf life. The problem in the quality of end-product can be caused by using material that is over-cured or prepared with an unfavorable curing cycle. Therefore, one of the most important steps in the process of developing novel systems is to understand the mechanism and kinetics involved in curing reactions. Therefore, the effect of the cure kinetics and rheological behavior of prepregs on the morphological, dynamic mechanical, mechanical, thermal, and chemical properties of composites should be investigated. Besides improvements in the mechanical properties such as tensile strength, interlaminar strength, flexural strength, and stiffness, composite materials must keep functionality at higher operating temperatures, providing high glass transition temperatures.

2.6. Nanoengineered (Hybrid) Composites

With the increasing demand for low density and high strength functional materials over the years, many developments have been studied on composite structures. Carbon fiber reinforced polymers (CFRP), which especially use the advantages of prepreg materials, meet this demand and are the most researched structures due to their mechanical properties/weight ratio.

Hybrid composites (also known as multiscale or hierarchical or nano-engineered composites) consist of at least two components with different size scales. The components usually consist of continuous fibers as in conventional composite structures and nano fillers that provide additional functional properties. Nano fillers are expected to be incorporated homogeneously into the matrix component of the composite structure and add many functional features such as stronger bonding with continuous fibers. As in the presented study, the incorporation of CNTs as a nanoscale filler into a polymer matrix with continuous fiber reinforcements to produce hybrid composites attracts attention as

one of the most well-seen subjects. The distribution of CNTs even in very small amounts into the polymer matrix has created great improvements, especially in the mechanical and thermal properties of the composite structure. Of course, one of the most important interests is the fabrication process chosen to distribute CNTs into the polymer matrix.

Resin transfer molding (RTM), vacuum-assisted resin transfer molding (VARTM), or wet hand lay-up process were generally performed for impregnating the continuous fibers with a CNT-resin mixture. In these processes, the resin infusion and consolidation of the composites in a single process brings several problems. One of them is that the resin integration, such as RTM, in a vacuum-assisted manner parallel to the fiber direction, results in the accumulation of CNTs in some regions. Hybrid composites can be produced using prepregs by incorporating CNTs in which the more systematic way (or multi-step) fibers are pre-impregnated with a resin in beta state.

In the presented study, CFRP hybrid laminates containing CNTs were produced using prepreg technology to create functional composite structures. Detailed information about CNTs, prepregs, and production methods will be given in the next chapters. The fibers that are fed continuously with the desired tension are impregnated by passing through the modified resin bath by incorporation of CNTs. Using the advantages of filament winding technology, the drum-type prepreg machine collects the impregnated fibers on a mandrel to produce 2D sheets.

2.7. General Structure of Laminated Composites

Laminated structures are composites that form high-strength structures with each successive layer. High-strength properties can be designed for different purposes with 2D layers stacked in different variations of fiber directions (Figure 2.6). FRP composite structures can be formed by stacking successive structures in a continuous or short fiber reinforced type [31-34]. The presented study focuses on laminated composite structures reinforced with continuous fiber. As mentioned, the mechanical behavior of composite structures can vary according to fiber directions, stacking ply orientations (stacking sequence), and thicknesses of successive layers. With this feature, composite structures have become the most popular structures of today, thanks to the contribution to be designed under the intended use [35]. Each of these successive layers may have different

fiber directions. One-ply can be formed using in a single direction (unidirectional) oriented fibers or bidirectional fibers such as woven fabric to meet the specific demands. Laminate structures usually establish a permanent bond with each ply by applying heat and/or pressure. The most distinctive features of the composite structure formed have very good mechanical properties in the fiber direction, while they are mechanically weaker in the transverse direction. It should be noted that when a force opposite to the direction of the fiber is applied, the composite structure fails more easily because the matrix with lower stiffness tries to carry this load.

Composite laminates can be divided into the following categories according to the stacking sequence: angle-ply laminate (e.g., 45/30/-45/-30), cross-ply laminate (e.g., 0/90/0/90), balanced laminate (e.g., 0/45/90/-45), symmetric laminate (e.g., 45/30/30/45), antisymmetric laminate (e.g., 45/30/-30/-45). In the presented study, hybrid composite structures formed by successive six plies with unidirectional 2D sheets in a cross-ply stacking sequence were investigated.

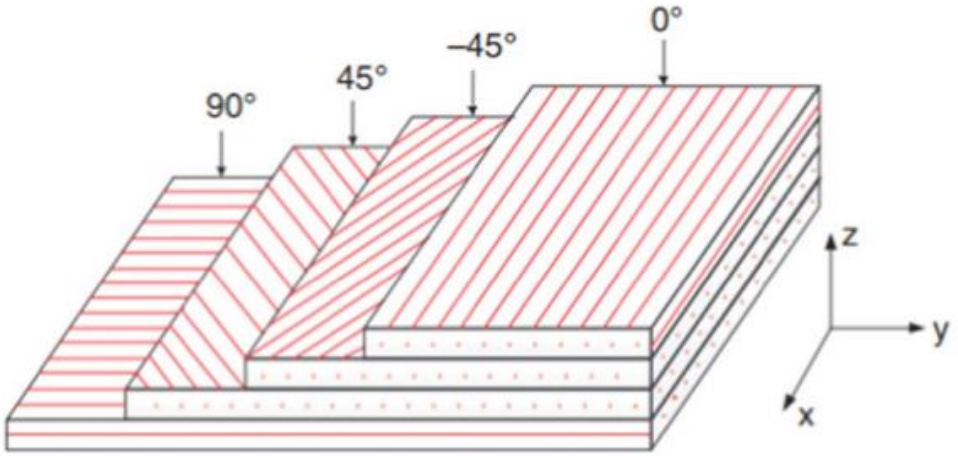

Figure 2.6. Schematic structure of HNTs from single tubular appearance to crystalline structure (Source: Zeng et al., 2014)

CHAPTER 3

PREPARATION OF NANOENGINEERED PREPREGS

3.1. Carbon Nanotubes (CNTs)

Carbon nanotubes (CNTs) are human-made tubes made of carbon structures with nanoscale diameters. Especially since the early 2000s, many articles have been published on CNTs and related fields, and many of these articles point to Sumio Iijima, who published an article of the incredible interest in Nature ("Helical microtubules of graphitic carbon") in 1991 as a starting point for multi-wall carbon nanotubes. The idea of using fillers, which are accepted as one-dimensional, is based on much older. Since 4000 BC, straw has been incorporated into the mud and used to obtain stronger building materials. With the development of technology, filler materials such as alumina, glass, boron, silicon carbide, and especially carbon began to be used during the production of FRP composites. These filling materials used to reinforce the matrix form composite structures with superior properties together with conventional fibers that act as a load carrier. Conventional fibers have mesoscale dimensions with micron diameter and millimeter lengths. Carbon fibers are used as primary materials, especially in the aerospace & defense industry, with mechanical properties reaching stiffness and strength values, typically in the range of 230-725 GPa and 1.5-4.8 GPa, respectively [36].

As described in the section on hybrid composites, polymer nanocomposites that can be used in a variety of structural and functional applications are manufactured by incorporating fillers with extraordinary mechanical, electrical, and thermal properties such as CNTs into their matrix [37,38]. CNTs superior properties can be summarized as follows: greater thermal conductivity (better than diamond), outstanding electrical properties (like copper), good mechanical strength (one hundred times the tensile strength of steel), high elastic modulus and aspect ratio, and lighter (one-sixth of the weight of steel). These tubes with unique properties consist of rolled graphene layer (s) to create a seamless cylinder. According to the number of tubes available in the layer structures, CNTs are defined as single-walled carbon nanotubes (SWCNTs) and multi-walled carbon

nanotubes (MWCNTs). Depending on the process for CNT fabrication, SWCNTs (Figure 3.1, left) are made of single graphene. On the other hand, MWCNTs (Figure 3.1, right) are made of two or more tubes which are concentric shells of graphene layers arranged around a hollow core with van der Waals forces between adjacent layers.

The physical properties of different carbon materials are given in Table 3.1. As can be seen in this table, these properties, which reveal the difference of CNTs from other carbon materials, help to create functional structures in many areas such as thermal conductors, energy storage, structural materials, and biological applications [39,40]. Since the chemical bonds of CNTs are completely composed of sp2 carbon-carbon bonds, it is defined as the strongest and stiffest material in the world [41-43]. Although thousands of articles have been written on the mechanical properties of CNTs, it has been observed that Young's modulus reached 1.2 TPa and tensile strength 50-200 GPa, although no consensus has been reached. The mechanical properties that differ according to the classification of CNTs are presented in Table 3.2 [44, 45].

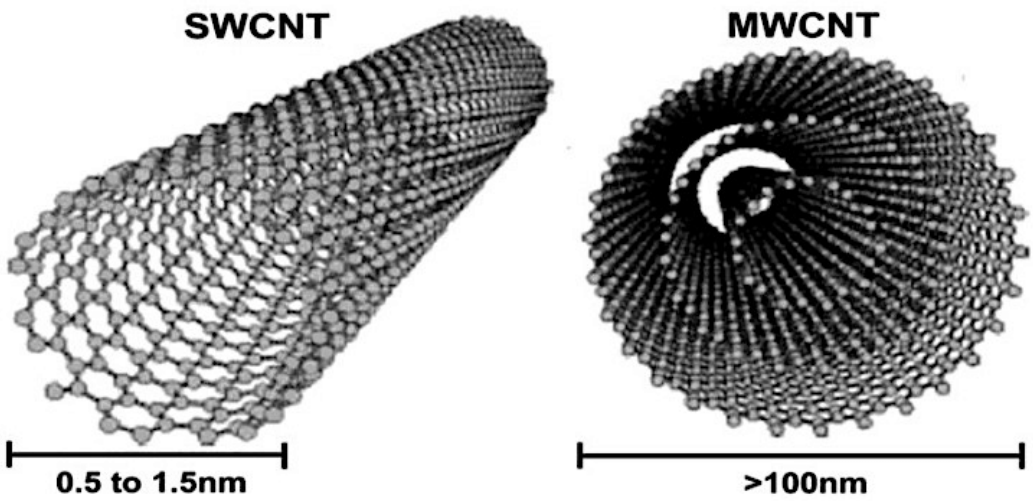

Figure 3.1. Classification of CNTs, (left) single-walled carbon nanotubes (SWCNTs) and, (right) multi-walled carbon nanotubes (MWCNTs) (Source: Siddiqui et al., 2010)

Table 3.1. Physical properties of different carbon materials

Property	C Material				
	Graphite	Diamond	Fullerene	SWCNT	MWCNT
Specific gravity (g(cm3)	1.9-2.3	3.5	1.7	0.8	1.8
Electrical conductivity (S/cm)	4000^{p} , 3.3^{c}	10^{-2}-10^{-15}	10^{-5}	10^{2}-10^{6}	10^{3}-10^{5}
Electron mobility ($cm^2/(V\ s)$)	2.0×10^{2}	1800	0.5-6	10^{-5}	10^{4}-10^{5}
Thermal conductivity (W/(m K))	298^{p} , 2.2^{c}	900-2320	0.4	6000	2000
Coefficient of thermal expansion (K^{-1})	-1×10^{-6p} 2.9×10^{-5c}	2×10^{-6}	6.2×10^{-5}	Negligible	Negligible
Thermal stability in air (C)	450-650	<600	600	>600	>600
p: in-plane; c: c-axis					

Table 3.2. Typical dimensions and mechanical properties of CNTs

Property	SWCNT	MWCNT
Length (micrometer)	~1000	<100
Diameter (nanometer)	0.4-2	2-50
Tensile Strength (GPa)	13-53	11-63
Tensile Modulus (GPa)	~1260	270-950

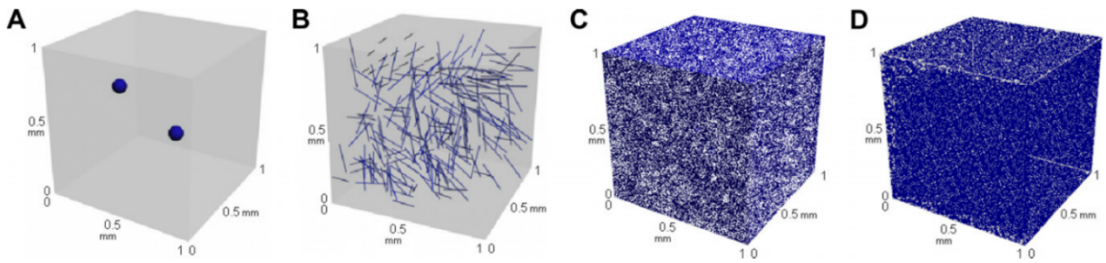

Figure 3.2. Distribution of micro- and nano-scale fillers of the same 0.1 vol.% in a reference volume of 1 mm3 (A: Al2O3 particle; B: carbon fiber; C: GNP; D: CNT) (Source: Siddiqui et al., 2010)

As mentioned earlier, Figure 3.2 is a very impressive image to visualize the distribution of micro and nanoscale fillers, such as respectively Al_2O_3 (A), and graphene (C), in a polymer matrix. In Figure 2.2, the fact that the fillers distributed in the matrix have different sizes and geometries gives information about their distribution behavior. The distribution of micro-scale fillers such as Al_2O_3 and carbon fiber (B) is homogeneous throughout the matrix, and the differentiation of their location and distribution can be easily noticed due to their size. However, it is almost impossible for the graphene and CNTs (D) added at the same volumetric ratio to be differentiated from each other and to be located at equal distances for the distribution. Particle agglomeration caused by electrostatic interaction and van der Waals force makes the dispersion of nanoscale fillers into the polymer matrix rather difficult. The aim here should be to minimize the attraction forces between each other and to create as small agglomeration groups as possible.

3.2. CNTs Market and Literature Forecast

According to Market Research Future, the CNTs Market is projected to reach US $ 6,026.4 Million by the end of 2027, with a CAGR of 20%, while it appears to be the US $ 1,659.8 Million in 2019. The increasing interest in CNTs in the aerospace & defense industry is also showing its effect in the global market. The increasing use of CNTs, both as a structural element and in the electrical and electronics industry, are the biggest factors

in the rapid growth of the market. Interest in CNTs is also increasing in the development of fuel cell vehicles in the automotive industry, which is one of the sectors closely related to the global economy. Composite sports equipment, which has not found its rightful place in Turkey, can be designed more lightly with high specific strength and specific stiffness gains with the inclusion of CNTs. All of these indicators can be seen with the number of patent applications made according to the years in Figure 3.2.

After the first CNT article was published in Nature in 1991, the first report [46] on the preparation of a CNT/polymer nanocomposite was published in 1994. Following this report, efforts have been made to obtain clearer information on the properties of CNTs, and as shown in Figure 3.3, academic studies on CNT and CNT/polymer nanocomposite have gained great momentum with the CNT fabrication at lower costs at the beginning of the 21st century. Based on the studies, it is divided into two main groups: structural and functional CNT / polymer nanocomposites [47]. In structural composites, the superior mechanical properties of CNTs such as high modulus, tensile strength, and stress against fracture are used to obtain structural materials with much more impressive properties. In functional composites, research is carried out with CNTs to improve the properties of the structure such as thermal, electrical, electromagnetic, and optical.

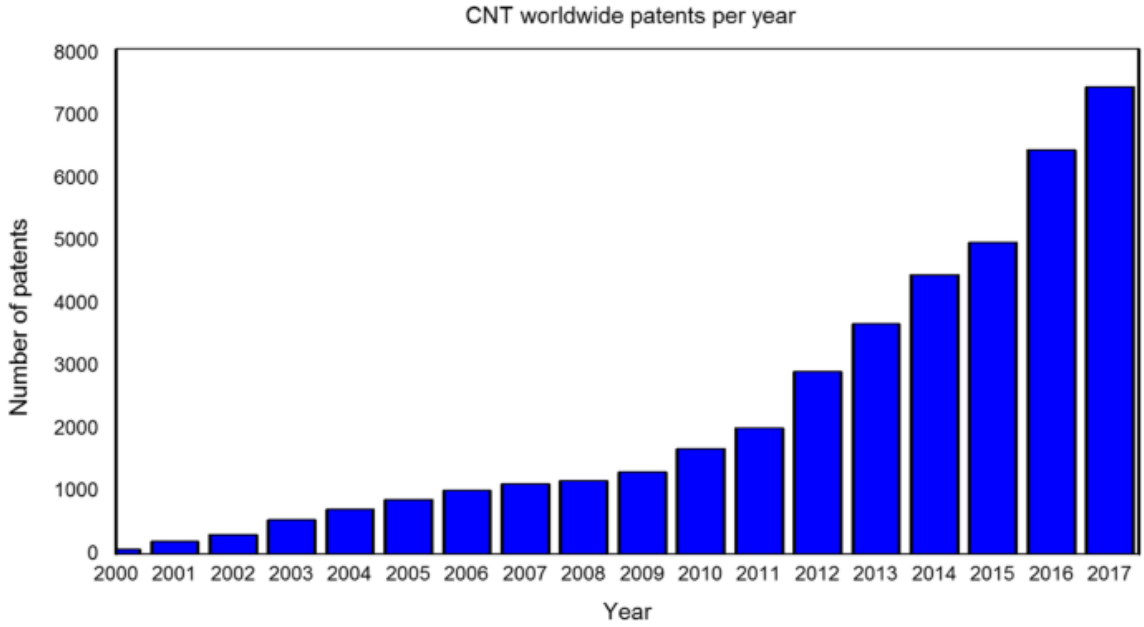

Figure 3.3. CNT worldwide patents per year

(Source: Venkataraman, 2019)

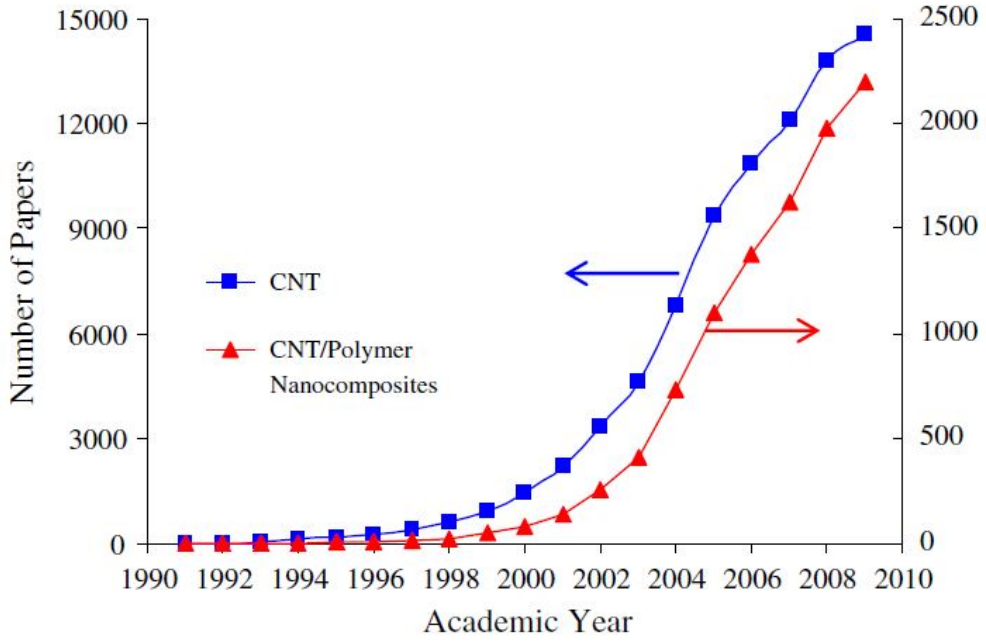

Figure 3.4. Number of papers about CNT and CNT/Polymer Nanocomposites according to the academic years (Source: Scopus)

3.3. Dispersion of CNTs

The most important factors on the success of CNTs in composite applications are directly related to homogenous and stability of the dispersion. The desired results could not be obtained with the inability to transfer the superior properties of CNTs to composite structures, and the weak interfacial interaction between nanofillers and polymer matrix [48-51]. CNTs tend to form agglomerates due to their van der Waals attraction and electrostatic properties between the nanotubes that make up their structure. Most of the time, these agglomerates cause large gaps in the composite structure and a decrease in mechanical, thermal, and electrical properties [52-54]. Besides these effects, it leads to a significant increase in the viscosity of the polymer due to its high aspect ratio (> 1000). The increase in viscosity leads to constraints for both the dispersion into the polymer and the manufacturing process. Because of these noticeable behaviors, it should usually be at levels less than 5 vol% in the polymer matrix [55, 56].

The dispersion of CNTs into the polymer matrix in composite applications is generally performed mechanically. The most common mechanical methods are ultrasonication, calendaring, ball milling, stir, and extrusion, respectively. While the dispersion of CNTs can be carried out with only one of these techniques, it can also be done in a multi-step manner. The comparison of various mechanical techniques for CNT dispersion in polymer composites is presented in Table 3.3.

3.4. Functionalization of CNTs

As mentioned earlier in this study, CNTs are found in clusters due to the carbon atoms in the CNT walls which are chemically stable due to the natural structure of the bond and van der Waals interactions that make their dispersion difficult in the polymer matrix. The biggest challenge in the development of nanostructured composites by incorporating the outstanding properties of CNTs into the polymer is to achieve a homogeneous and stable dispersion. Therefore, it has been observed that the functionalization process was applied in most of the studies performed to overcome the problem [57-60]. With the functionalization process, the performance of the CNT / polymer nanocomposite is improved by its positive effect on the distribution of CNTs in the matrix and the interfacial interactions between the CNT and the polymer. By changing the surface properties of CNTs with functionalization, the possibility of bonding with the medium in which it will be dispersed is increased. These methods have been studied in two groups as chemical functionalization and physical methods that depend on interactions between active molecules on CNTs and carbon atoms. Table 3.4 provides the advantages and disadvantages of functionalization techniques [61].

Table 3.3. The comparison of various mechanical techniques for CNT dispersion in polymer composites

Technique	Factor			
	Damage to CNTs	Suitable Polymer Matrix	Governing Factors	Availability
Ultrasonication	Yes	Soluble, low viscous polymer or oligomer, monomer	Power and mode of sonicator, sonication time	Commonly used in lab, easy operation and cleaning after use
Calendaring	No	Liquid polymer or oligomer, monomer	Rotation speed, the distance between adjacent rolls	Operation training is necessary, hard to clean after use
Ball milling	Yes	Powder polymer or monomer	Milling time, rotation speed, size of balls, balls/CNT ratio	Easy operation, need to clean after use
Shear mixing	No	Soluble polymer, low viscous polymer or oligomer, monomer	Size and shape of the propeller, mixing speed and time	Commonly used in lab, easy operation and cleaning after use
Extrusion	No	Thermoplastics	Temperature, configuration and rotation speed of the screw	Large-scale production, operation training is necessary, hard to clean after use

Table 3.4. The comparison of various functionalization techniques for CNT treatment

Functionalization	Method	Damage to CNTs	Interaction with polymer	Re-agglomeration of CNTs in matrix
Covalent	Incorporation of functional groups	Yes	Strong	Yes
Non-covalent	Polymer wrapping	No	Variable	No
	Surfactant adsorption	No	Weak	No

3.4.1 Covalent Functionalization of CNTs

Covalent functionalization is the chemical process that is based on the covalent linkage of the functional groups onto the carbon scaffold of CNTs. Chemically functionalized CNTs can form strong interfacial bonds with many polymers and enable CNT-based nanocomposites to achieve high structural and functional properties, making them the primary material in many usage areas. Defect functionalization, which is also applied in the presented study, is one of the methods used for the covalent functionalization of CNTs. This process creates chemical junction points in defect sites such as open ends and/or holes in sidewalls in the hexagonal graphene frame, pentagonal or heptagon irregularities in CNTs (Figure 3.5). Oxygenated areas are also one of the defect sites. Strong bonds can be established with the polymer by forming defects in the sidewalls and open ends of CNTs by an oxidative process with strong acids such as HNO_3, H_2SO_4, or their mixture [62]. As a result of the oxidation process, bonds with carboxylic acid (–COOH) or hydroxyl (–OH) groups are observed on the sidewalls of CNTs.

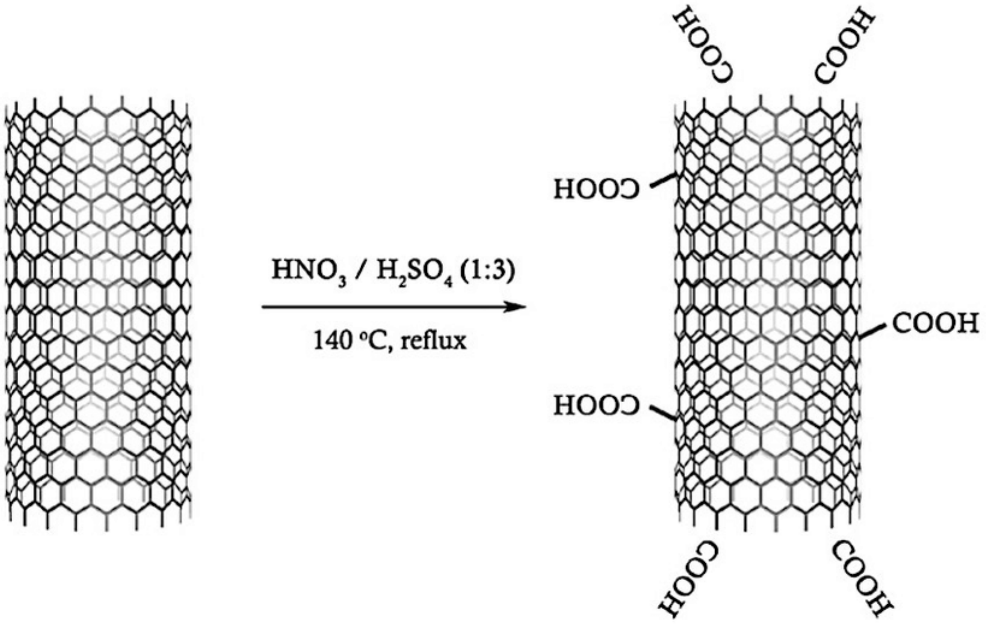

Figure 3.5. The forming defects in sidewalls of CNTs by an oxidative process with strong acids such as HNO_3, H_2SO_4 or their mixture, also known as acid treatment (Source: Dimitrios et al., 2008)

3.4.2 Non-covalent Functionalization of CNTs

The covalent functionalization process creates the possibility of damaging consequences for CNTs, especially during the ultrasonication process. This damage usually occurs by shortening the length of CNTs and may negatively affect functional properties such as thermal and electrical. Another method developed as an alternative to this method is non-covalent functionalization and it is used to improve the interface properties of nanotubes for the same purpose. Much research has not been done on this subject in the presented thesis, but the process mainly involves van der Waals, π-π or CH-π interactions between polymer molecules and the CNT surface [63-65]. The two main approaches to non-covalent functionalization are polymer wrapping and surfactant-supported dispersion. Although it does not cause any damage on CNTs, its bond with the medium in which it is dispersed is weaker.

3.5. Prepreg Preparation by Filament Winding Technology

Filament winding is a manufacturing technique mainly used to produce open (cylinders) or closed-end structures (pressure vessels or tanks). The filament winding technique is a low-cost, efficient manufacturing process typically used in the mass production of continuous fiber-reinforced composite components with a sophisticated machine and software system. As can be seen in Figure 3.7, this process involves winding the filaments under a certain tension and at desired angles on a rotating mandrel. As the mandrel rotates around the spindle, a pay-out eye on a carriage passes horizontally flush with the axis of the rotating mandrel, placing the filaments in the desired pattern or angle. Before the filaments reach the mandrel, they are impregnated with resin in a bath. After the mandrel is completely coated to the desired thickness, the resin curing stage is reached. Depending on the resin system and curing properties, usually the rotating mandrel is placed in an oven. After the resin cures, the mandrel is removed or extracted leaving the hollow final product.

With this process, after determining the details of each layer, winding angle, span, offset distance, and other parameters, anyone adapts the filament winding according to the direction of how loads will be applied to the part, and lighter and stronger structures can be created. Thus, the highlighted advantage of the filament winding manufacturing technique is a highly automated manufacturing process that can produce different fiber orientations with different mechanical properties. It is possible to convert it to a drum-type prepreg machine with a little modification to the winding process. This method, which is more suitable for 2D UD sheet prepregs, is directly related to the viscosity of the resin used. The resin systems selected in the range that will ensure sufficient wetting of the fibers are used in the production of UD prepreg. Unlike the filament winding process, the fibers collected on the mandrel are taken to the furnace so that the resin reaches the b-stage point instead of curing. After this process, the prepreg plates that reach good tack properties are stored in a freezer between -4 and -12 °C and kept ready for future use. Details and visuals of the drum-type prepregging system used in the presented thesis are given in the experimental chapter.

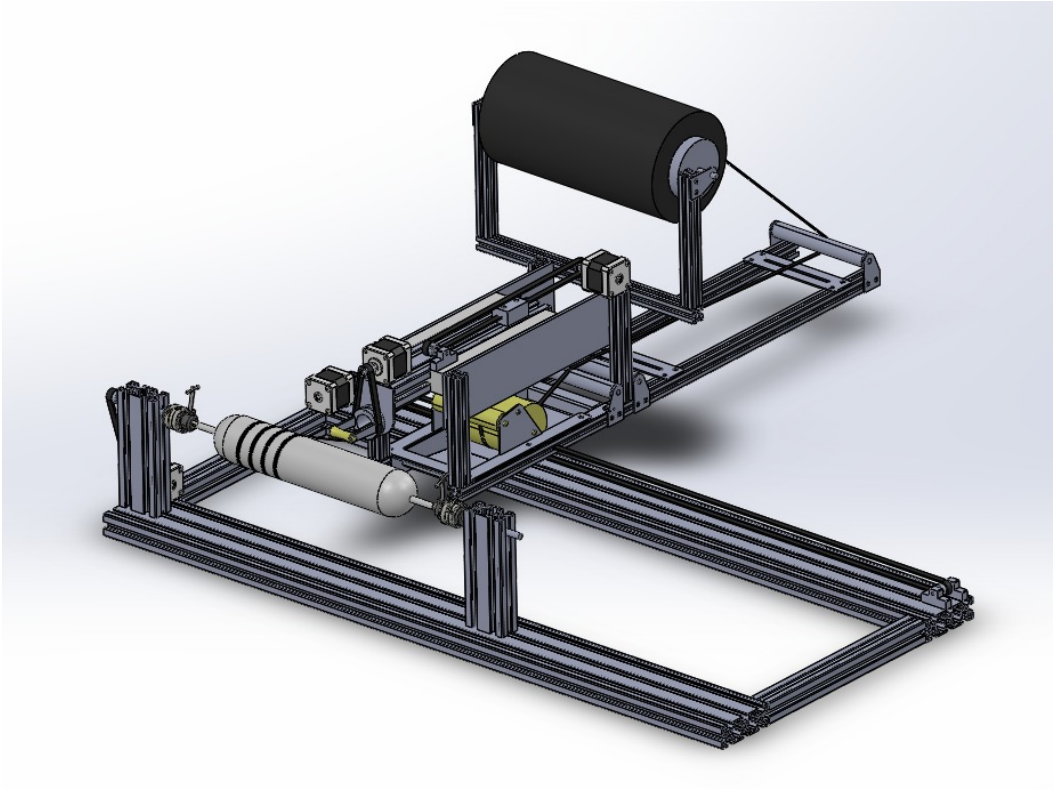

Figure 3.6. Image of desktop filament winding machine designed by the researcher for future studies

Preparation of CNT/polymer resin systems can be performed by in situ polymerization which is an efficient method to provide homogeneous dispersion of CNTs in an epoxy polymer. In this method, CNTs are first mixed with monomers after being dispersed in a solvent. These monomers are then polymerized with the addition of a hardener or curing agent. While the dispersion process can be done in one of the aforementioned mechanical ways, it can also be applied in a multi-step way. The polymerization reactions are stopped at the b-stage point in resin suitable for prepreg production, and the vacuum bagging arrangement is prepared for composite production so that the curing reactions take place at high temperatures. One of the major advantages of this method is that a strong bond can be formed between functionalized CNTs and the polymer matrix, which will directly affect the improvement of the mechanical properties of the manufactured composite.

3.6. Literature review of composites containing CNTs

Functional composites can be investigated under three main categories in terms of their contents. These can be defined as two-phase, three-phase, and multi-phase composites, respectively, as shown in Figure 3.8. Studies in the literature show that composites formed in three and multi-phase are generally called hybrid structures.

As stated before, the technique used for CNT dispersion when producing functional composites affects the mechanical properties of CNT / polymer nanocomposites. A remarkable study on this subject is summarized in Table 3.5 [66]. The results show the flexural properties of CNT / polymer nanocomposites (NK-50, epoxy) produced by different dispersion techniques. As can be seen from the results, the best CNT distribution, improvement in flexural strength and modulus were achieved using a calendaring machine. The probe sonication also made a positive contribution to both properties.

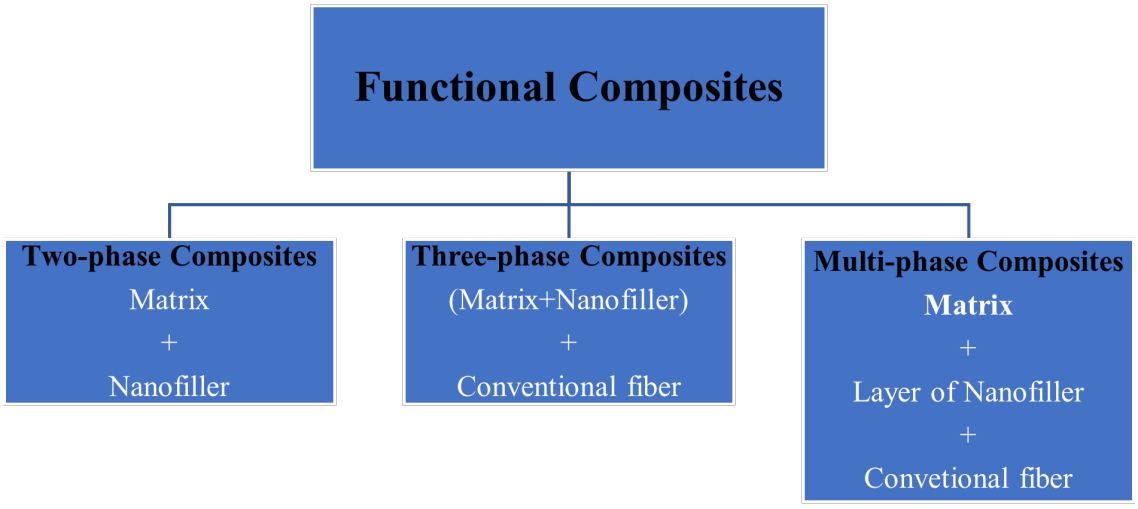

Figure 3.7. Main types and components of the functional composites

Table 3.5. The results for the flexural properties of CNT / polymer nanocomposites (NK-50, epoxy) produced by different dispersion techniques

Dispersion Technique	Flexural Modulus	Flexural Strength
Neat epoxy	3.43 (+0.00%)	140.0 (+0.00%)
Sonication in the water bath	3.41 (-0.58%)	144.1 (+2.93%)
Shear mixing	3.36 (-2.08%)	140.4 (+0.29%)
Probe sonication	3.47 (+1.17%)	142.7 (+1.93%)
Calendaring	3.65 (+6.41%)	145.2 (+3.71%)

It has been proven that the chemical and physical functionalization of CNTs so that does not take place in the matrix as agglomerates increase interfacial adhesion. The results obtained on the mechanical properties of CNT / thermosetting polymer nanocomposites as a result of the functionalization of CNTs are summarized in Table 3.6. These results show that the functionalization of CNTs improves the mechanical properties of nanocomposites such as modulus, strength, and toughness. Data in brackets present the percentage enhancement on mechanical properties by incorporation of functionalized CNTs.

Sun L. et al [67] investigated the effect of incorporation of pristine and functionalized SWCNT on epoxy Young's modulus and tensile strength. Based on the results presented, the incorporation of pristine SWCNT increased the epoxy Young's modulus and tensile strength by 18% and 16%, respectively. Functionalized SWCNTs incorporated by oxidation functionalization increased the increments to 27% and 17%, respectively.

Bekyarova et al. [68] studied the effect of functionalized SWCNTs as nano reinforcement for carbon fiber/ epoxy composites. After SWCNTs functionalized with carboxylic acid groups (SWCNT-COOH) were dispersed in epoxy, the vacuum-assisted resin transfer molding was used for fabricating SWCNT-COOH/epoxy/CF composites. The results showed that the incorporation of SWCNT-COOH improves the mechanical properties of the composites as a 40% enhancement of the shear strength with the addition of 0.5 wt. %. SWCNT-COOH.

Table 3.6. The results for mechanical properties of CNT / thermosetting polymer nanocomposites as a result of different functionalization techniques

Ref.	Matrix	Functionalization technique	CNT content	Enhancement of mechanical properties		
				Modulus (%)	Strength (%)	Toughness (%)
[69]	Epoxy	Amino treatment	0.10 wt.%	2.1 (6.7)	-2.2 (3.1)	17 (19)
[70]	Epoxy	Surfactant treatment	0.25 wt.%	8.6 (24)	6.8 (20)	35 (60)
[71]	Epoxy	Organic silane	0.25 wt.%	8.7 (22)	3.6 (18)	-22 (8.5)
[72]	Polyurethane	Acid treatment	10 wt.%	340 (500)	51 (111)	-
[73]	Vulcanized rubber	Acid treatment	25 phr	444 (594)	175 (244)	-

In Table 3.8, the contribution of the incorporation of chemically functionalized CNTs to the epoxy matrix and conventional carbon fiber on the mechanical properties of hybrid composites is summarized for other studies. When a literature review is made on prepregs, it is seen that there is not much work on fabrication techniques and characterization for nano-engineered prepregs.

Siddiqui et al. [74] published one of the most comprehensive studies about nanoengineered prepregs. It is a study that emphasizes the effects of CNTs on prepreg production parameters and resin that curing characterization of the prepregs obtained

afterward. The viscosity of the resin is the most important factor in prepreg production, and the addition of CNTs is known to increase viscosity. The results showed that high-speed shear mixing, and functionalization of CNT is an important factor in reducing the viscosity of CN / polymer nanocomposites. Thermal characterization results showed that the catalytic activity of the CNTs did not have a significant effect for 0.5 wt. % filler content, while the CNTs act as catalyzers when the content was 1.0 wt. %. The degree of cure was fallen for prepregs containing 0.5-1.0 wt. % CNT than without or containing less weight of CNT.

Garcia et al. [75] studied interlaminar properties of unidirectional prepregs containing aligned carbon nanotubes. Aligned CNTs were applied into the prepregs by using transfer printing technology at high temperatures and maintained CNT alignment in the transverse direction. The results indicated that the CNT-modified interface was observed to increase fracture toughness between 1.5 and 2.5 times in Mode I, and 3-times in Mode II.

Chen et al [76] modified the surface of carbon nanotubes by the functional reactor to disperse into the epoxy matrix, which was prepared for carbon fiber reinforced prepregs. The results showed that distribution was more homogeneous with modified CNTs. Moreover, the mechanical strengths of modified CNT-added nano-prepregs are higher than those of unmodified CNT-added nano-prepregs.

Tariq et al. [77] investigated the effect of CNT content on the mechanical properties of CFRP composites. The results were summarized in Table 3.7 as the mechanical improvements and properties of MWCNT–CF composites. Researchers have stated that while nano fillers are generally expected to improve matrix-dominant properties, they also have a positive effect on fiber-dominant properties in this study. Data in brackets present the percentage enhancement on mechanical properties by incorporation of functionalized CNTs.

Table 3.7. The effect of functionalized CNT content on mechanical properties of CFRP composites

The sample that containing various amounts of MWCNTs	Tensile Strength (MPa)	Ultimate strain (%)	Young's modulus (GPa)	Flexural Strength (MPa)	Flexural Modulus (GPa)
0 wt. %	415	0.75	51.9	715 (30%)	14.9
0.15 wt. %	541 (30%)	0.94 (15%)	60.8 (17%)	927 (30%)	18.7 (26%)
0.25 wt. %	606 (46%)	0.96 (28%)	65.1 (26%)	944 (32%)	29.6 (98%)
0.50 wt. %	579 (40%)	1.10 (47%)	55.6 (7%)	887 (24%)	16.2 (9%)
0.75 wt. %	530 (28%)	1.45 (93%)	52.1 (0.6%)	732 (3%)	16.0 (8%)

Table 3.8. The contribution of the incorporation of chemically functionalized CNTs to the epoxy matrix and conventional carbon fiber on the mechanical properties of hybrid composites

Ref.	A hybrid CF-CNT fabrication method	Matrix	% increase in flexural strength	% increase in flexural modulus	% increase in interfacial shear strength (IFSS)	% increase in interlaminar shear strength (ILSS)
[78]	Chemical Functionalization	Epoxy	-	-	-	18
[79]	Chemical Functionalization	Epoxy	59	54	27	-
[80]	Chemical Functionalization	Epoxy	-	-	70	-
[81]	Chemical Functionalization	Epoxy	-	-	43	13
[82]	Chemical Functionalization	Epoxy	-	-	26	-
[82]	Chemical Functionalization	Epoxy	-	-	72	-
[83]	Chemical Functionalization	Epoxy	20	-	-	13
[84]	Chemical Functionalization	Epoxy	-	-	-	32
[85]	Chemical Functionalization	Epoxy	-	-	83	48
[86]	Chemical Functionalization	Epoxy	-	-	273	-

CHAPTER 4

CURE KINETICS OF THERMOSETTING MATERIALS

4.1. Curing Mechanism

Hybrid composites (also known as multiscale or hierarchical or nanostructured composites) consist of at least two reinforcements of different size scales. These reinforcements are generally applied as micro-scale continuous fibers and nano-scale fillers. An important feature of hybrid composites is that they both have the advantages of traditional fiber-reinforced composites and benefit from the functionality gain by incorporating carbon nanotubes into the resin. One of the most remarkable challenges to be overcome with the use of epoxy resins in pre-impregnated systems is that they pass complex reaction stages during the curing process. [88]. This has been the subject of many studies involving handling and extending the shelf life of prepregs without sacrificing advantageous properties such as high glass transition temperatures (Tg), high modulus, and weight ratios [89-92]. In recent years, the essential reason for the growing popularity of CNTs as nano-scale reinforcements is not only excellent mechanical properties but also CNTs can provide high thermal conductivity throughout the resin system [93-97].

The mechanical and thermal properties of prepreg systems are linked to cross-linking reactions that occur during the epoxy curing process [98]. Epoxy resin is a thermosetting material that can form a three-dimensional network when it reacts with the hardener. Since it is an exothermic process, the heat of the reaction is released during the curing reaction. The curing mechanism is quite complicated as epoxy resin is subjected to many physical and chemical reactions during crosslinking [99, 100]. These chemical reactions play an important role in resin morphology, which determines the properties of cured thermoset resin and its composites. Since crosslinking continues after production, prepregs should be stored in a cold environment. In this way, it may be possible to extend the shelf life. The problem in the quality of end-product can be caused by using material that is over-cured or prepared with an unfavorable curing cycle. Therefore, one of the most important steps in the process of developing novel systems is to understand the

mechanism and kinetics behind curing reactions. Most of the studies on fiber-reinforced epoxy composites have been related to the final properties of the material in the literature. The focus is on studying the curing of composites, as optimizing work on processing products becomes more important today.

The incorporation of well-dispersed carbon nanotubes directly affects the curing reaction of the epoxy resin. Understanding the curing mechanism of the CNT / epoxy composite should be a priority for the design, analysis, and optimization of manufacturing materials. Therefore, there is a need to understand the nature of the prepreg processing because the final properties of hybrid composites depend heavily on the curing conditions [111-113]. Understanding the effects of nano-sized materials on the curing process will enable innovative developments for novel prepregs. In this part, the fundamentals of cure kinetics have been presented for the epoxy resin system incorporating single-wall carbon nanotubes (SWCNTs). Differential scanning calorimetry (DSC) is the most widely used technique to monitor the cure of solid-state processes. Also, the required kinetic parameters can be obtained using relatively simple isoconversional methods. CNTs often act as catalysts in the early stages of the curing reaction [114,115]. Therefore, the excessive decrease in activation energy for a prepreg process may shorten the gel time available to produce prepregs and cause the shelf life of prepregs to decrease.

4.2. Cure Reaction of Epoxy Resin

Epoxy resins generally have poor mechanical, chemical, and heat resistance properties before curing. However, three-dimensional cross-linked thermoset structures with superior properties are formed by reacting with suitable chemical agents. This process is known as the curing or gelation process [116]. Several types of chemicals are used to cure epoxies, such as including amines, imidazole, anhydrides, and photosensitive chemicals [117]. Also, curing may be taken place by reacting an epoxy with itself. As a result of curing, the structure gains resistance, durability, versatility, and adhesion properties. Any molecule containing reactive hydrogen could theoretically react with the active groups of the epoxy resin to form these three-dimensional structures (cross-linking). These co-reactants (hardeners) are usually amines, acids, acid anhydrides, phenols, alcohols, and thiols. The curing of epoxy resins is an exothermic reaction or

heat-generating. As it cures, the epoxy passes from the liquid state, through a gel state, before it reaches a solid-state. The curing of epoxide groups with amine hardeners as it is presented in this thesis shows that the primary amine hydrogen reacts with the epoxy resin, and then the secondary amine hydrogen is formed, which can react with the other epoxy ring. The mechanism of curing epoxy resins with amine hardeners can be seen in Figure 4.1 [118].

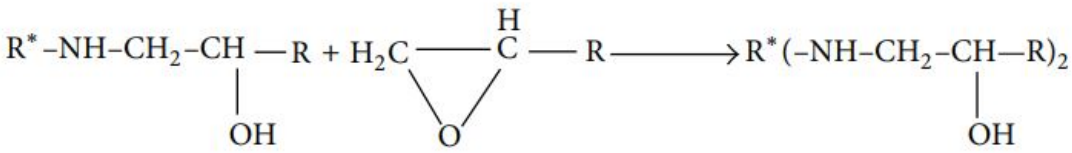

Figure 4.1. Illustrating mechanism of curing of epoxy resins with amine hardeners (Source: Mohammed Reza, et al., 2013)

While some epoxy resin/hardener systems cure at ambient temperature, most require heat input. Commonly used combinations provide the environment for curing at temperatures up to 150 ° C, while this temperature is up to 200 ° C for primary aerospace components. In case of insufficient heat input during curing, a network with incomplete polymerization is formed, resulting in reduced mechanical, chemical and heat resistance. Therefore, the curing temperature typically must reach the glass transition temperature (Tg) of the fully cured network for the final structure to achieve maximum properties.

The degree of cured resin gives an idea about the suitability of the resin available to bind the two prepreg layers during the final curing of the laminate formation. A prepreg will not show optimum mechanical properties if it is not fully cured. If the percentage of the cured resin is too high, there will be less chance of crosslinking during curing because of hindering chain mobility. It will form a weaker bond between the two subsequent layers.

4.3. Heat Flow Measurements by Differential Scanning Calorimeter

Cross-linking during the curing process can be monitored by Differential Scanning Calorimetry (DSC). The thermal analysis of partially cured prepreg samples provides generating a series of time-temperature-degree of cure diagrams. DSC can measure the heat during the exothermic or endothermic process, providing information on cure and degradation reactions. This method, which is used to measure the enthalpy changes occurring in a sample, also provides information for determining the thermal transitions of polymers. Therefore, thermograms obtained from DSC are used to achieve high-quality parts by optimizing kinetic parameters and curing cycles. The presentative thermogram of DSC is presented in Figure 4.2. There are two methods of thermal analysis kinetics, isothermal and non-isothermal methods. Non-isothermal heat treatment is applied at a constant heating rate where the temperature depends linearly on time. In contrast to non-isothermal heat treatment, the isothermal run sample is kept constant at the desired temperature for a while.

DSC is a popular method for determining the heat of reaction, the onset and offset of cure temperatures, degree of cure, cure kinetics, and Tg. It is possible to create optimum processing conditions by using these parameters presented in Figure 4.3. The heat of the reaction is a change in the enthalpy (energy) that is released during chemical reactions of epoxies. The degree of cure reveals the conversion achieved during cross-linking reactions. Cure kinetics are also known as kinetic triplets which are the activation

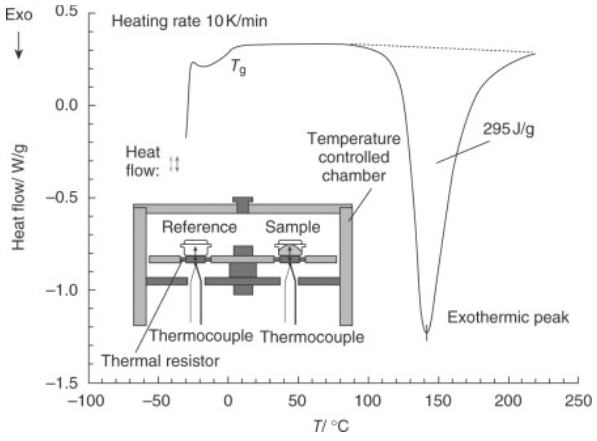

Figure 4.2. DSC heat flow vs. temperature of epoxy resin during full crosslinking (Source: PerkinElmer)

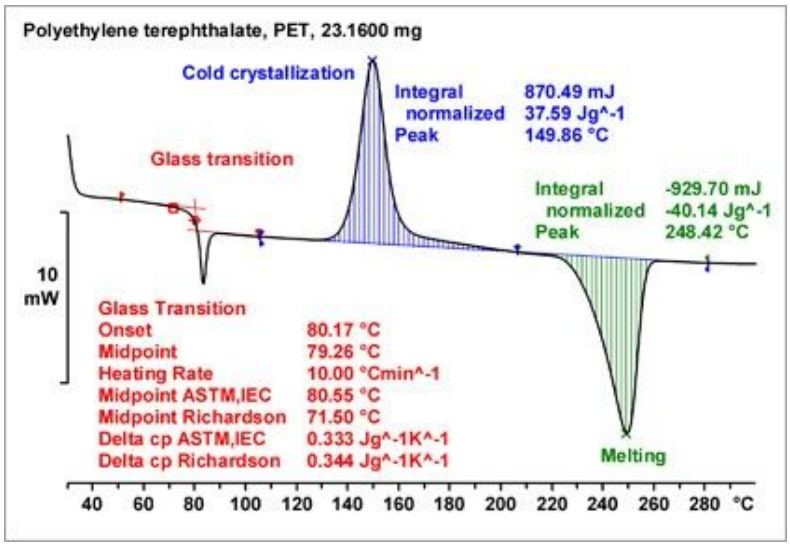

Figure 4.3. Finding glass transition temperature, onset-offset temperature, and total heat of reaction from heat flow curves (Source: Mettler Toledo)

energy, the pre-exponential factor, and the reaction model. Activation energy is the energy value that must be exceeded for a chemical reaction to occur. The amount of energy that causes all molecules in one mole of a substrate to transition into a transition state is related to the activation energy. Every chemical reaction has specific activation energy. The higher the activation energy of a reaction, the more difficult it will be to start that reaction. A reaction that does not occur spontaneously at room temperature can be carried out by heating the reactants (thus reaching the activation energy). In addition, the activation energy of a reaction can be reduced with the help of a catalyst, as CNTs do in an epoxy system.

4.4. Fundamentals of Cure Kinetics

The curing reaction of an epoxy resin is an exothermic reaction in which heat is generated. That energy dissipation during the cross-linking reactions is proportional to the number of consumed reactive groups [119]. Therefore, the process rates play important roles for thermal analysis which is initiated by a change in temperature. The

rate of reaction can be defined in terms of the temperature, T and the degree of cure (extent of conversion), α, as follows:

$$\frac{d\alpha}{dt} = k(T)\, f(\alpha) \tag{4.1}$$

where $k(T)$ is the rate constant and $f(\alpha)$ is the reaction model.

Eq. (4.1) express the rate of reaction for a single-step process. The mechanism of reaction processes of thermosetting materials generally includes several steps but one of them describes the overall kinetics. The rate constant deals with the temperature dependence while the reaction model is linked to the degree of cure. The degree of cure, α, can be expressed as the conversion achieved during the curing process [120]. It starts from 0 to 1 while the reaction is progressing from initiation to completion. The degree of cure is calculated experimentally as a fraction of the total heat released in the process:

$$\alpha = \frac{H_t}{\Delta H} \tag{4.2}$$

where H_t is the amount of heat released in time t and ΔH is the total heat of reaction. The area under the exothermic peak gives the amount of heat. Rate constant depends on the temperature and is expressed by the Arrhenius equation:

$$k(T) = A\, exp\left(-\frac{E}{R\,T}\right) \tag{4.3}$$

where E and A are kinetic parameters, the activation energy, and the pre-exponential factor, and R is the universal gas constant. The pre-exponential factor introduces the frequency of vibrations of the activated complex [121]. Temperature is controlled as a linear heating program by DSC instrument in non-isothermal measurements and described as follows:

$$\beta = \frac{dT}{dt} = const. \tag{4.4}$$

The process rate expressed by the degree of cure is a function of the reaction model. These reaction models show a wide variety as a solid-state in literature, some of them are given in Table 4.1. There are many reaction models, but they are examined under three main types: acceleration, deceleration, and sigmoidal (also known as autocatalytic). These kinetic curve shapes are given in Figure 4.4 with the numbers 1, 2, and 3 respectively. Thermosetting materials exhibit the sigmoidal behavior (i.e., Avrami-Erofeev models) that the initial stage is accelerating while the final stage is decelerating [122]. This means that the rate of reaction achieves its maximum at the intermediate values of the degree of cure.

Combining Eqn. (4.1) and (4.3), the rate of reaction can then be formed as:

$$\frac{d\alpha}{dt} = A\ exp\left(-\frac{E}{R\,T}\right) f(\alpha) \tag{4.5}$$

The resulting equation can be used for any temperature program with some modification. Combining Eqn. (4.1), (4.3) and (4.4) yields a resulting equation for non-isothermal (constant heating program) conditions:

$$\frac{d\alpha}{dT} = \frac{A}{\beta}\ exp\left(-\frac{E}{R\,T}\right) f(\alpha) \tag{4.6}$$

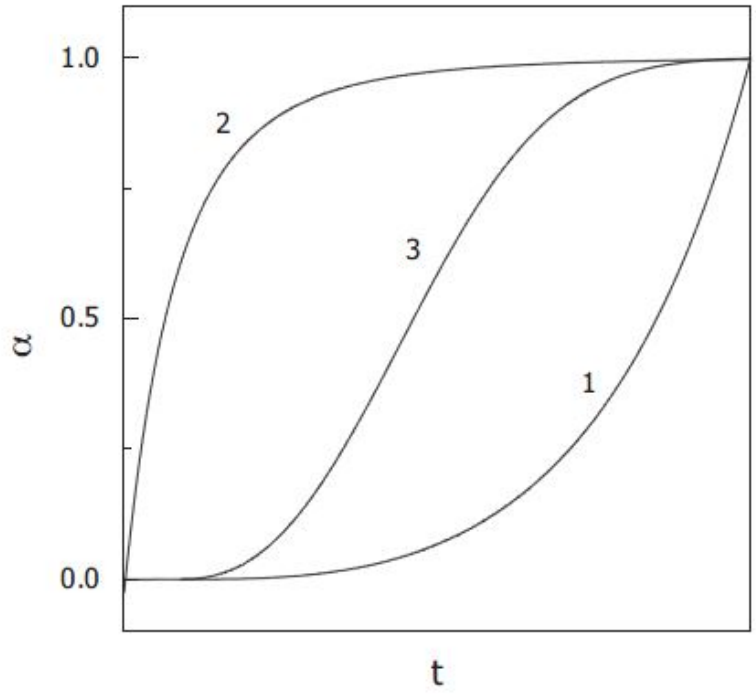

Figure 4.4 Kinetic curve shapes of α vs. t for (1) accelerating, (2) decelerating, and (3) sigmoidal (Source: Sergey et al., 2011)

Integration of Eq. (4.5) yields:

$$g(\alpha) \equiv \int_0^{\alpha} \frac{d\alpha}{f(\alpha)} = A \int_0^{t} exp\left(-\frac{E}{R\,T}\right) dt \tag{4.7}$$

where $g(\alpha)$ is the integral form of reaction to the model. For constant heating rate conditions, the integral form changes from time to temperature:

$$g(\alpha) = \frac{A}{\beta} \int_0^{T} exp\left(-\frac{E}{R\,T}\right) dT \tag{4.8}$$

Although Eq. (4.8) does not have an analytical solution, approximate solutions were applied in the past. These approaches have pioneered the development of integral methods. Modern integral methods realize the precise solution of integrals using numerical integration.

Table 4.1. Some of the kinetic models used in the solid-state kinetics [28]

	Reaction Model	Code	$f(\alpha)$
1	Power law	P4	$4\alpha^{\frac{3}{4}}$
2	Power law	P3	$3\alpha^{\frac{2}{3}}$
3	Power law	P2	$2\alpha^{\frac{1}{2}}$
4	Power law	P2/3	$\frac{2}{3}\alpha^{-\frac{1}{2}}$
5	One-dimensional diffusion	D1	$\frac{1}{2}\alpha^{-1}$
6	First Order	F1	$1-a$
7	Avrami-Erofeev	A4	$4(1-a)[-\ln(1-a)]^{\frac{3}{4}}$
8	Avrami-Erofeev	A3	$3(1-a)[-\ln(1-a)]^{\frac{2}{3}}$
9	Avrami-Erofeev	A2	$2(1-a)[-\ln(1-a)]^{\frac{1}{2}}$
10	Three-dimensional diffusion	D3	$\frac{3}{2}(1-a)^{\frac{2}{3}}[1-(1-a)^{1/3}]^{-1}$
11	Contracting sphere	R3	$3(1-a)^{2/3}$
12	Contracting cylinder	R2	$2(1-a)^{1/2}$
13	Two-dimensional diffusion	D2	$[-\ln(1-a)]^{-1}$

The purpose of kinetic analysis of polymeric reactions is to establish mathematical relationships between the process rate, degree of cure, and temperature. The most common way is to find a kinetic triplet (A, E, and $f(\alpha)$or $g(\alpha)$). After evaluating a single kinetic triplet for a single-step reaction, multi-step kinetics are predicted by substituting it into Eq. (4.5). The basis of thermal analysis is the interpretation of experimentally determined kinetic triplets. With this analysis, predictions can be made about process rate and material lifetimes.

Eqn. (4.5) provides the necessary conditions to apply different kinetic methods [123]. Isocoversional methods are one of the impressive ways to find kinetic parameters without assuming a reaction model. The common assumption of all isoconversional

methods is that the reaction rate only depends on the temperature at a constant degree of cure. Taking the logarithmic derivation of Eq. (4.1) at a constant degree of cure yields:

$$\left[\frac{\partial \ln\left(\frac{d\alpha}{dt}\right)}{\partial T^{-1}}\right]_{\alpha} = \left[\frac{\partial \ln k(T)}{\partial T^{-1}}\right]_{\alpha} + \left[\frac{\partial \ln f(\alpha)}{\partial T^{-1}}\right]_{\alpha} \tag{4.9}$$

The second term of the right-hand side of Eq. (4.9) is zero because of the common assumption and introduces:

$$\left[\frac{\partial \ln\left(\frac{d\alpha}{dt}\right)}{\partial T^{-1}}\right]_{\alpha} = -\frac{E_{\alpha}}{R} \tag{4.10}$$

As can be seen in Eq. (4.10) activation energy, E_{α}, can be determined by using the temperature dependence of reaction rate. That is why isoconversional methods are often referred to as model-free methods without assuming a reaction model. A series of dynamic scans with different heating rates have to be performed to evaluate more precisely the temperature dependence of the isoconversional rates. There are generally two categories of isoconversional methods: differential and integral. Kissinger–Akahira–Sunose (KAS) and Flynn–Wall–Ozawa (FWO) are the most common integral isoconversional methods in the literature [124, 125]. In addition, although the Kissinger method has some limitations, it has an advantage in determining the activation energy due to its easy use [126]. The equations of the aforementioned methods are presented below, respectively.

Kissinger–Akahira–Sunose (KAS) Method:

$$\ln\left(\frac{\beta_i}{T_{\alpha,i}^2}\right) = Const - \frac{E_{\alpha}}{R\,T_{\alpha}} \tag{4.11}$$

Flynn–Wall–Ozawa (FWO) Method:

$$\ln(\beta_i) = Const - 1.052\frac{E_\alpha}{R\,T_\alpha} \tag{4.12}$$

Kissinger Method:

$$\ln\left(\frac{\beta_i}{T_p^2}\right) = Const - \frac{E}{R\,T_p} \tag{4.13}$$

4.5. Literature Overview of Effect of CNTs on Cure Kinetics

In recent years, interest in the modeling of epoxy-based nanocomposite processing has increased to obtain high-quality parts by optimizing curing cycles and parameters [127-131]. Thus, experimental studies for the cure cycles can be reduced to a minimum. Using nanofillers in the resin system may have a considerable impact on the heat of reaction, ΔH, degree of cure (α), and kinetic triplet, such as activation energy (E_α). Borchardt and Daniels [132] have obtained the kinetic parameters using a single DSC measurement. Moreover, Kissinger [133], Ozawa [134], Flynn–Wall–Ozawa [135], and Kissinger–Akahira–Sunose (KAS) [40] models have been used for multiple dynamic scans with more precision. Isoconversional (model-free) models are the type of kinetic models and provide information about kinetic analysis of solid-state reactions without an explicit kinetic model. It is very difficult to define the complete curing reaction of the epoxy resin system simply because many reactive processes take place at the same time.

These models are useful for the study of the complex curing process. However, there are not many studies yet on how the material affects the curing mechanism because of the use of nanomaterials in hybrid prepreg systems. Siddiqui et al [136] studied the effect of multi-walled carbon nanotubes (MWCNTs) on the cure behavior of prepregs of carbon fiber-reinforced polymer (CFRP). The degree of cure is lower for the prepregs containing 0.5–1.0 wt.% MWCNTs than neat prepregs. Costa et al [137] focused on understanding the cure behavior of the Carbon/epoxy 8552 thermoplastic toughened

prepreg using DSC, DMA, and rheometer. Dynamic DSC scans were performed to obtain kinetic parameters incorporating with nth order reaction model. The results showed that the heating rate more reliable to fabricate the polymeric composite is 2.5 °C.min-1. Wu et al. [138] analyzed the curing behavior of high temperature curing epoxy resin prepreg in fiber metal laminates using DSC. Kinetic parameters were determined by the autocatalytic reaction model. The activation energy of the epoxy resin was 62.178kJ/mol and the reaction orders were 0.314 and 1.2157, the total reaction order was 1.5297. Kumar et al [139] studied cure cycle optimization of resin transfer molding type epoxy resin system containing MWCNTs for the manufacture of composite structures. Dynamic Mechanical Analysis (DMA) was performed to optimize the viscosity profile of the modified resin system.

The studies mentioned above and presented in Table 4.2 present some controversial behavior regarding the effect of CNT on the curing process of epoxy resin. Generally encountered results are given in order: an increment in thermal conductivity because of the excellent CNT thermal conductivity; an increase or decrease in viscosity; a catalytic effect by reducing activation energy. The common feature of the mentioned studies is the homogeneity of the CNT dispersed in the epoxy resin and the viscosity of the medium seems to be most responsible for the controversial behavior of the structures containing nano-fillers. For instance, the effect of pristine CNTs can give rise to a faster recovery or sometimes slower. Therefore, the effect of nanoscale fillers on the curing reaction depends on parameters such as the length and diameter of the CNT, the purity, type and number of chemical groups attached to the walls, the amount of CNT, the dispersion method, etc. In other words, composites prepared with the same CNT type may lead to different dispersion degrees of CNTs and different viscosities in epoxy resin. Another example is amine functionalized CNTs that can catalyze the curing reaction, but if added in a large quantity will increase the viscosity of the uncured resin and inhibit the curing reaction. Thus, dispersion homogeneity is one of the most effective factors that will determine the curing reaction of epoxy / CNT composites. It can be said that the heterogeneous CNT dispersion decelerates the reaction rate and reduces the heat-curing reaction [140, 141].

To observe the effect of CNTs on the curing reaction of the epoxy resin, it is necessary to obtain information on CNT dispersion homogeneities, such as the aspect ratio of the CNTs, the amount added, the purification, and dispersion method. Also, CNTs are often used as catalysts in the early stages of the curing reaction due to CNT thermal

conductivity (especially when added in large amounts) and to the presence of functional chemical groups such as amine, hydroxyl, or fluorine. Since the chemical structures of these amine groups have similar properties to that of the hardener, they act as a curing agent and the hydroxyl group can catalyze the ring-opening of the epoxy. The lowest degree of cure behavior is coming from the increase in viscosity. It is caused by the addition of CNT, hindering the mobility of the epoxy chains. Figure 4.5 summarizes the possible effects of CNTs on the curing reaction of the epoxy resin [142].

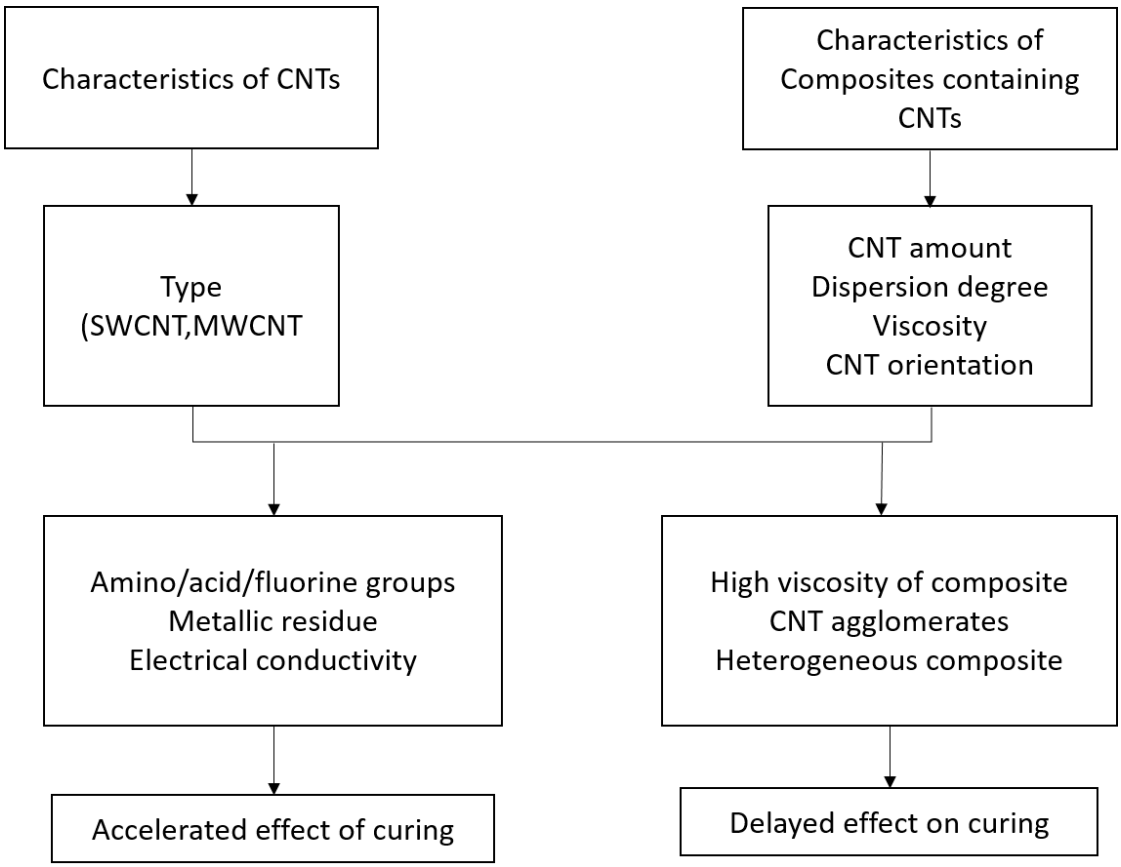

Figure 4.5 Effects of parameters on curing reaction of CNT/epoxy systems

Table 4.2. Kinetic Parameters of epoxy cure reaction [143]

No	CNT type	wt.% CNT	Dispersion	Enthalpy (ΔH)	Activation Energy
1	A	5, 10	Regular	$\Delta H^A < \Delta H^J$	-
2	B	1	Regular	$\Delta H^B < \Delta H^J$	-
3	C	0.5	-	-	$E^C > E^J > E^D$
4	D	0.5	High	-	-
5	E	1	Low	$\Delta H^E < \Delta H^F < \Delta H^J$	$E^E > E^J > E^F$
6	F	1	High		-
7	D	1	High	$\Delta H^D < \Delta H^J$	$E^D < E^J$
8	C	1	Low	$\Delta H^C < \Delta H^J$	$E^C \sim E^J$
9	D	2	High	$\Delta H^D < \Delta H^J$	$E^D < E^J$
10	C	2	Low	$\Delta H^C < \Delta H^J$	$E^E \sim E^J$
11	A, G, H, I	-	-	$\Delta H^H < \Delta H^G < \Delta H^A < \Delta H^I < \Delta H^J$	$E^I < E^J < E^G < E^A < E^H$
A ≡ SWCNT; B ≡ mixture of SWCNT, double-walled carbon nanotube, triple-walled carbon nanotube; C ≡ MWCNT; D ≡ Functionalized MWCNT with amine groups; E ≡ Functionalized MWCNT with carboxyl groups; F ≡ Functionalized MWCNT with fluorine groups; G ≡ Functionalized SWCNT with amine groups; H ≡ cut-SWCNT; I ≡ Functionalized SWCNT with epoxide groups; J ≡ Neat epoxy					

4.6. A New Numerical Approach: Nonlinear Fitting

It is proposed a new algorithm (GMN) for determining pre-exponential and activation energy of curing process by researchers of the presented thesis and Prof. Gamze Tanoğlu's research group (Murat Öz, Neslişah İmamoğlu). This method is based on the combination of the fitting for the measured conversion values via the least-squares minimization technique and linear fitting for the kinetic parameters. Experimentally determined differential scanning calorimetry (DSC) data sets for an epoxy resin functionalized by single-wall carbon nanotubes are used for the verification of the

proposed method. The results obtained from the proposed algorithm are also compared with the methods reported in the literature.

It is supposed that the experimental data $T = [a_1, a_2 \ldots, a_n]$ and $\alpha = [b_1, b_2, \ldots, b_n]$ temperature and conversion are given. It is considered the activation function as follows:

$$\alpha(T) = A(tanh(B(Tn - C) - 3) + 1) \tag{4.14}$$

where *A, B,* and *C* are unknowns. It is supposed to be fit a function that has a form in Eqn. (4.14). For this purpose, the nonlinear least square method is used. The error between the experimental result and activation function is defined by the following function.

$$E(A,\ B,\ C) = \sum_{n=1}^{N} (yn - A(tanh(B(Tn - C) - 3) + 1))^2 \tag{4.15}$$

The nonlinear least-square procedure requires finding a minimum error function. To find the minimum, the following conditions are applied.

$$\frac{\partial E}{\partial A} = 0, \qquad \frac{\partial E}{\partial B} = 0, \qquad \frac{\partial E}{\partial C} = 0 \tag{4.16}$$

The partial derivative of $E(A, B, C)$ concerning *A, B,* and *C* are:

$$\begin{aligned} \frac{\partial E}{\partial A} &= \sum_{n=1}^{N} 2(-tanh(B(Tn - C) - 3))\,(yn \\ &\quad - A(tanh(B(Tn - C) - 3) + 1)), \\ \frac{\partial E}{\partial B} &= \sum_{n=1}^{N} 2AB(sec\,h\,sec\,h(B(Tn - C) - 3)^2)(yn \\ &\quad - A(\tanh(B(Tn - C) - 3) + 1)), \end{aligned} \tag{4.17}$$

$$\frac{\partial E}{\partial C} = \sum_{n=1}^{N} -2AB(sec\,\mathrm{h}\,sec\,\mathrm{h}(B(Tn - C) - 3)^2)(yn - A(\tanh(B(Tn - C) - 3) + 1)).$$

Combining (4.16) and (4.17), it is obtained system of the nonlinear equation as follows:

$$0 = \sum_{n=1}^{N} 2(-\tanh(B(Tn - C) - 3))\,(yn - A(\tanh(B(Tn - C) - 3) + 1)), \tag{4.18}$$

$$0 = \sum_{n=1}^{N} 2AB(sec\,\mathrm{h}\,sec\,\mathrm{h}(B(Tn - C) - 3)^2)(yn - A(\tanh(B(Tn - C) - 3) + 1)), \tag{4.19}$$

$$0 = \sum_{n=1}^{N} -2AB(sec\,\mathrm{h}\,sec\,\mathrm{h}(B(Tn - C) - 3)^2)(yn - A(\tanh(B(Tn - C) - 3) + 1)). \tag{4.20}$$

When the partial derivative in Eqn. (4.18), (4.19), and (4.20) are set equal to zero, the nonlinear system of equations is obtained. The Newton Method is used to find the *A, B,* and *C*. Iterative formula of Newton Method for nonlinear systems is given as follows:

$$z^{k+1} = z^k - J^{-1}(z^k)\begin{pmatrix} F(z^k) \\ G(z^k) \\ S(z^k) \end{pmatrix} \tag{4.21}$$

where z^k is equals to the

$$z^k = \begin{pmatrix} A^k \\ B^k \\ C^k \end{pmatrix}$$

And $J^{-1}$the inverse the of the Jacobian matrix,

$$\mathrm{J(z)}=\begin{pmatrix} \frac{\partial E}{\partial A} & \frac{\partial E}{\partial B} & \frac{\partial E}{\partial C} \\ \vdots & \ddots & \vdots \end{pmatrix}$$

To start Newton's iterative method, an initial condition has to be applied.

This section, it is seeking for values of pre-experimental factor A and activation energy E which are given in Eqn. (4.6). There are four unknowns as A, E, α, and $f(\alpha)$ in Eqn. (4.6). The function of $\alpha(T)$ is obtained in the previous section approximately. In Table 4.1, there are the different choices of $f(\alpha)$. For the model most suitable choice is:

$$f(\alpha) = \alpha^m(1-\alpha)^n \tag{4.22}$$

where m, n are positive real numbers. As a result, there are only two unknowns A and E in Eqn. (4.6). To find these unknowns, the data linearization technique is used.

The first step is to take the logarithm of both sides of the Eqn. (4.6):

$$\ln\left(\frac{\beta}{f\ (\alpha)}\right) + \ln\left(\frac{d\alpha}{dT}\right) = \ln(A)\ e - \frac{E}{R\ T} \tag{4.23}$$

This results in a linear relationship between the new values X and Y:

$$Y = \overline{A} + E\ X \tag{4.24}$$

where Y, A, and X can be calculated by the linear fitting method.

$$Y = \ln\left(\frac{\beta}{f\ (\alpha)}\right) + \ln\left(\frac{d\alpha}{dT}\right)$$

$$\overline{A} = \ln(A)$$

$$X = -\frac{1}{R\ T}$$

CHAPTER 5

OUT OF AUTOCLAVE PROCESSING

5.1. Prepreg Processing

Advanced composite materials generally form from pre-impregnated carbon fiber reinforcement with either a unidirectional or woven architecture within an epoxy [144-146]. The semi-solid resin is at the B stage before the processing. Composite structures are fabricated with the application of heat and pressure to the stack of layers arranged in a certain order. Prepregs can be processed in different ways that the most common processing techniques are autoclave and out-of-autoclave methods. Historically, autoclave processing has been used to manufacture primary structures for aerospace applications. The autoclave is a pressure vessel that provides the curing conditions for composite production in which vacuum, pressure, heating rate, and curing temperature are controlled (Figure 5.1). The high compaction pressure (4-8 bar) provided by the autoclave gives a chance to fabricate superior quality components containing high fiber volume (55-65%) and low void contents (less than 2%) [147, 148].

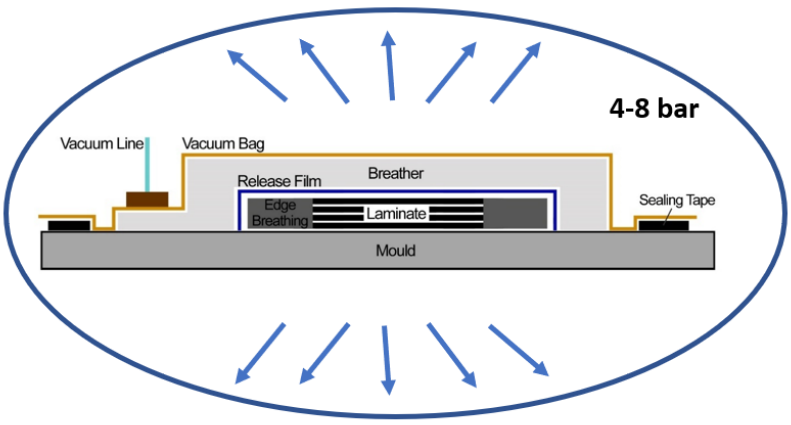

Figure 5.1. Schematical view of autoclave processing during fabrication

Compaction pressure acts as a spring analogy that compacts a stack of fiber to a certain fiber volume fraction. Entrapped gases will dissolve into the resin at a certain level of hydrostatic pressure which is approximately 3.5 bar [149]. This pressure describes the resin pressure which mostly depends on temperature, moisture, surface tension, and resin formulation. In this process, a stack of plies consist of prepregs are laid out on tooling, closed with a vacuum bag, and placed in the nitrogen environment. With the application of pressure and heat, the resin viscosity decreases and wets the reinforcement fibers, and finally takes the final shape of the mold in a laminated form by allowing void mitigation before curing [150]. High processing pressures provide better compaction for thicker sections of complex shapes. Long cure cycles are required because the large autoclave mass takes a long time to heat up and cool down. Sometimes slow heat-up rates are required to guarantee even temperature distribution on the tooling and composite components. In addition, due to high investment costs, high energy consumption, operation danger, and size limitations, it has gradually begun to be replaced by out-of-autoclave (OoA) processing methods [151]. One of these methods is vacuum bag-only (VBO) processing in which the same vacuum bag technique will be introduced in the next heading. The only difference of VBO is that lay-up is placed in an oven instead of a pressurized vessel. The stack of plies is oven cured under vacuum bag conditions which include 1 bar compaction pressure (Figure 5.2).

5.2. Out-of-Autoclave (OoA) Prepregs

Achieving advanced composite material has taken major steps with the use of prepreg. Out-of-autoclave composite processing has been used for the fabrication of primary structures over the last 30 years. The first generation OoA prepregs were designed with low curing temperatures (60 °C) to eliminate the disadvantages of the autoclave such as part and tooling costs [9-11]. With developments in resin chemistry, it is enabled the improvement of a new generation of OoA prepregs, curing in the 80–200 °C temperature range [152]. In addition, OoA prepregs have allowed the production of larger structures by eliminating size restrictions. Vacuum bag processing consists of the placing and sealing of a plastic bag over a stack of plies before evacuating all the air. It is suitable for the monolithic components of varying thickness and sandwich structures. The

applied pressure in VBO processing is the pressure between vacuum bag pressure (500-900 kPa) and the atmospheric pressure (1 bar), providing to press the individual plies together [153]. During applied pressure, the viscosity of the resin decreases with the performing heating scheme as molecular mobility increases. When the cross-linking reaction progresses, the viscosity starts to increase, hindering the mobility of chains. Eventually, a three-dimensional network provides stiffening the materials and forming the final shape of a composite structure during the cure cycle [154,155].

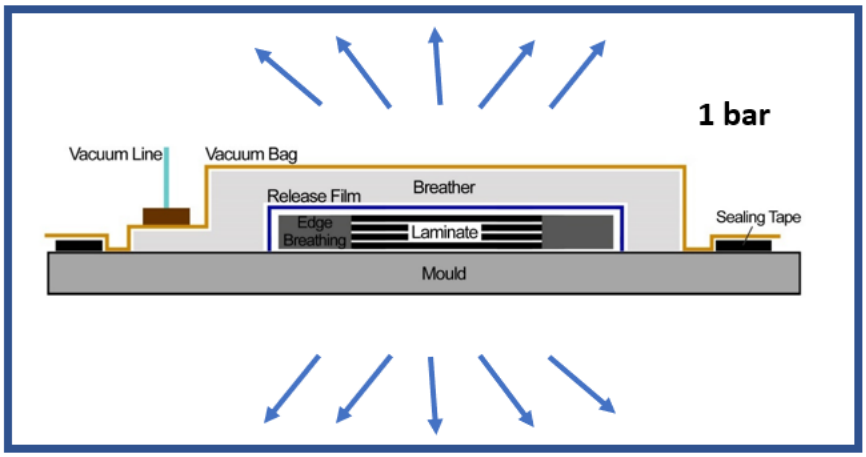

Figure 5.2. Schematical view of out of autoclave processing during fabrication

However, composites manufactured with first-generation OoA prepregs had poor surface quality and mechanical properties with extensive porosity due to low compaction pressure. Void content limited their use of application [156]. Besides, VBO processing depends on the air permeability (or evacuation of entrapped gas) to achieve similar quality to autoclave processed laminates. Voids take generally their source from air entrapped during lay-up, volatiles in the resin mixture, and moisture contained in the material [157]. Entrapped gas cannot be dissolved in the resin solution due to low compaction pressure. On the other hand, the requirements are less than 2% void content and high fiber volume content (>50%) for aerospace primary structures [157]. OoA prepreg systems must be specifically designed to meet these requirements without the autoclave, although the compaction pressure does not exceed 1 bar. Evacuation of the entrapped gas is the key

point for OoA prepreg laminates similar quality to autoclave processed laminates. Air permeability and resin chemistry of OoA prepregs have been optimized to achieve high mechanical properties while it is using VBO compaction pressure. To get low void content, the system should work well with the following parameters: air pathways (initial dry regions, sometimes called Engineered Vacuum Channels, EVACs), edges breathing and vacuum level. Air pathways are created as initial dry regions before curing through partial impregnation (Figure 3 (A)). These regions are completely wetted during the resin curing cycle and take their final form before consolidation. Meanwhile, edges breathings are working for evacuation of entrapped gases from laminate. The vacuum level is also an important parameter to reduce residual air in the vacuum bag lay-up. The stages of the traditional OoA processing are as follows.

• Prepreg layers are removed from their protective films and adhered to on top of each other.

• The surfaces are rolled to provide an effective adhesion.

• After the lay-up is completed, the system is surrounded with perforated or unperforated nylon (perforated/unperforated film).

• Then the breather fabric is laid, which will ensure the removal of excess resin and effective vacuum distribution.

• Finally, the system is put under vacuum using sealing paste and vacuum bag.

• The prepared system is placed in the furnace and the thermoset-based resin is cure under vacuum and heat.

One of the outlines that the presented thesis emphasizes is the processing of OoA prepregs. The basics of air permeability, void mitigation, resin impregnation, and curing process are presented in the next part.

5.3. Out of Autoclave (OoA) Processing Steps

The main processing steps of the VBO technique are listed as shown below step by step.

Lamination

Lamination is generally done by automated fiber placement (AFP), automated tape-laying (ATL), and hand lay-up. Hand lay-up has long been a standard method for composite fabrication processes, but it may not work well with complex mold geometries including sharp and concave corners. Prepreg fiber reinforcements generally have two different sides a dry and resin-rich side. The dry side includes initial dry regions also known as "engineered vacuum channels (EvaCs)" in Figure 5.4 (A). EvaCs permit air extraction by forming a permeable vascular network. Surface quality can be improved by laying the dry side of the prepreg towards the mold side as can be seen in Figure 5.3. Lamination is the adaptation stage to mold shape and first ply consolidation.

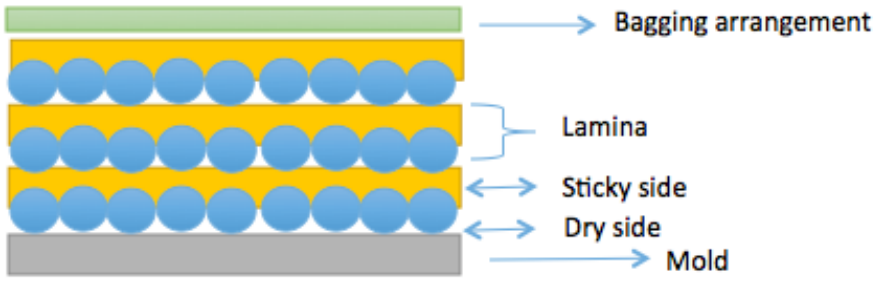

Figure 5.3 Orientation of the prepregs in the bagging arrangement during lamination

Vacuum bag lay-up

Bagging techniques are essential to achieve with OoA prepreg based laminates similar quality to autoclave processed laminates. Vacuum bagging quality mostly depends on the gas extraction and vacuum level of the bag arrangement. Vacuum bag processing includes vacuum line, vacuum bag, and sealant tape, breather fabric, release film, edge dam, peel ply as shown in Figure 5.4 (B). Following descriptions of the assembly, components are recommended to better understand the intended use.

- Release agent provides easy removal of cured laminate from the tool.
- Peel ply (optional) allows pathways of volatiles and excess resin bleeding in a vacuum bag process.
- Release film prevents the resin flow towards an upper layer and can be perforated to form porous media for air and volatile pathways.

- Breather fabric ensures that the applied vacuum is distributed evenly over the whole assembly and helps to remove the air and volatile substances coming from the laminate.
- Edge dam allows in-plane gas transport through the breather to improve the extraction from the laminate.
- Caul plate (optional) helps to prevent out-of-plane ply wrinkling.
- Vacuum bag and sealant tape are used to remove air from the assembly in leak-free condition.

Entrapped gas can propagate both through-thickness and in-plane directions before cross-linking reactions. Therefore, the boundaries of the assembly have to possess permeability skills to allow gas migration from the laminate to the breather fabric. For in-plane permeability, these boundaries are a kind of porous dams placed around the prepreg stack. Non-perforated films should be used so that the air flow is in the in-plane direction only. Sealant tape and fiberglass cloth can be used to connect the edges of the laminate. For through-thickness permeability, peel plies and perforated films are used to form gas pathways before and during the cure of the prepreg stack. Both air permeability systems are presented in Figure 5.5.

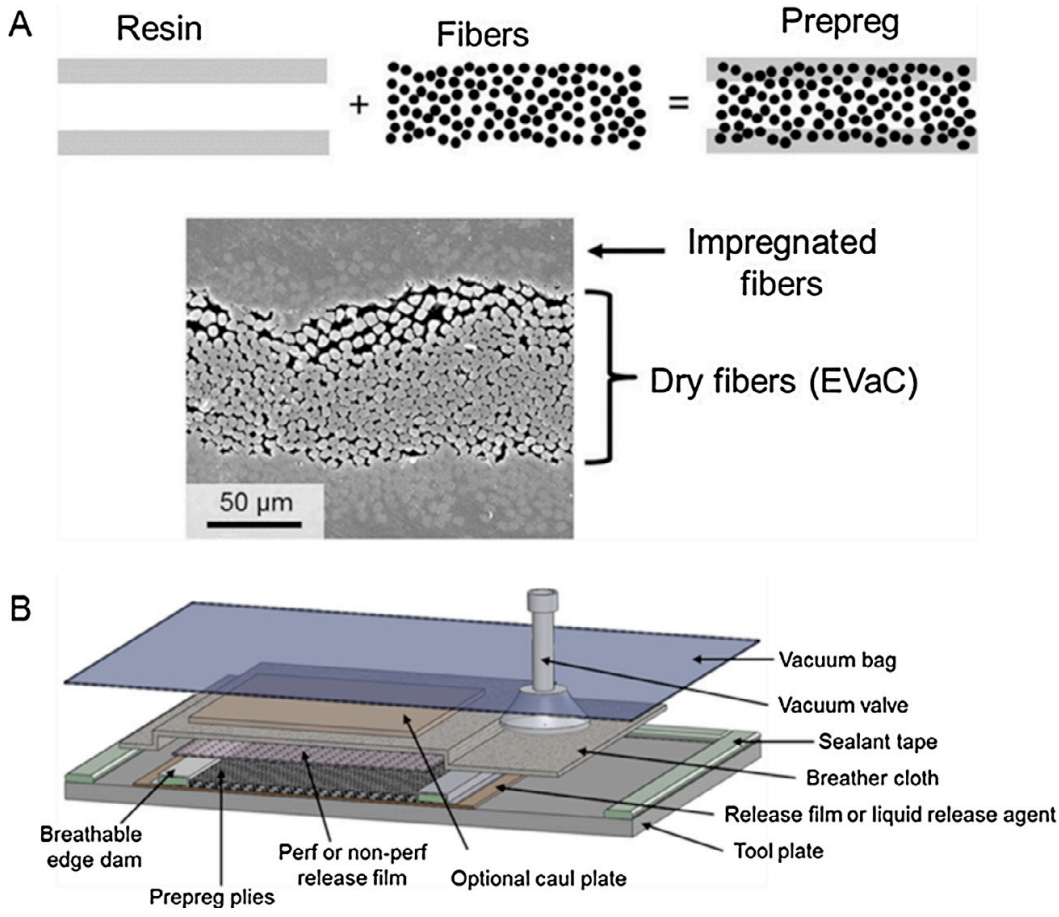

Figure 5.4. (A) Schmetical and SEM view of the engineered vacuum channels (EvaCs), (B) Bagging lay-up arrangement (Source: S.R. Nutt et al., 2015)

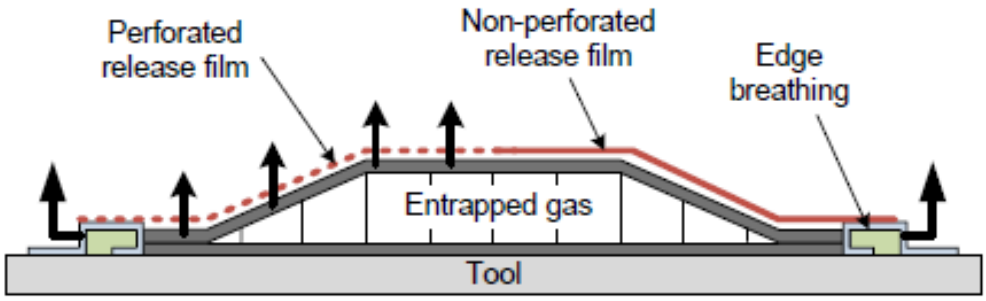

Figure 5.5. Lay-up variations in through-thickness and in-plane directions for air permeability from laminate to breathers (Source: J. Kratz, 2013)

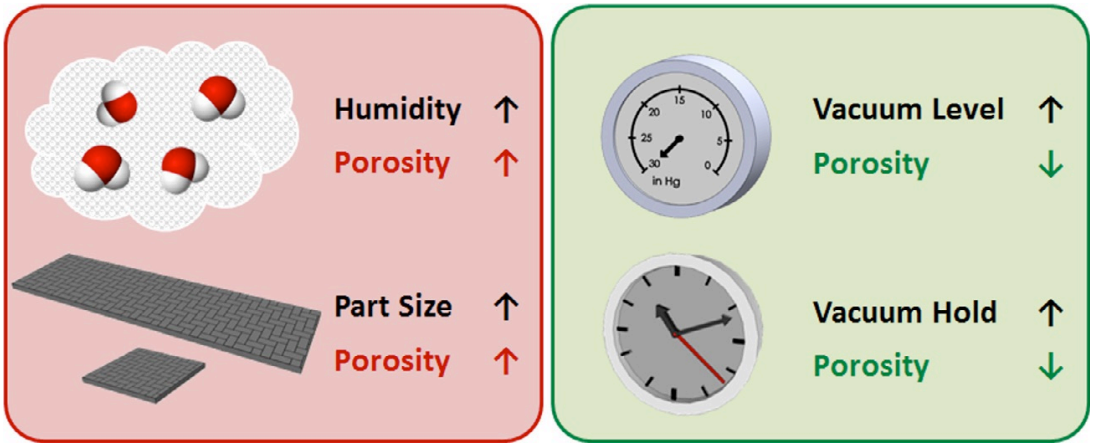

Figure 5.6. Effect of processing parameters on porosity for OoA process
(Source: S.R. Nutt et al., 2015)

The quality of vacuum is another essential process parameter for OoA prepreg-based composites to remove air from the prepreg lay-up. Moreover, the vacuum provides a consolidating pressure for oven curing. It is recommended that the vacuum pressure level do not drop more than 0.068 bar within 10 minutes. Increasing relative humidity and reduced vacuum levels each increase the void content and their combination causes this content to increase exponentially. The effects of various parameters on void content can be summarized in Figure 5.6.

Debulking

Before the curing process starts, the air and volatiles should be extracted from the bagging assembly as much as possible. Debulking process is used to ensure good mold adhesion and void-free parts for prepreg-based laminates. Uncured prepreg stack is kept at room temperature under vacuum conditions during debulking. In OoA processes, debulking time depends on the air permeability system and thickness of the stack of plies. Moreover, the air permeability of the prepreg is reduced during debulking.

Consolidation

Consolidation is generally focused on the behavior of the fibers, resin, and voids during curing processing. Moisture has to be evacuated before achieving a high degree of cure. At this stage, the prepreg stack is heated up to curing temperature and kept for a while. Resin rheology determines the quality of the final product by influencing the flow

characteristics. It is critical to provide sufficient flow to fill the EVaCs. The OoA prepreg consolidation process is shown schematically in Figure 5.7. In the beginning, a stack of partially impregnated plies is unconsolidated under ambient pressure. Each ply includes aligned fibers, surrounding resin, micro-voids, and macro-voids. Micro voids occur between individual aligned fibers, while macro-voids take place within the resin regions located around the fibers. Air is evacuated through the vacuum line when the vacuum is applied, the macro-void content decreases, and the stack of plies is compacted at ambient temperature. During heating to cure temperature, resin viscosity decreases and flows easily into the initial dry regions (EvaCs) to form void-free parts.

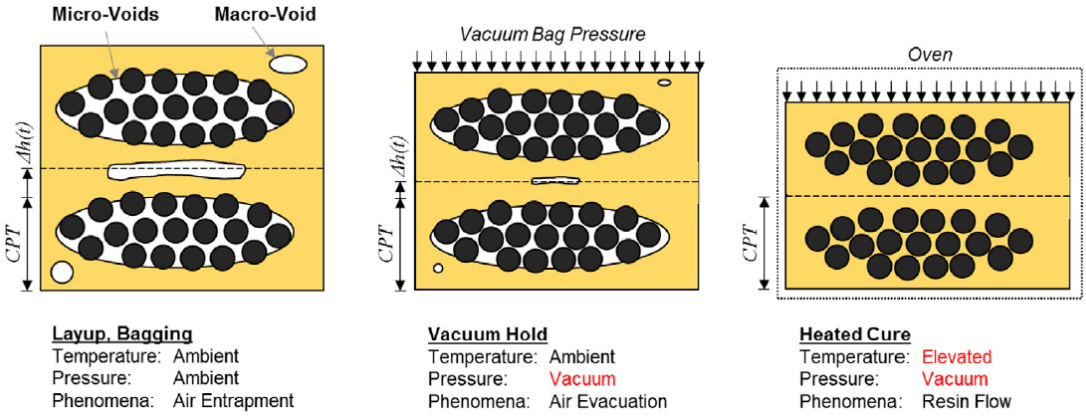

Figure 5.7. Steps of the OoA prepreg consolidation process during heating up (Source: S.R. Nutt et al., 2015)

For instance, viscosity of the MTM44-1 resin system drops from the 500 Pa.s (at 25 ºC) to 10 Pa.s (at 130 ºC, curing temperature) to impregnate the fibers. Fully impregnation cannot be achieved since the presence of large amounts of dry fibers. will hinder the resin flow. If is a small volume of dry fibers exists during the impregnation, there will be restricted flow paths, causing insufficient air permeability. Moisture remains the same between the layers at room temperature debulking. With the increase in the temperature, the moisture that becomes volatile blows away from the environment. On the other hand, prepreg air permeability starts to decrease due to the resin filling the dry areas. This will serve as the driving force behind a laminate with a high void content.

Also, the heat up rates affects the resin viscosity, flow, and laminate surface quality. Generally, fast heating rates are suitable for thin components and slow heating rates (i.e., 2,5 °C/min) are used for large and thick components.

Curing Process

Consolidation and air evacuation continue until gelation. The resin changes its phase from fluid to gel during an early stage of the curing process. Activation energy is the energy value that must be exceeded for a chemical reaction to occur. A reaction that does not occur spontaneously at room temperature can be carried out by heating the reactants (reaching the activation energy). Meanwhile, the viscosity of thermoset resin begins to increase caused by cross-linking reactions that occur during the curing process. The transition from liquid to rubber is also known as gelation linked to the cross-linked 3-D network structure of the thermosetting material. As the progress of the cross-linking reaction, the physical state of the thermoset transforms to a state of the glassy solid (vitrification), providing the final part with high glass transition temperature and mechanical properties. Vitrification state takes place at which the glass transition temperature of the resin system is equal to the cure temperature. During the curing process, representative evolution of the resin viscosity of a thermosetting material is presented in Figure 5.8.

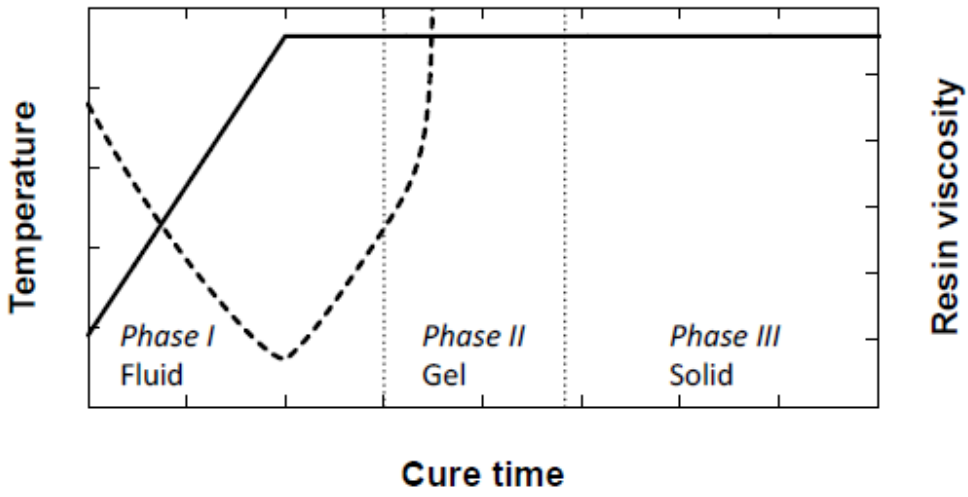

Figure 5.8. The representative evolution of the resin viscosity of a thermosetting material during fabrication (Source: Palardy-Sim, 2015)

Post-curing Process

For some thermoset resin systems, the curing process is followed by a post-cure at elevated temperature to complete cross-linking and achieve high glass transition temperature and degree of cure. Post-curing completes the polymerization reaction and further develops high-temperature mechanical properties for some epoxies. After post-curing processing, composite laminate is kept for cooling to room temperature. Thermosetting materials generally achieve full curing at room temperature for 7-10 days. Therefore, post-curing is going to not affect physical properties after thermosetting materials get full cure at room temperature.

5.4. Literature Review of OoA Processing

The key to the fabrication of void-free parts using out-of-autoclave methods is that create open-cell porosity into the prepreg by partial impregnation. The first paper presenting low-temperature VBO prepregs was published by Rebecka and Boyd. Over a year after this publication, Boyd, J. studied the influence of voids on the shear strength of the laminate. This result indicated that shear strength decreases with an increase in void content. Olivier et al. presented that void contents which are less than 2 % can provide an improvement on modulus and strength for a unidirectional carbon/epoxy laminate.

Centea and Nutt [158] investigated the effect of ambient pressure, vacuum quality, air evacuation, and fiber bed architecture on porosity for OoA prepregs. Reduced ambient pressure and insufficient vacuum quality caused to increase in void contents within resin-rich regions due to a lower ratio of resin to void pressure.

As mentioned above, one of the important parameters that affect the void content is the degree of impregnation. Prepreg format plays a crucial role in part quality for composites produced using vacuum bag only (VBO) techniques. Definition of the degree of impregnation of OoA prepregs is given schematically in Figure 5.10. Thorfinnson and Biermann [159] indicated that fully impregnated prepregs caused fabrication laminates with higher porosity than partially impregnated prepreg. The most important source of this issue is that structures with high DOI increase porosity by preventing air permeability pathways. Also, fiber volume fraction decreases with increasing implementation during preparing prepregs.

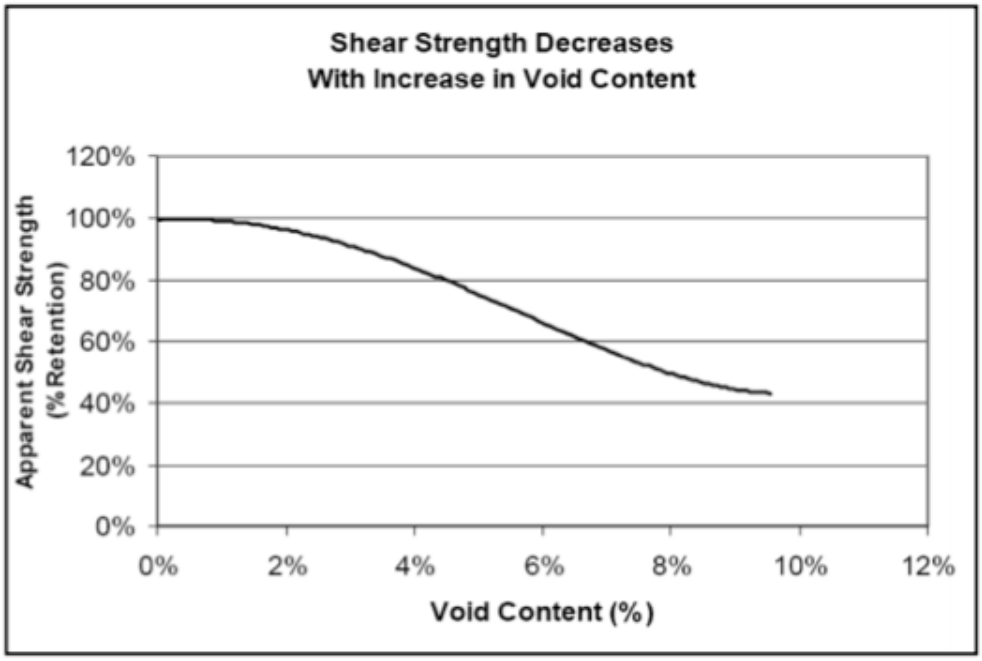

Figure 5.9. Influence of voids on the apparent shear strength
(Source: Boyd, J., 2003)

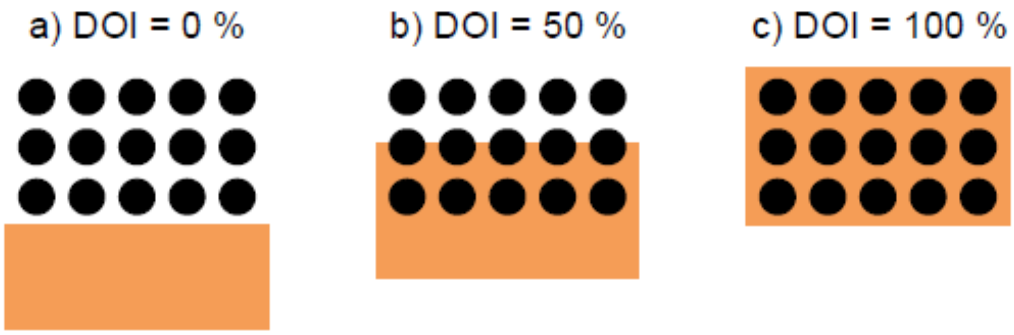

Figure 5.10. Various concentrations of degree of implementation (DOI), a) 0 %, b) 50 %, c) 100 % (Source: Thorfinnson, B.,1986)

Several authors have studied the air permeability of OoA prepregs and emerged two major inferences. Through-thickness air permeability seems more efficient because of short flow lengths. However, S.R. Nutt indicated that in-plane permeability (~10-14 m^2) is about four orders of magnitude greater than transverse permeability (~ 10-18 m^2).

Average in-plane permeabilities are relatively lower than other porous materials, and debulking time needed to evacuate most of the entrapped air is long in the processing of prepreg cure. Average room-temperature types of air permeabilities of various commercial prepregs are shown in Table 5.1.

Nutt and Hu [160] studied the effects of debulking on-air evacuation on both plain weave (PW) and unidirectional (UD) prepregs. Figure 5.11 shows void content as a function of time in PW and UD prepreg. The initial void content was ~35% for PW laminate because of the naturally contained air. The air evacuation rate is lower during vacuum holding at room temperature than during heating up to curing temperature. Despite this, in both fiber bed architectures, void content dropped significantly to 0.3% within an hour. Initially, UD prepregs consist of a lower void content of 13%. However, the results showed that the air evacuation of inter-ply air was much slower in UD prepregs. The void content dropped to 6% and 3%, when a 4-hour debulking was performed at 20 ° C and 60 ° C, respectively.

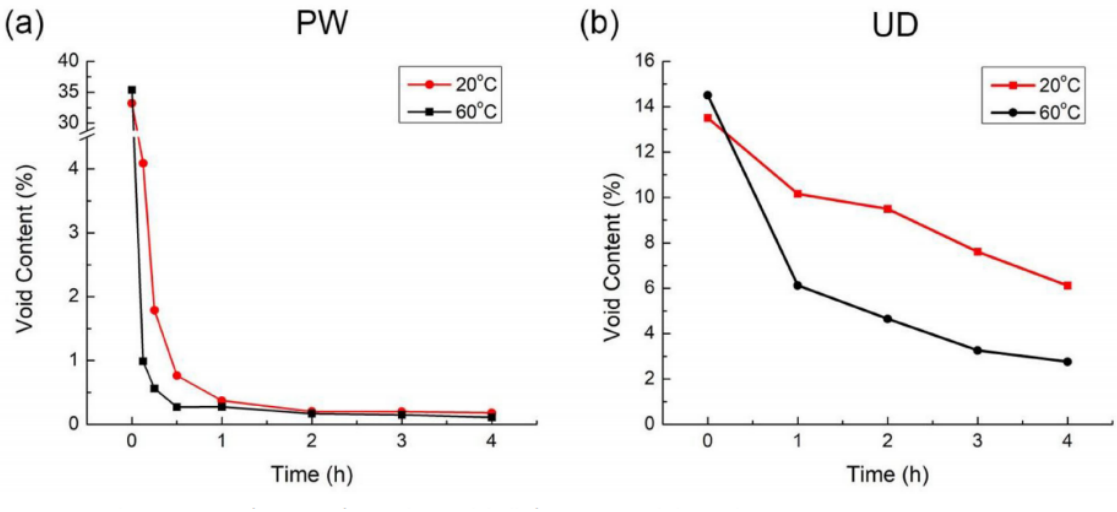

Figure 5.11. Void content as a function of time in PW and UD prepreg
(Source: Nutt and Hu, 2020)

Table 5.1. Average room-temperature types of air permeabilities of various commercial prepregs

No	Direction	Manufacturer	Resin	Fiber bed	Permeability (m^2)
1	In-plane	ACG	MTM45-1	5HS	3.3 x 10-14
2	In-plane	Cytec	5320	5HS	8.5 x 10-15
3	In-plane	Cytec	5320	PW	7.3 x 10-15
4	In-plane	Average			1.6 x 10-14
5	Transverse	Cytec	MTM45-1	5HS	1 x 10-18
6	Transverse	Cytec	5320	5HS	1.6 x 10-17
7	Transverse	Cytec	5320	PW	6.4 x 10-17
8	Transverse	ACG	VTM264	UD	5 x 10-18
9	Transverse	Average			2.5 x 10-17
5HS = 5-harness satin, PW = Plain weave, UD = Unidirectional					

The effect of VBO process parameters on mechanical properties attracted enormous attention in the literature. For instance, Vo et al. [161] studied the effect of post-cure temperature on the resin-dominated properties of an OoA prepreg (Cytec 5320/8HS). Laminates were fabricated using a cure cycle consisting of a two-hour cure at 93 °C and a post-cure at temperatures between 99 °C and 143 °C. The results indicated a direct relationship between the degree of cure, the average compressive strength, and glass transition temperature. All three properties increased with the application of higher post-curing temperature, as well as improved resin properties and fiber-resin bonds.

M. Danzi studied the effect of compaction pressure on fiber volume content at the laboratory of composite materials and adaptive structures in ETC Zurich. Figure 5.12 shows the compaction pressure required to compact a stack of fiber to a certain fiber volume fraction. This curve is characteristic of the textile. Due to the low compaction pressure (1bar), the maximal achievable fiber volume content is between 50 and 55%, depending on the textile used.

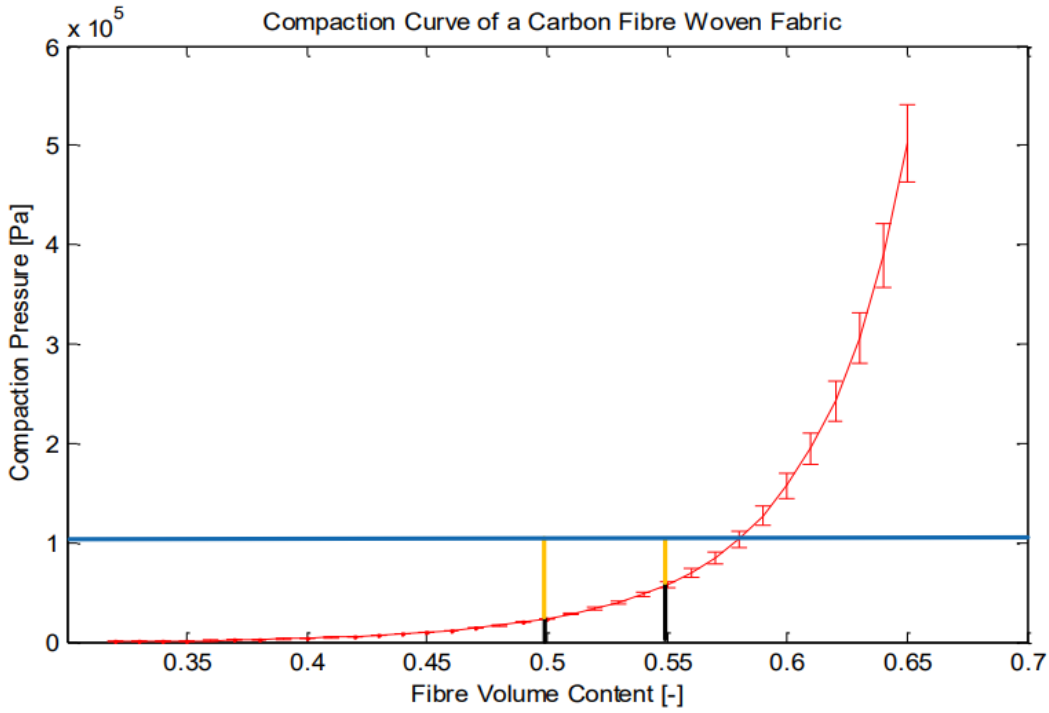

Figure 5.12. Fiber volume content for compaction pressure

(Source: M. Danzi, 2017)

CHAPTER 6

MATERIALS AND EXPERIMENTAL METHODOLOGY

6.1. Material Preparation

6.1.1. Epoxy Resin System

The properties of the resin system suitable for solvent-type prepregs in composite applications are presented in Table 6.1. The solvent of epoxy between 10% and 20% can be added to the resin system, depending on the amount of CNT and prepreg process.

Table 6.1. The properties of the resin system suitable for solvent-type prepregs in the presented study

Name	F-RES 21 (Epoxy) / F-HARD 22 (Hardener)
Weight fraction (wt. %)	100/21
Viscosity (mPa.s)	500-800 (at 25 °C)
Gelation Time	80 °C: 30 minutes
Prepreg curing at three different schemes (4-layer of 245g/m^2 carbon fiber reinforcement)	10 hours at 90 °C 35 minutes at 120 °C 20 minutes at 150 °C
Tensile Strength after curing	80 MPa
Tensile Modulus after curing	3.3 GPa
Supplier	FİBERMAK Composites

6.1.2. Single Wall Carbon Nanotubes (SWCNTs)

When embedded into a resin system, well-dispersed SWCNTs create a 3D reinforced and conductive network that provides improved mechanical and thermal properties and has minimal effect on the other properties of the final product. Properties of SWCNTs which is the highest purity on the market are listed in Table 6.2.

Table 6.2. The properties of pure SWCNTs used in the presented study

Name	High purity TUBALL™ graphene nanotubes
CNT content (wt. %)	≥80
Number of layers of CNT	1
The outer mean diameter of CNT (nm)	1.6 ± 0.4
Length of CNT (mm)	>5
Metal impurities (wt. %)	≤15
Moisture (wt. %)	<5
Length-to-diameter ratio	10^3–10^4
Surface area (m^2/g)	1000
G/D ratio	>90
Supplier	TUBALL™

6.1.3. Carbon Fiber (CF)

The properties of the continuous CF reinforcement used in this research are given in Table 6.3.

Table 6.3. The properties of the continuous CF reinforcement used in the presented study

Name	A-42 Carbon Fiber
Description	Continuous Carbon Fiber Reinforcement
Filament	12K
Tensile Strength (MPa)	4200
Tensile Modulus (GPa)	240
Strain (%)	1.8
Density (g/cm^3)	1.78
Yield Tex (g/1000m)	800
Supplier	AKSACA™

6.2. Sample Preparation

6.2.1. Neat Epoxy Resin Sample

Neat epoxy resin systems were prepared using a mechanical mixing method, shown in Figure 6.1. For the chemical reaction to take place smoothly, the resin and hardener must be homogeneously dispersed in the mixture. This situation depends on good mixing. In mixtures that are not made homogeneously, curing problems occur in local areas or all areas. The mixing ratios belonging to the type of resin used must be

strictly observed. The mixture was stirred for 15 minutes at a rate of about 1500 rpm, using IKA Eurostar 20. Finally, resin system samples were degassed in a vacuum oven for 15 minutes at 50 °C.

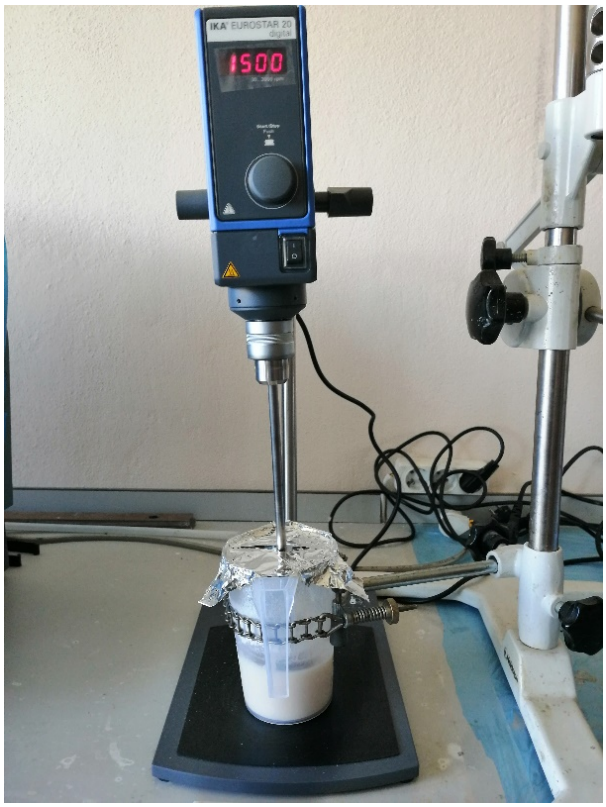

Figure 6.1. The mechanical high-speed mixing setup for preparing neat epoxy resin system

6.2.2. Epoxy Resin Sample Containing SWCNTs

6.2.2.1. Acid Functionalization of SWCNTs

The solution containing 15 mL H_2SO_4, 5 mL HNO_3 and 0.1 g SWCNT was sonicated for 2 hours. As a next stage, the solution was kept in the fume hood for 15 hours. Then, 5 mL HCl was added to the solution and shaken slowly. Thereafter, 60 mL

NH_4OH was slowly poured into the mixture until the completion of the gas release. This step was aimed to neutralize it. The pH value of the mixture is expected to be around 7. After neutralization, the solution was vacuum filtered using 0.2 µm cellulose acetate filter paper (Figure 6.4). An amount of distilled water was added to the mixture by observing pH in the range of 5.5-6. The obtained solution was mixed by a mechanical stirrer at 2000 rpm and filtered again. After completion of the chemical functionalization stage, SWCNTs were dispersed in acetone to remove any residuals by using sonication for 30 minutes. The final product was dried in the oven for a night at 50 ^{o}C. As a result of the treatment process, dry functionalized SWCNTs (F- SWCNTs) were obtained as a powder form (Figure 6.5). The schematic illustration of the processes is given in Figures 6.2 and 6.3, respectively.

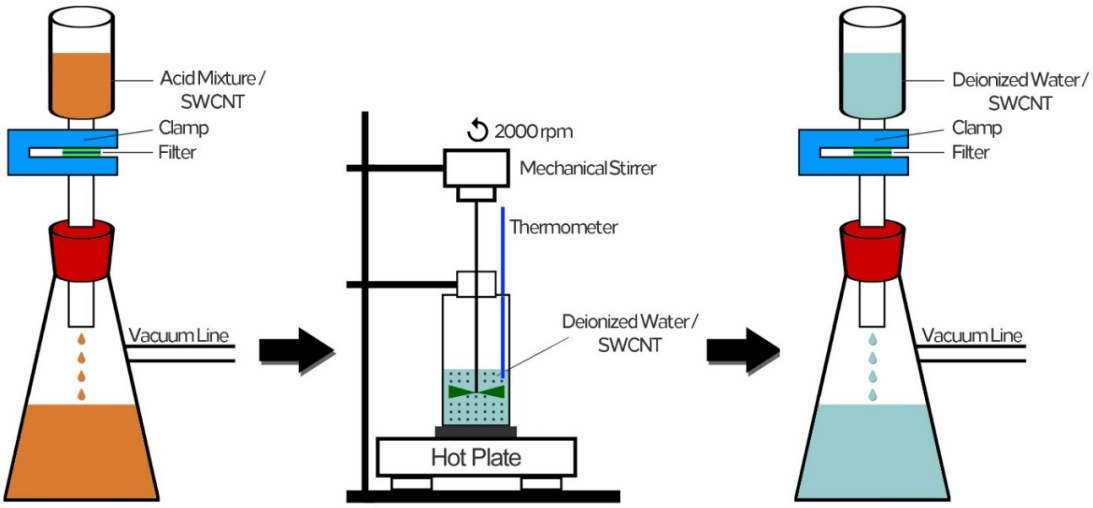

Figure 6.2. Schematic illustration of the vacuum filtration stage of functionalized SWCNTs

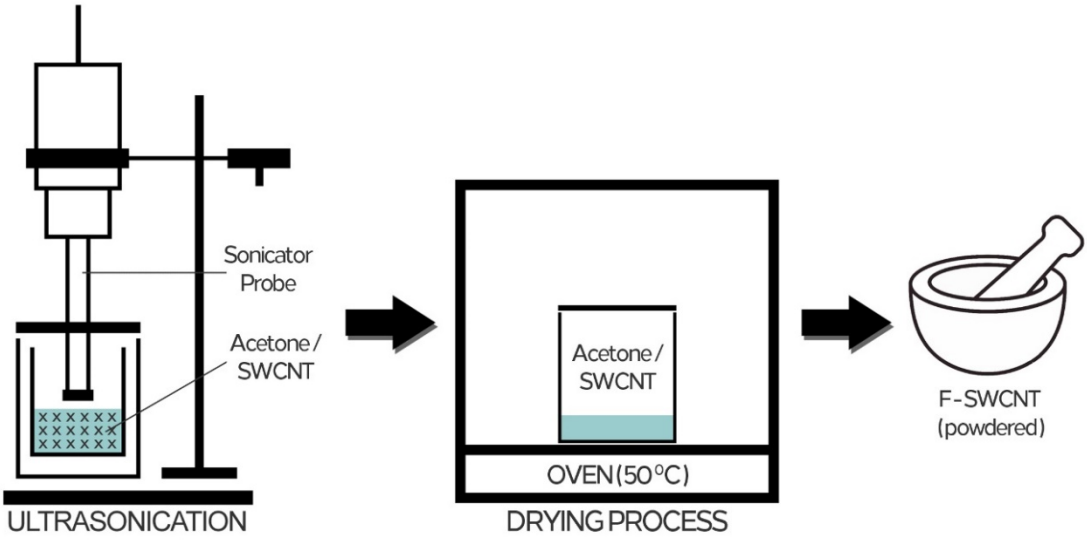

Figure 6.3. Schematic illustration of drying processes of functionalized SWCNTs

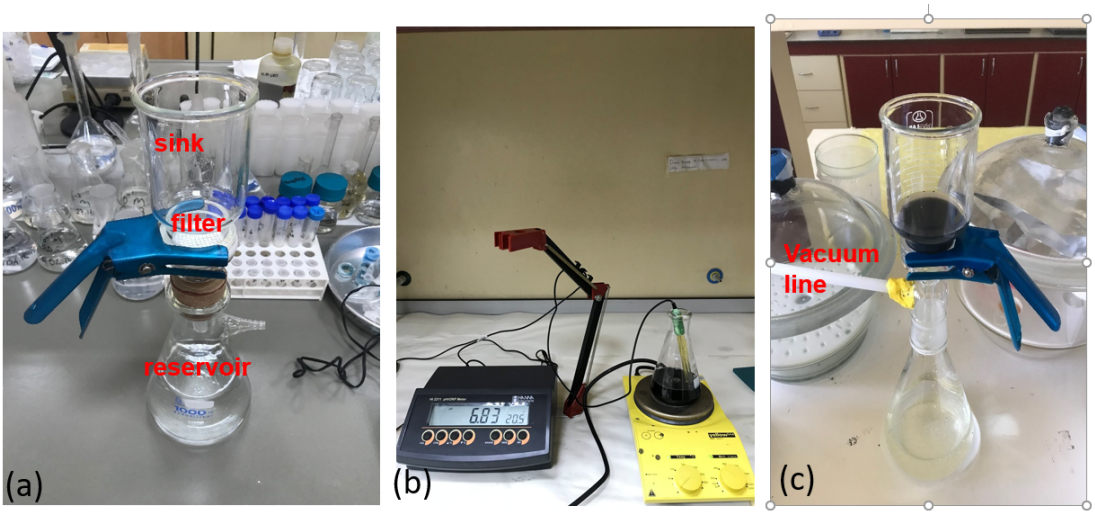

Figure 6.4. Steps of acid treatment, (a) vacuum filtration setup, (b) neutralization of the solution, (c) vacuum filtration using 0.2 µm cellulose acetate filter paper

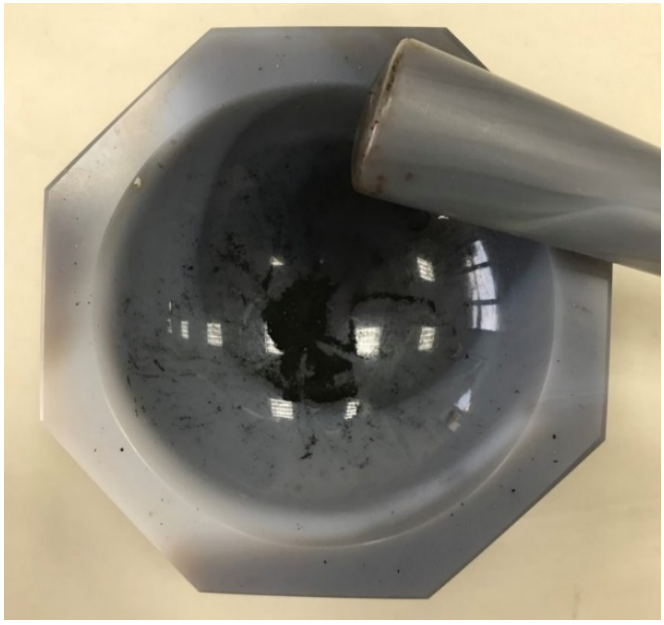

Figure 6.5. Powder of F-SWCNTs after drying process

6.2.2.2. Dispersion of Functionalized SWCNTs within Resin System

Physical methods were applied for dispersing F-SWCNTs within the epoxy resin system, as schematically illustrated in Figure 6.6. In the first stage, F-SWCNTs were sonicated in the solvent (F-Prepreg) of the resin system for 15 minutes. Then, the solution was poured into epoxy resin (RES-21) and mixed by ultrasonication technique for 90 minutes. After the addition of the hardener, all the components of the resin system were mixed mechanically at 2000 rpm for 15 minutes. The un-modified resin system contained epoxy (RES 21), hardener (21 wt.% of epoxy), and its solvent (10 wt.% of whole resin system). Since the added F-SWCNTs would affect the viscosity of the resin system, a parametric study was carried out by adding 10% (neat), 12% (0.05 wt. % F-SWCNT), 14% (0.1 wt. % F-SWCNT), and 16% wt. (0.2 wt. % F-SWCNT) of solvents, respectively. Finally, a modified resin system containing F-SWCNTs was ready for nano-engineered prepreg fabrication.

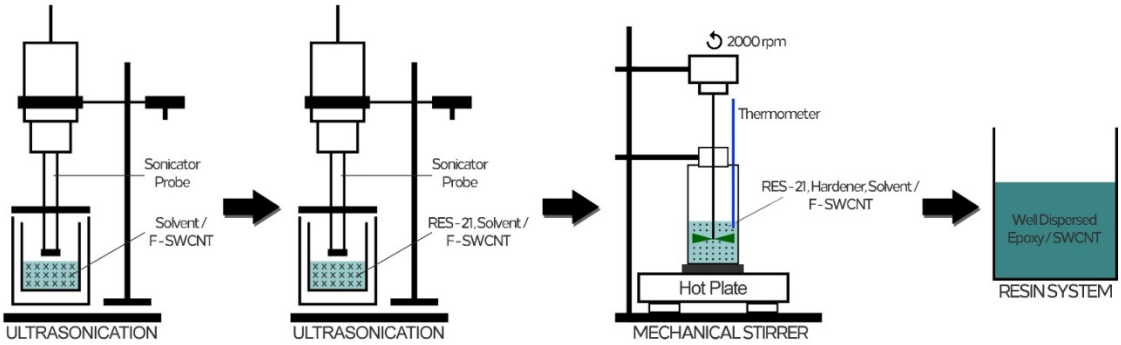

Figure 6.6. Schematic presentation for dispersion of functionalized SWCNTs within epoxy resin system

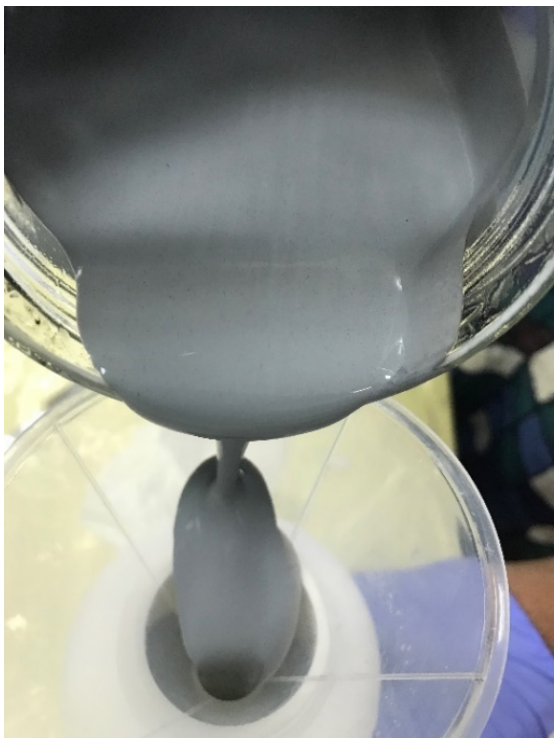

Figure 6.7 Epoxy resin system containing 0.025 wt.%. F-SWCNT

6.2.3. Preparation of Prepregs with/without SWCNTs

6.2.3.1 Drum-type Winding

Filament winding is a manufacturing technique mainly used to produce open (cylinders) or closed-end structures (pressure vessels or tanks). The filament winding technique is typically a low-cost, efficient manufacturing process used in the mass production of fiber-reinforced composite components, typically with a sophisticated machine and software system. This process involves winding the filaments under tension on a rotating mandrel. As the mandrel rotates around the rotation axis, the pay-out eye on a carriage passes horizontally concerning the axis of the rotating mandrel, placing the filaments in the desired pattern or angle. The desired pattern per circuit is applied on the mandrel while impregnated in a bath with resin (Figure 6.8). The hoop pattern, in which the winding angle is 90°, creates UD products. After the mandrel is completely wrapped to the desired thickness, the resin curing stage is reached. Depending on the resin system and curing properties, usually the rotating mandrel is placed in an oven. The filament winding machine was modified by utilizing a solvent dip (solution impregnation) method using modified F-SWCNTs dispersed within the epoxy resin system and carbon filaments. The prepreg system was controlled by the fiber feeding mechanism, and the rate of rotation of the mandrel in the control unit (Figure 9). This production method is also known as drum-type prepregging. Fundamentals of the winding machine are shown schematically in Figure 6.8. The resin system was prepared as described in the material section. The tensioned continuous fiber tows were passed feeding mechanism through a resin bath before hoop winding over a mandrel, which was covered by a release layer (Figure 6.10-12). Approximately 750-850 grams of resin systems (resin, hardener, and its solvent) were used per production. After completion of the winding of the UD prepreg, the solvent was evaporated from the prepreg, and the resin reached B-stage using a drying oven according to the resin formulation given in the material section (Figure 6.12). Prepregs had two different sides as a dry and resin-rich side. Dimensions of the manufactured prepreg were 600 mm x 1000 mm.

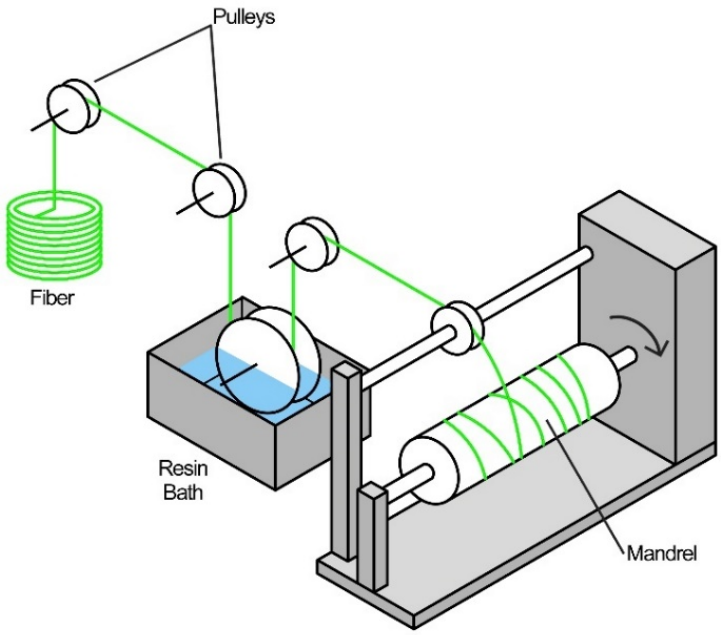

Figure 6.8. Schematic of the drum-type prepregging machine

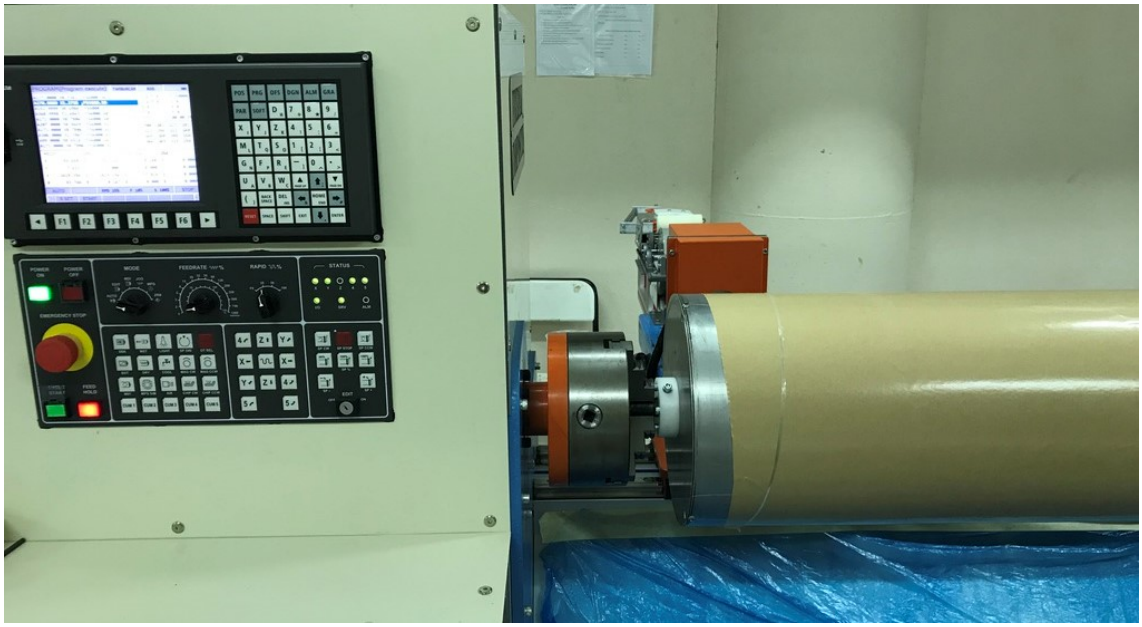

Figure 6.9. Control unit of the filament winding machine

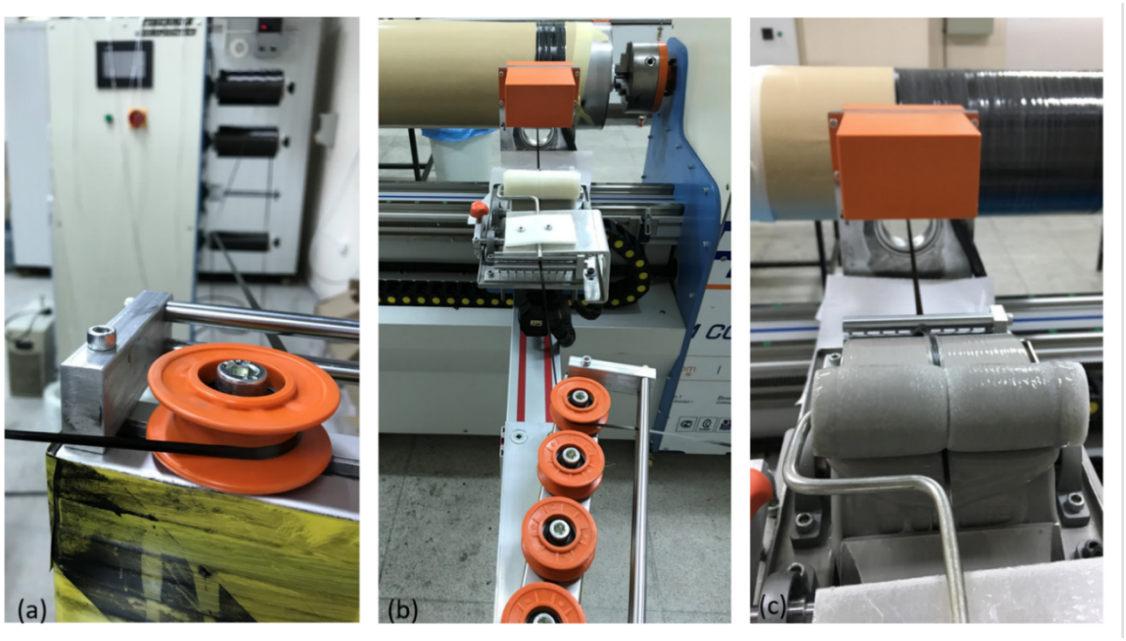

Figure 6.10. Components of the drum-type prepregging system, (a) tensioned fibers, (b) feeding mechanism, and (c) drum wheel of the resin bath

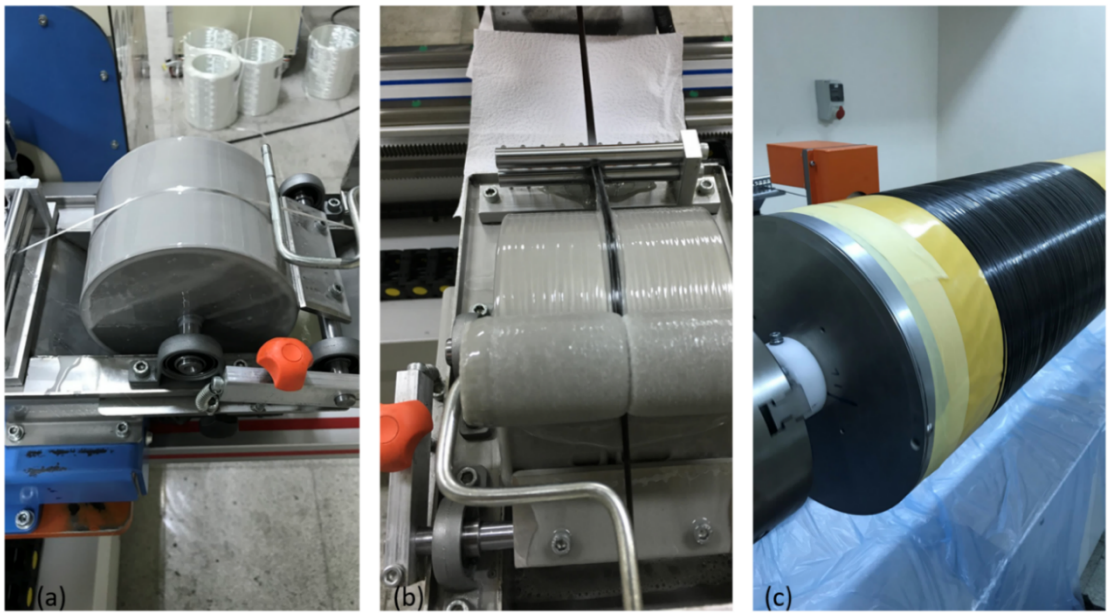

Figure 6.11 (a) Original resin bath, (b) modification by adding sponge before fibers (c) reach the mandrel

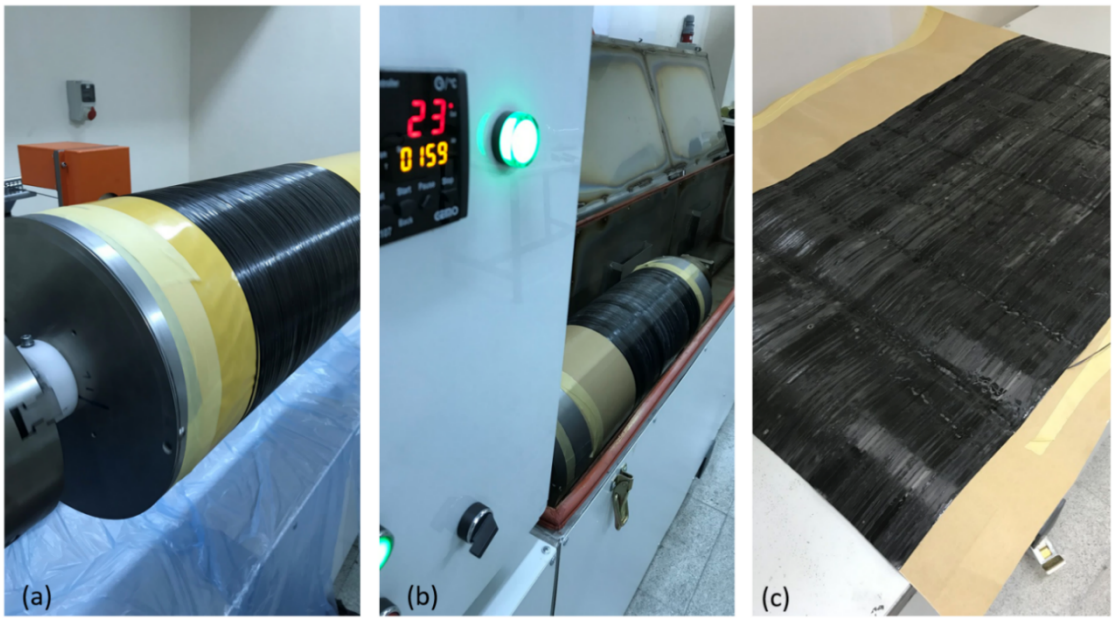

Figure 6.12. (a) Completion of the winding on a mandrel, (b) the solvent was evaporated from the prepreg using a drying oven (c) before placing in a freezer

6.2.4. Fabrication of Hybrid Composites

6.2.4.1. Vacuum-Bag-Only (VBO) Processing

UD Carbon prepregs with/without F-SWCNTs of dimensions 600 mm x 1000 mm were given an adequate one day of the freezer before processing. All the steps described in the previous chapter were applied as seen in Figure 6.13. Lamination was done by hand lay-up and stacked with six layers of 0°/90°/0°/90°/0°/90° orientations. For in-plane permeability, boundaries were kind of porous dams (fiberglass cloth) placed around the prepreg stack. For through-thickness permeability, peel plies were used to form gas pathways before and during the cure of the prepreg stack. The vacuum bag was closed to get ready for debulking time.

Before the curing process started, the air and volatiles were extracted from the bagging assembly. Uncured prepreg stack was kept at room temperature under vacuum

condition during four an hour for debulking. The temperature and pressure scheme of the curing process concerning the time is shown in Figure 14. The heating rate was 2.5 °C/min during cross-linking reactions. The dimensions of the fabricated prepreg laminate were 500 mm x 500 mm x 3 mm.

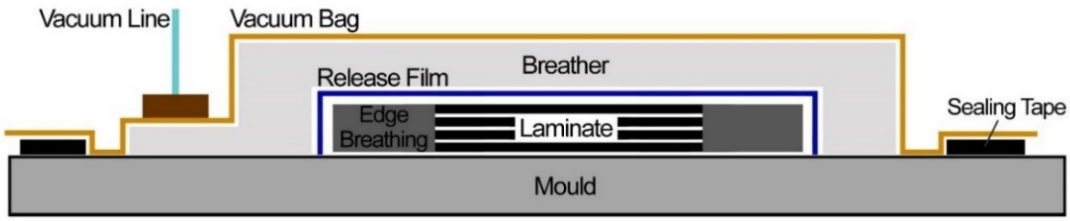

Figure 6.13. Schematic layup of the VBO technique for OoA processing

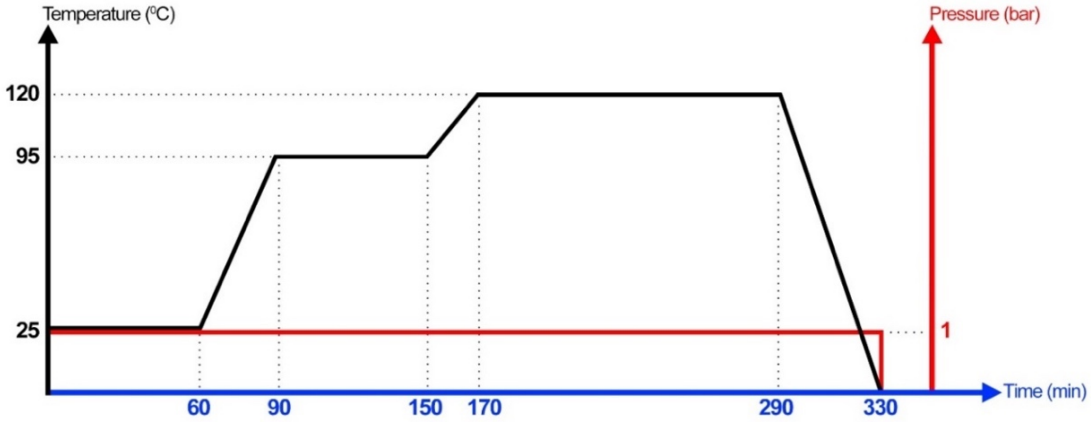

Figure 6.14. The cure cycle of the prepreg based composite in the oven

Figure 6.15. The representative vacuum bagging arrangement in a temperature-controlled oven

6.3. Characterization

6.3.1. Rheological Characterization of Epoxy Resin

The rheological behaviors of reference (neat) epoxy suspensions prepared as described in the subtitle of 6.2.1 were measured by an oscillatory rheometer (TA Instruments™) with a 25 mm parallel plate geometry and 0.5 mm sample gap. Rheological studies were carried out to select a suitable matrix material and identify optimal prepregging parameters. The viscosity changes were measured on an oscillatory rheometer (TA 300, TA instrument in Figure 6.16) using a parallel plate geometry (with 40mm flat plate and 300 μm in the gap) was used of this purpose.

Figure 6.16. Oscillatory rheometer (TA Instruments^{TM})

6.3.2. Optical Characterization of SWCNTs

6.3.2.1. Fourier Transform InfraRed (FTIR) Spectroscopy

FTIR spectroscopy was performed to determine carboxylic groups (-COOH) on the walls of powder-type SWCNTs / F-SWCNTs using the PerkinElmer Spectrum Two on transmission mode. The powdered SWCNTs with/without functionalization were collected on paper tape and placed on the measuring table (Figure 6.17). The resin samples for FTIR were prepared from the residue in the resin bath after the prepregging. One drop from the solution was placed on the measuring plate. The wavenumber range of the spectroscopy was from 4000 to 650 cm^{-1}.

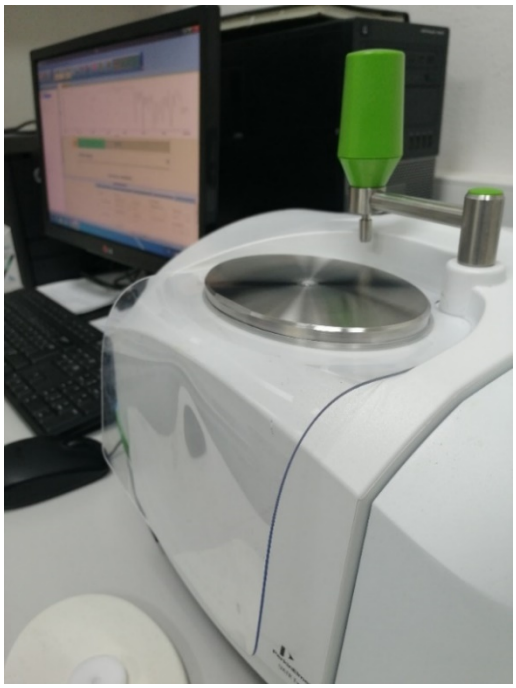

Figure 6.17. The setup of an FTIR spectrometer, PerkinElmer Spectrum Two

6.3.3. Thermal Characterization of Prepregs

6.3.3.1 Differential scanning calorimetry (DSC)

Temperature variations during curing determine the degree of cure of the prepreg system. The degree of curing is highly dependent on the heat of the reaction. The results of the DSC experiments are heat flux curves concerning time and temperature. Samples consisting of 3–6 mg mixtures were placed in aluminum pans and 50mL/min of N_2 purge in DSC 50, Shimadzu series (Figure 6.18). Dynamic scans for each sample were performed at different heating rates (2.5, 5, 10, and 20 °C/min) from room temperature up to 250 °C in an N_2 atmosphere. The upward peaks formed in the DSC thermograms show that the reaction is exothermic.

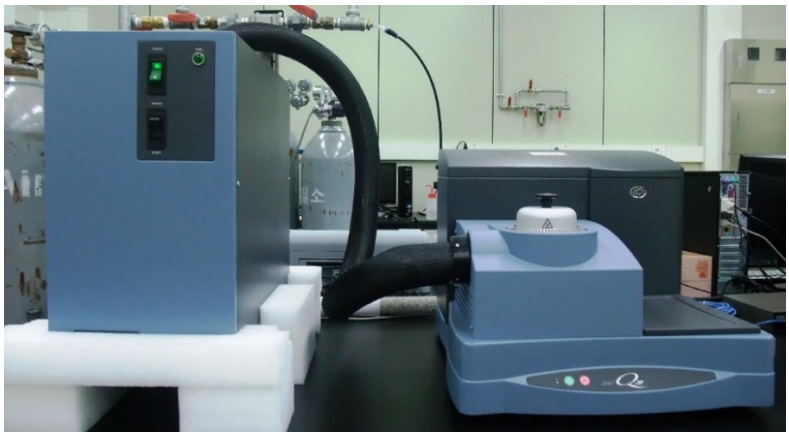

Figure 6.18. The setup of DSC, 50, Shimadzu series

6.3.4. Microstructural Characterization of Hybrid Composites

The microstructural characterization for the cross-section of the hybrid composites was investigated by Leica Optical Microscope. The cross-sectional chips of the specimens were placed into the epoxy resin to get stubs. Following mounting in stubs, the samples were ground, washed, and polished to obtain microstructure without any scratch under the optical microscope. This method provides to study the distribution of carbon fibers in the epoxy matrix.

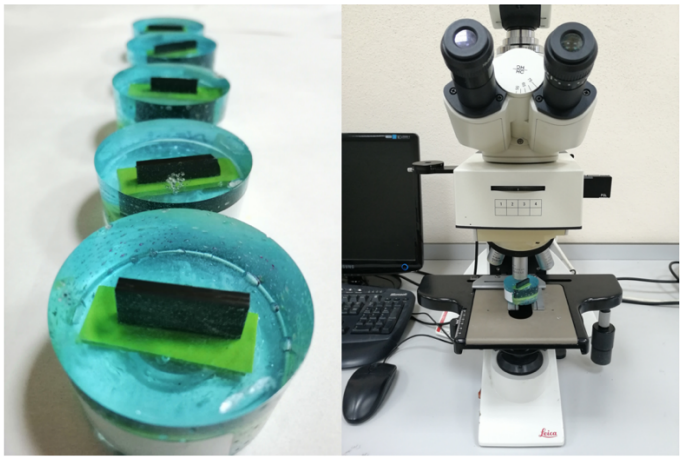

Figure 6.19. Specimens of CFRP in Epoxy Stubs and Optical Microscope

6.3.5. Mechanical Characterization of Hybrid Composites

6.3.5.1. Tensile Test

Specimens were subjected to a controlled tension until failure using a Shimadzu AGS-X Universal test machine with a crosshead speed of 2 mm/min (Figure 6.20). The tension tests were performed using at least three specimens and tensile strength, modulus of elasticity, and strain at break values was calculated. ASTM D3039 standard procedure was followed for the tensile test.

$$\sigma_i = \frac{P_i}{A} \tag{6.1}$$

where σ_i is the tensile stress at ith data point, MPa, P_i is the load at ith data point, N, and A is the average cross-sectional area, mm^2.

Figure 6.20. CFRP standard tensile test setup

6.3.5.2. Charpy Impact Test

The amount of energy absorbed by hybrid composites was evaluated. The absorbed energy levels were determined by comparing the notch toughness of the composites. The tests were performed using a falling-hammer-type Ceast™ impact tester (Figure 6.21). Charpy impact strength of notched specimens, $\boldsymbol{a_{cU}}$, expressed in kilojoules per square meter, was calculated using the following equation according to the ISO 179-1:2000 standard**:**

$$a_{cU} = \frac{E_c}{h * b_N} \times 10^3 \tag{6.2}$$

where $\boldsymbol{a_{cU}}$ is the Charpy impact strength of notched specimens, in kilojoules per square meter, E_c is the energy, in joules, absorbed by breaking the test specimen, h is the thickness, mm, of the test specimen, b_N is the remaining width after notching, mm, of the test specimen.

Figure 6.21. Charpy Impact tester

6.3.5.3. Short-Beam Shear (SBS) Test

SBS test was performed to evaluate the interlaminar shear strength (ILSS) of the hybrid composites using a Shimadzu AGS-X Universal test machine. It indicates the performance of a composite under shear-like loading conditions. For this reason, the short beam shear test is used to compare the relative performance of composites containing various filler content. The load was applied at the center of the specimen placed upon two lower supports (Figure 6.22). Short-beam strength of the specimens, $\boldsymbol{\sigma_{sbs}}$, expressed in MPa, was calculated using the following equation according to the ASTM D2344 standard:

$$\sigma_{sbs} = 0.75 \times \frac{P_m}{b\ h} \tag{6.3}$$

where $\boldsymbol{\sigma_{sbs}}$ is the short-beam strength, MPa, $\boldsymbol{P_m}$ is the maximum load observed during the test, N, $\boldsymbol{b}$ is the measured specimen width, mm, and $\boldsymbol{h}$ is the measured specimen thickness, mm.

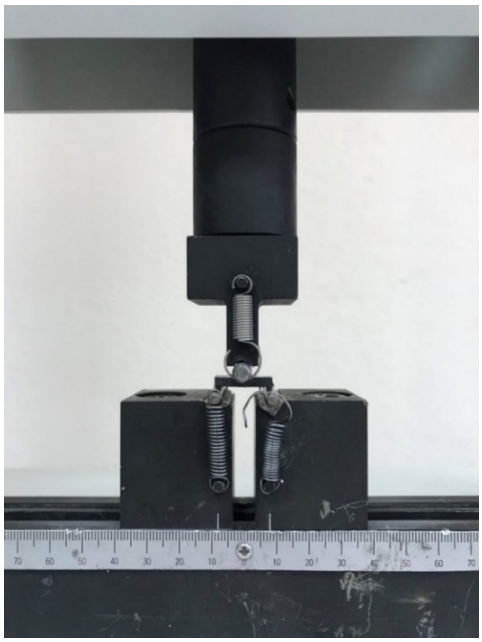

Figure 6.22. SBS specimen placed upon two lower supports

6.3.5.4. Three-Point Bending Test

Three-point bending tests were performed using Shimadzu AGS-X Universal test machine with a test speed of 2 mm/min. The three-point bending test method was used to measure the behavior of hybrid composites subjected to simple beam loading (Figure 6.23). Flexural stress of the specimens, σ_f, expressed in MPa, was calculated according to the ASTM D790 standard:

$$\sigma_f = \frac{3\,P\,L}{2\,b\,d^2} \tag{6.4}$$

where $\boldsymbol{\sigma_f}$ is the flexural strength, MPa, $\boldsymbol{P}$ is the load at a given point on the load-deflection curve, N, $\boldsymbol{L}$ is the support span, mm, $\boldsymbol{b}$ is the width of the specimen thickness, mm, and $\boldsymbol{d}$ is the depth of the specimen thickness, mm.

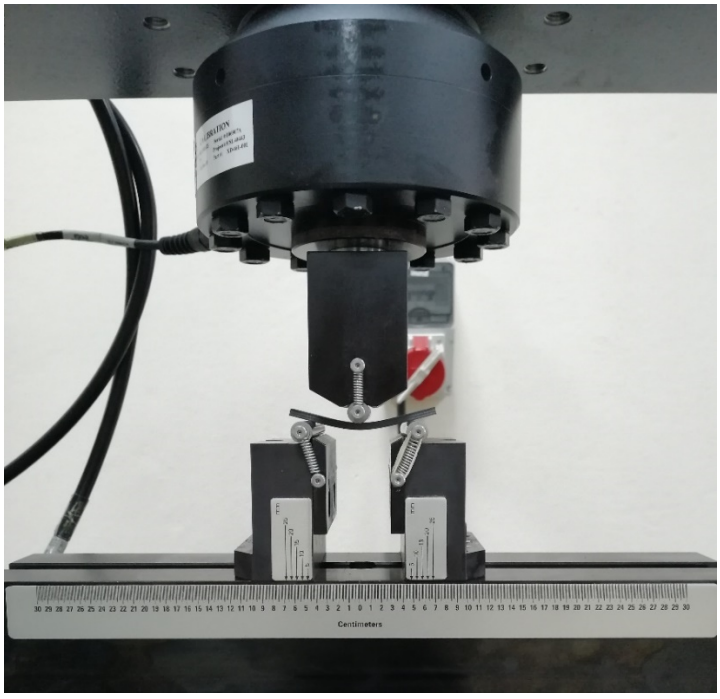

Figure 6.23. The specimen on two support anvils and bending it through applied force

6.3.6. Chemical Characterization of Hybrid Composites

Fiber volume fraction, which is the percentage of fiber volume in the entire volume of CFRP, was measured by the acid digestion method. This method consists of digesting the epoxy resin using an acid that does not affect the fibers and fillers. After digestion, the remaining fibers are washed with acetone, dried at 100 °C, and weighed (Figure 6.24). The volume fraction of both the fiber and the matrix in the laminate can be determined by knowing the initial weight of the composite sample as well as the densities of the fiber and resin. Separation of fibers from the resin was performed according to the ASTM D-3171 standard.

Figure 6.24. Fiber volume fraction determination of carbon-epoxy composites containing F-SWCNTs using an acid digestion

6.3.7. Thermomechanical Characterization of Hybrid Composites

6.3.7.1. Dynamic-Mechanical Analysis

The thermo-mechanical behavior of the samples was determined based on the dynamic mechanical analysis (DMA) method using TA™ Q800. DMA is a useful technique for calculating the storage modulus (E′), loss modulus (E″), and loss factor (tan δ) and glass transition temperature (Tg). The storage modulus shows the ability of the material to store deformation energy elastically. The loss modulus is related to the dissipated energy in the material. The loss factor is the meaning of the ratio between the loss modulus and storage modulus. Tg can be defined as the center of the glassy and rubbery states of a polymer or polymer composite. It is the peak point of the tan delta. A dynamic force was applied at a frequency of 1 Hz in three-point bending mode. The temperature was elevated from 20 to 200 C with a ramp of 5 C / min. The dimensions of specimens were set at 10 mm x 65 mm x 3 mm.

Figure 6.25. The setup of DMA, TA Instruments™ Q800

CHAPTER 7

RESULTS AND DISCUSSIONS

SEM image of pure SWCNT, which is manufactured by chemical vapor deposition (CVD), is shown in Fig. 7.1. Pure SWCNT's diameters and lengths vary of 2 nm and 5-10 μm, respectively. Due to van der Waals forces, the need for surface modification is obvious to distribute SWCNTs displayed as cluster form homogeneously in the medium.

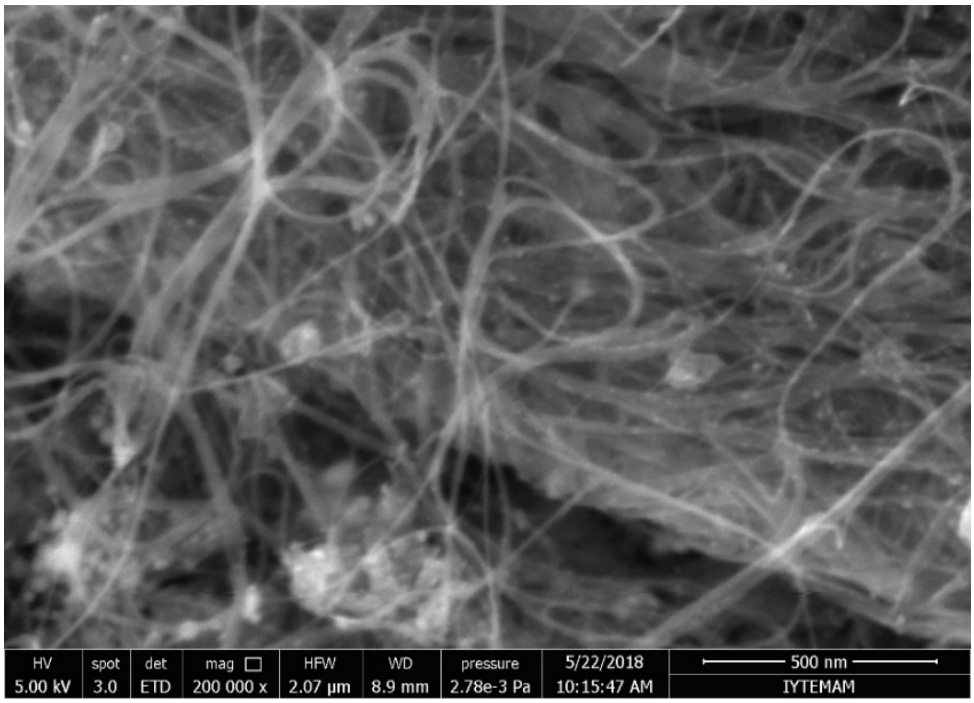

Figure 7.1. SEM images of pure SWCNTs from PİNHAS A.Ş.

7.1. Acid Treatment of SWCNTs

Functionalized SWCNTs (F- SWCNTs) were obtained through oxidizing SWCNTs in order to create carboxyl and hydroxyl groups in their surfaces. One of the disadvantages of the ultrasonication process is that it increases the temperature of the environment during the process and damages the carbon nanotubes. The shock waves that occur during sonication cause shear forces and these forces divide individual nanotubes into smaller pieces, reducing the average individual length of the CNTs. When graphene layers are destroyed, it causes a significant reduction in their mechanical properties. To prevent effect on their behavior, many studies have stated that the solution temperature should be kept below 50 °C by using cooling jackets and ice baths [1,2]. Figure 7.2 given below shows the change of the solution temperature overtime during the ultrasonication process in the presented study. Temperature variation was achieved with a thermocouple placed in the solution. In the early stages of the process, the temperature tends to rise excessively, and the temperature was kept constant around 40 °C during the process after a short time utilizing the ice bath.

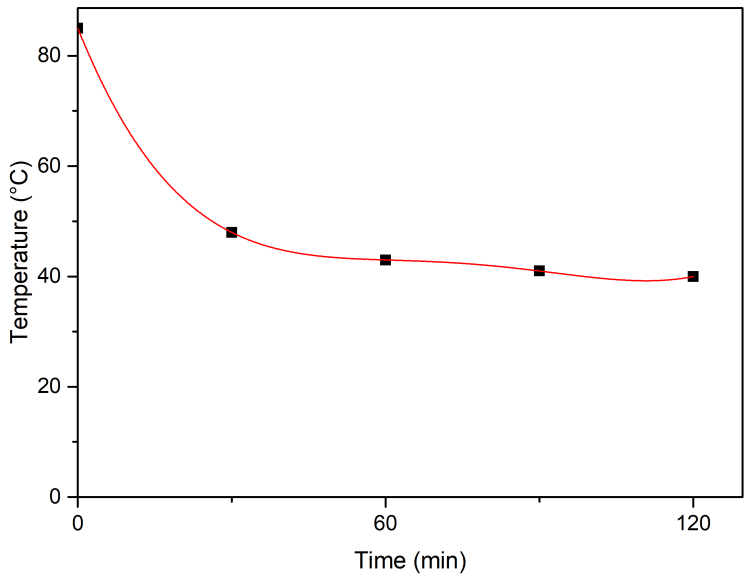

Figure 7.2. The temperature change in the acid treatment during the ultrasonication process

While ensuring the dispersion of the CNTs in the acid solution, it is aimed not to create defects in the structure of the CNTs by applying short-term ultrasonics. Ultrasonic waves were applied for two minutes on and two minutes off, to prevent both overheating and deterioration of their structures. Through the acid treatment, the pristine SWCNTs can be purified and oxidized with carboxyl, and hydroxyl groups created on the surface of SWCNTs. The oxidization of SWCNTs bundles provide increasing the solubility of SWCNTs in polar media and is more easily incorporated in an epoxy resin. To avoid agglomeration, the presence of functional groups (carboxyl, and hydroxyl groups) at the sidewalls of SWCNTs is useful for dispersing homogeneously. It can provide homogeneous distribution for a long time by providing electrostatic stability in the solution [3].

Figure 7.3 represents the first view of dispersibility of pristine (a) and F-SWCNTs (b) in water after 2 hours of ultrasonication. Figure 7.4 shows the dependency of dispersibility of pristine (left) and F-SWCNTs (right) in water as a function of time after 1-hour (a) and 2-hours (b).

After the success of the dispersion of functionalized SWCNTs in water was observed, a small sample was taken and kept in the fume hood to check for a longer time. After dispersed in water (left), the first precipitates (agglomerations, right) in solution after about 3 months was shown in Figure 7.5.

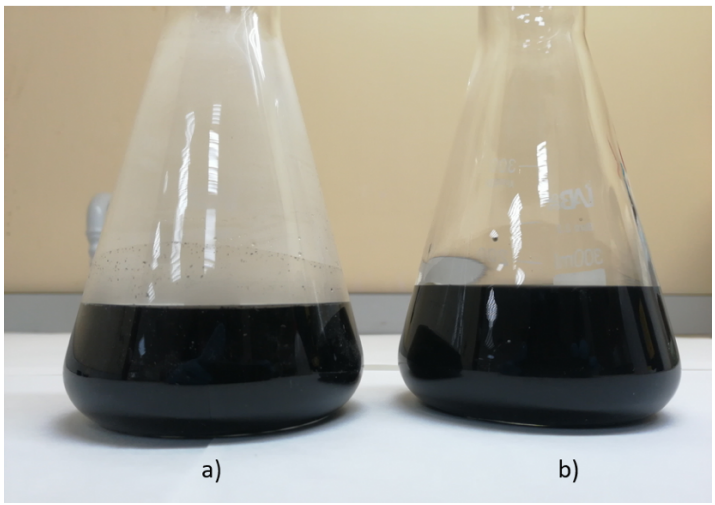

Figure 7.3. The image of dispersibility of (a) pristine and (b) F-SWCNTs in water after 2 hours of ultrasonication

Figure 7.4. Images of pristine (un-modified) and functionalized F-SWCNT /epoxy sonicated after 2-hour preparation stage. (left) Pristine SWCNTs/epoxy, (right) 0.05wt. % F-SWCNTs

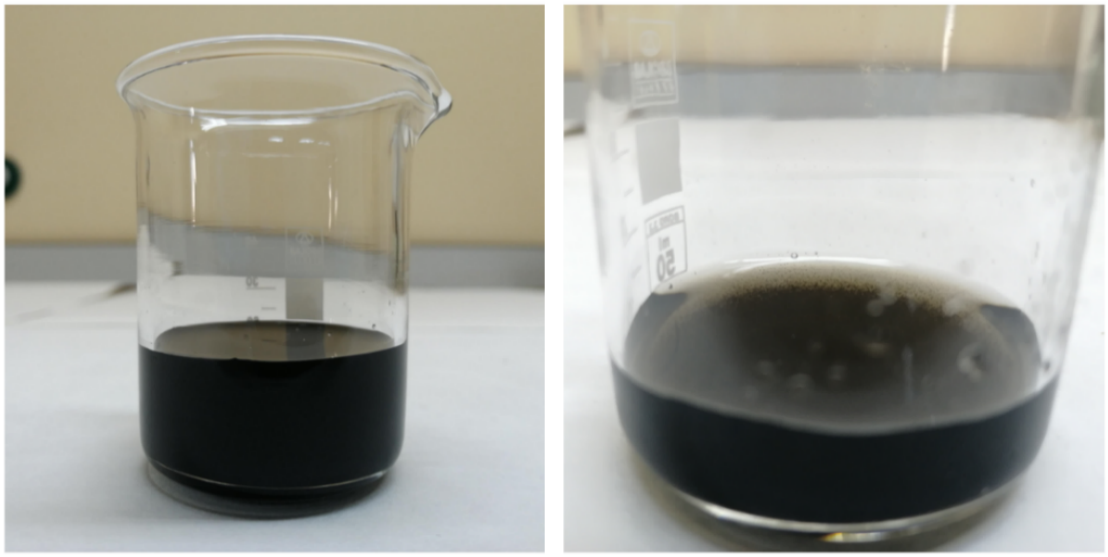

Figure 7.5. Images of functionalized F-SWCNT /epoxy after three months. (left) First-day view, (right) The precipitates (agglomerations,) in solution after about 3 month

7.2. Dispersion of F-SWCNTs within Epoxy Resin System

The stability of the mixture was checked before prepregging by incorporating the functionalized carbon nanotubes into the epoxy resin. A visual test is performed on a macro-scale, observing well-dispersed samples. Several samples were collected during the multi-step mixing process. By use of the combination of the different techniques, the well-dispersed sample was obtained. This technique is a model that there are no visible clouds of agglomeration in it and the mixture is homogeneous on the macro scale. The appearance of functionalized SWCNT (F-SWCNT) /epoxy blends after preparation as presented in the experimental section is shown in Figure 7.6. The samples were also used for rheology, DSC, and FTIR analysis.

To monitor the success of incorporating functionalized carbon nanotubes into epoxy resin, they were subjected to the same mixing steps with the pristine samples. After a short time, an amount of 0.025 wt. % pristine SWCNT /epoxy system resulted with the agglomerates of the carbon nanotubes formed by the effect of Van der Walls forces, while stable dispersion of various amounts of F-SWCNTs within the epoxy resin was observed, as shown in Figure 7.7, b-d.

Figure 7.6. The image of functionalized SWCNT (F-SWCNT) /epoxy blends after preparation as presented in the experimental section

Figure 7.7. Images of pristine (un-modified) and F-SWCNT /epoxy blends after 1-hour preparation stage. (left) Pristine SWCNTs/epoxy, (right) 0.05, 0.1, and 0.2 wt. % functionalized F-SWCNTs/epoxy blends, respectively

The most important factor in achieving the superior performance of composites carbon fiber reinforced by incorporating CNT is the homogeneous distribution of nano-fillers in any solvent and matrix system and the protection of the stabilization of this distribution. The presented study provided homogeneity of well-dispersed samples for prepregging by minimizing agglomeration of the distribution of F-SWCNTs in the epoxy resin using multi-step dispersion techniques.

7.3. Rheological Behavior of Neat Epoxy Resin

Viscosity is the most important parameter for preparing prepregs to achieve good wetting of fibers. Siddiqui et al. noticed that viscosity must be between 1.5 – 2.5 Pa.s for processing. Also, it has been made very clear that high mixing speeds are an effective parameter in preventing CNTs from agglomerating. In the presented study, rheological characterization was performed to the neat epoxy samples mixed at 1500 rpm, considering these important inferences. Samples were obtained by adding 10% wt. solvent into the epoxy resin with the recommendation of the manufacturer was subjected to rheological tests. As can be seen in Figure 7.8, the viscosity changes of the neat sample against temperature were obtained. It shows that the resin systems being approximately

40 °C during the prepreg process will ensure that it coincides with the specified viscosity range.

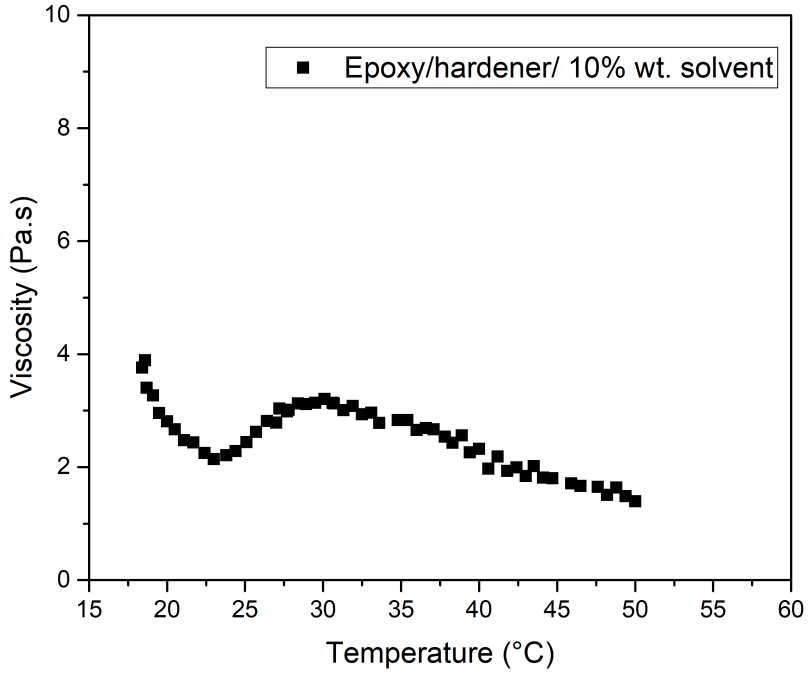

Figure 7.8. The effect of temperature on viscosity of the neat epoxy resin

Therefore, the solution was stirred on the hot plate at the desired temperature. Since the added F-SWCNTs would affect the viscosity of the resin system, a parametric study was carried out by adding 10 wt.% (neat), 12 wt.% (0.05 wt. % F-SWCNT), 14 wt.% (0.1 wt. % F-SWCNT), and 16 wt.% wt. (0.2 wt. % F-SWCNT) of solvents, respectively. For future studies, the effect of the amount of solvent to be added on the viscosity ranges for F-SWCNTs of different variations should be investigated.

7.4. FTIR Spectra of SWCNTs and F-SWCNTs

FTIR analysis were performed for the investigation to characterize the functional groups created on carbon nanotubes. The FTIR spectroscopy studies show the identification of the functional groups on the walls of SWCNTs because of

functionalization. The FTIR was performed using two types of samples: pristine SWCNTs and functionalized F-SWCNTs. FTIR spectra from pristine SWCNTs show a peak at around 2000 which refers to the backbone of the pristine SWCNT, as seen in Figure 7.9. The strong peak of SWCNTs backbone is reduced in functionalized SWCNT spectra. It means, the structure of carbon bonds has been broken and added new functional (polar) groups utilizing functionalization.

The FTIR spectra of the functionalized F-SWCNTs are presented in Figure 7.10. Peaks between 2600 and 3700 cm^{-1} are the characteristics of C-H vibrations and O-H bonds. These peaks can be related to the carboxylic groups (-COOH). Absorption bands in the range between 1600 and 1800 cm^{-1} are the characteristics of the C=O bond type from carbonyl and carboxyl groups. The presence of C-O bond type from alcohol and carboxylic acids is observed around 1000-1250 cm^{-1}. Moreover, peaks between 900 and 1400 are related to the O-H, and around 680-880 cm^{-1} are related to the C-H bonding type. Acid treatment of SWCNT with a combination of HNO_3 and H_2SO_4 indicated successful oxidation of SWCNTs. So, the new chemical bonding groups are identified after the functionalization of SWCNTs, and these groups are expected to improve the extend of dispersion of the SWCNTs within the liquid resin.

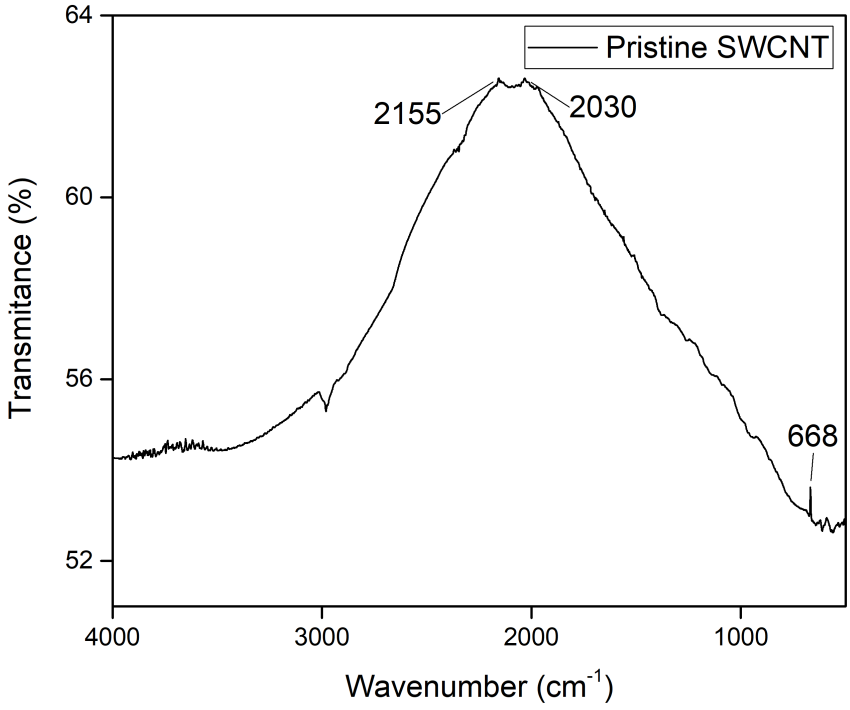

Figure 7.9. FTIR Spectra of Pristine SWCNTs

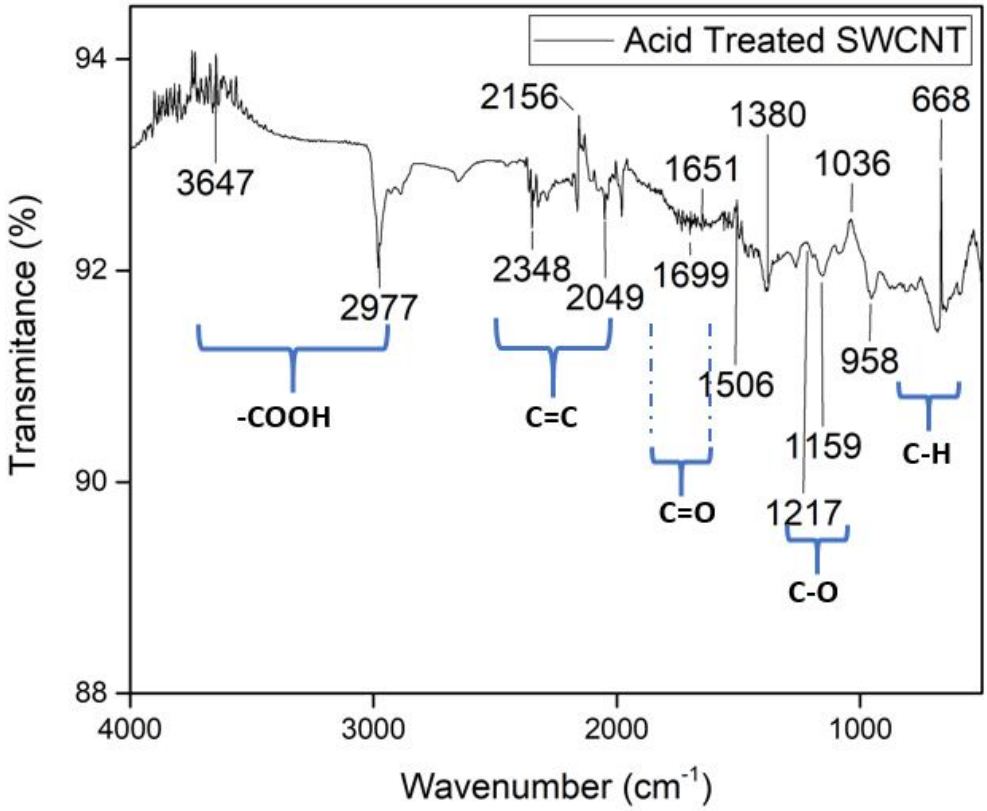

Figure 7.10. FTIR Spectra of Functionalized F-SWCNTs

Figure 7.11 shows the FTIR spectra of the neat epoxy, and it blends. As the amount of SWCNTs in the blends were small, no distinct difference in the spectra was observed. However, the effect of the epoxy matrix is realized by increasing the transmittance values. The transmittance values were around 99% with the added epoxy while it was 93% with powder F-SWCNT. There are no insignificant changes in transmittance values observed with F-SWCNTs added in different variations.

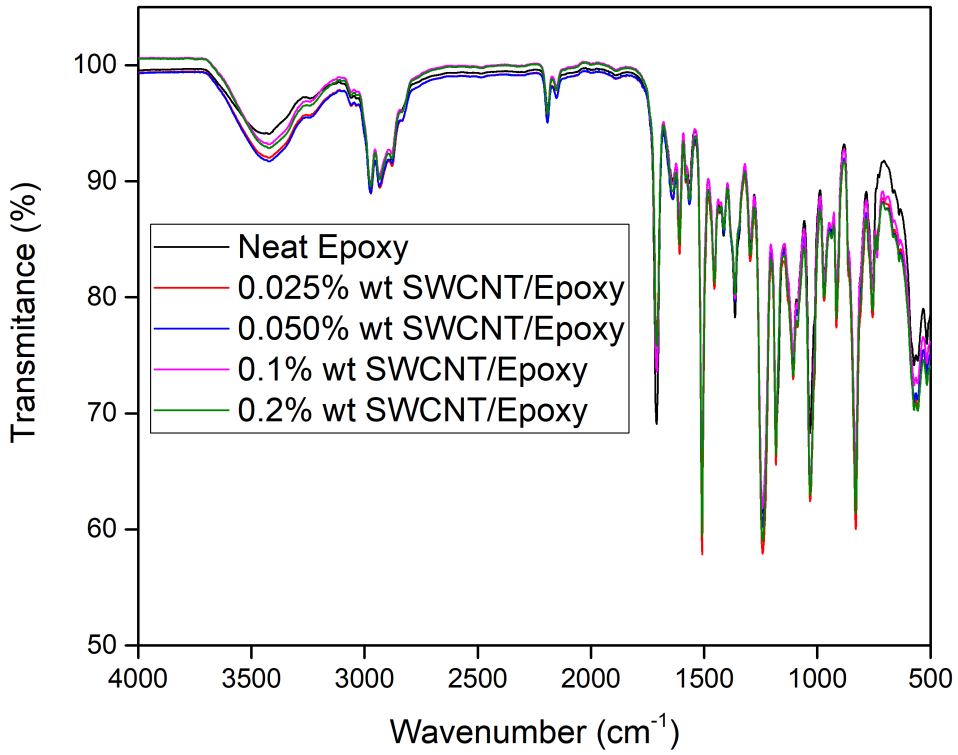

Figure 7.11. The FTIR spectra of the epoxy resin containing various amounts of F-SWCNTs

7.5. Thermal Properties and Curing Behaviors of Prepregs with/without F-SWCNTs

The non-isothermal curing reaction of carbon fiber/epoxy-based prepregs with/without F-SWCNTs as a function of the curing temperature was shown in Figure 7.12 at different heating rates. Only one exothermic peak has risen in the temperature range for all prepreg types, (a)-(d). Since thermal degradation peaks were observed on polymer after 250 °C, the graphs were cut from this point. Therefore, the area above the peak at the exothermic reaction was used to measure the reaction enthalpy (the total heat of reaction) by using OriginPro.

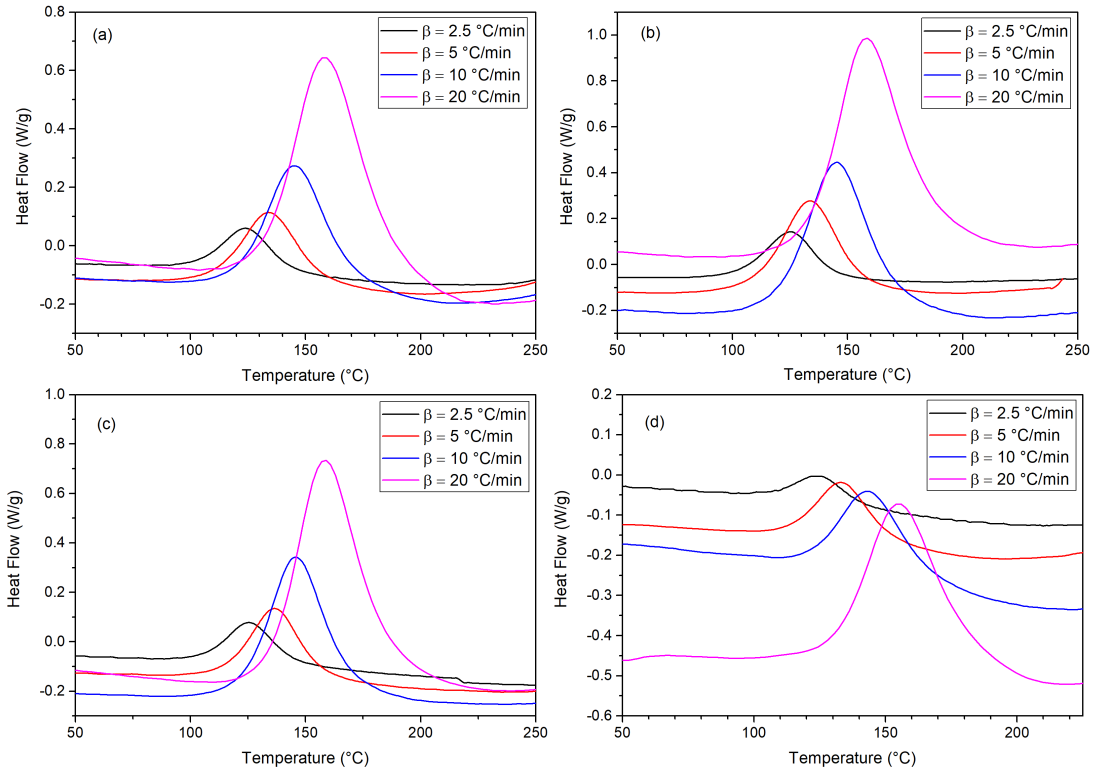

Figure 7.12. Non-isothermal curing DSC curves for different prepreg systems, containing (a) 0.0 wt. % (neat) (b) 0.05 wt. % (c) 0.1 wt. % and (d) 0.2 wt. % F-SWCNTs at different heating rates

Onset temperature (T_{onset}), the peak temperature (T_p), offset temperature (T_{offset}), and reaction enthalpy (ΔH) were obtained and listed in Table 1. The temperature at which the curing starts is very important to create hybrid composites from the prepared prepregs. As seen in the table, the T_{onset} temperature of prepregs varies around 100 °C according to the amount of SWCNTs included. With the increase in heating rate, the exothermic peak shifted to the right. T_{onset}, $T_{p,}$ and T_{offset} temperatures also increased with the increase of heating rate. It is shown that the T_{onset} of the curing reaction was lower for slower heating rates. The lower heating rate allows enough time for more chemical groups to be involved in the reaction. Moreover, the enthalpy almost kept constant within about ±5%. with the increase of the heating rate. One of the important parameters is that the calculated reaction enthalpy depends strongly on the type of baseline used. Small differences may be due to the choice of baseline and thermal degradation at higher heating rates.

Table 7.1. Onset temperature, the peak temperature, offset temperature, and reaction enthalpy

Sample	β (°C/min)	T_{onset} (°C)	T_p (°C)	T_{offset} (°C)	ΔH (J/g)
Neat	2.5	105.2	123.8	139.8	43.63
	_5	116	133.1	149.1	46.76
	_10	121.3	143.2	164.7	44.05
	_20	134	155.1	178.6	45.86
	Average				45.07
0.05 wt.% F-SWCNT	_2.5	105.4	124.1	140.7	97.58
	_5	111.6	133.8	153.6	97.54
	_10	121.2	145.2	168.6	94.04
	_20	133.6	158.2	185.1	95.17
	Average				96.08
0.1 wt.% F-SWCNT	_2.5	101.8	125.1	141.1	146.26
	_5	109.5	133.9	151.1	150.98
	_10	119.8	145.2	169.3	146.22
	_20	134.8	158.5	186.3	138.08
	Average				145.38
0.2 wt.% F-SWCNT	_2.5	104.7	125.3	146.7	113.07
	_5	112.8	136.5	157.3	110.73
	_10	122.8	145.2	167.2	114.33
	_20	138	158.5	184.7	108.16
	Average				112.25

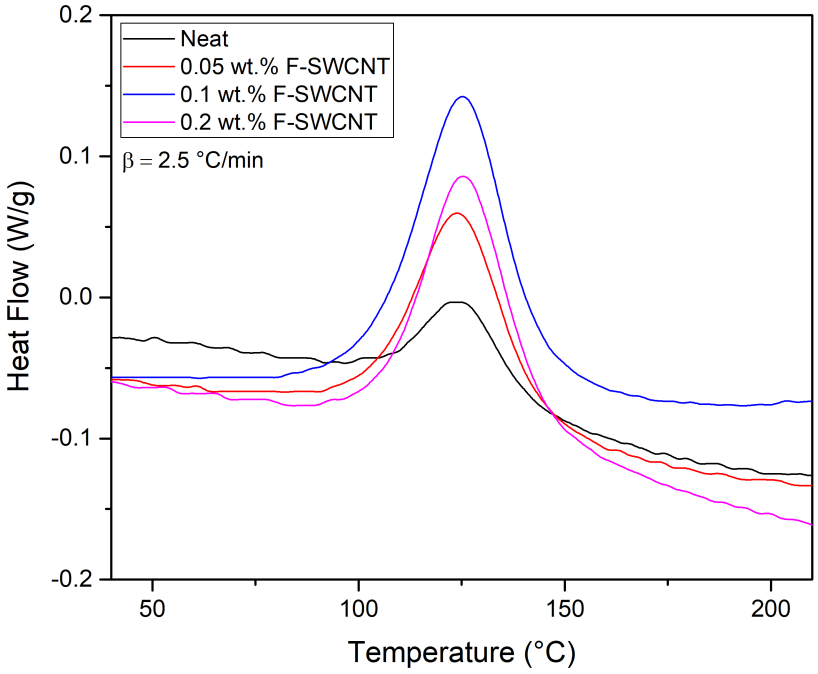

Figure 7.13. Non-isothermal curing DSC curves for various F-SWCNTs content at 2.5 °C/min

Compared to the CF/neat epoxy prepreg, the curing heat of 0.05 wt. and 0.1 wt. % F-SWCNT systems significantly increased (Figure 7.13). The reason for this may be that the presence of the solvent (F-Prepreg) of the resin system causes a decrease in viscosity which increases the mobility of the reactive species and results in a higher heat of reaction. Choi et al. have already reported similar results. They found that the incorporation of pure and functionalized carbon nanotubes (azomethine ylide groups) into an epoxy matrix led to a shift of the peak temperature to higher values. In addition, an increase of enthalpy and activation energy values was observed, reflecting its influence on the curing reactions. However, it was observed that the tendency for rising the curing heat disappears as the content of F-SWCNTs is above 0.1 wt.%. This decay on the heat of reaction at 0.2 wt.%. content of F-SWCNT may associate with the non-homogeneous dispersion and the formation of CNT agglomerations at high contents. The CNT agglomerations in the matrix system may cause an increase in viscosity by neutralizing the solvent which lowers the mobility of reactive species.

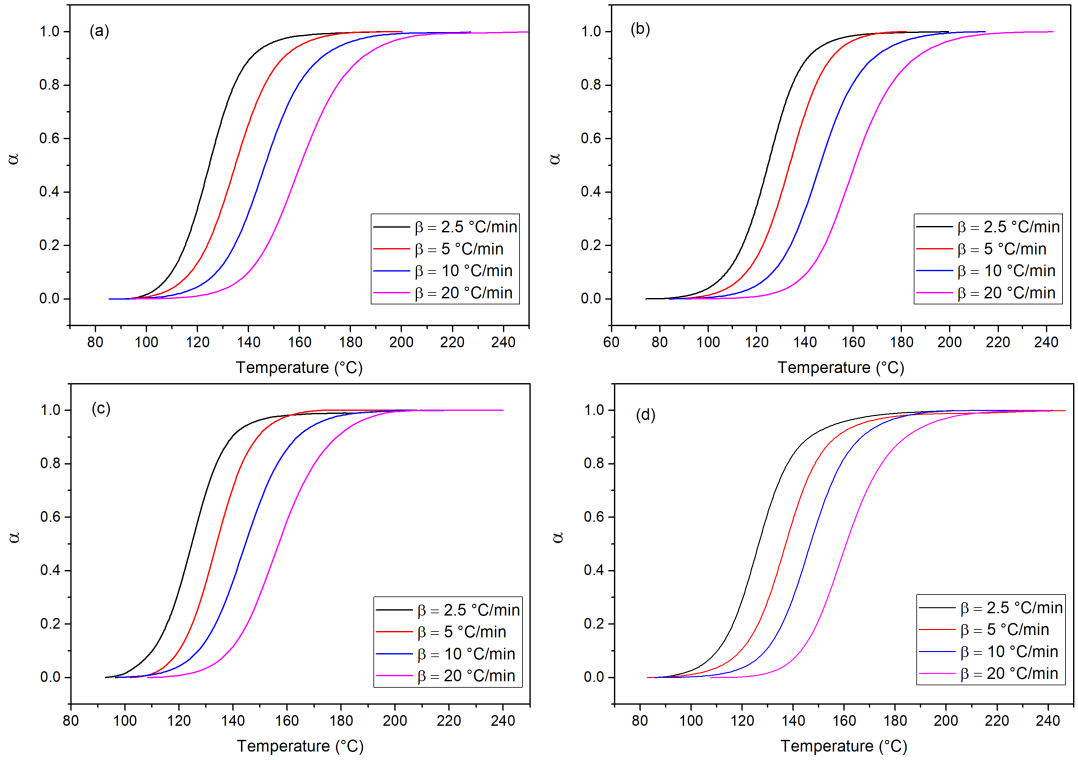

Figure 7.14. Temperature dependent degree of cure (conversion) for different prepreg systems, containing (a) 0.0 wt. % (neat) (b) 0.05 wt. % (c) 0.1 wt. % and (d) 0.2 wt. % F-SWCNTs at different heating rates.

Figure 7.14 shows the conversion vs. the temperature for various prepreg systems at various heating rates. The degrees of conversion have been obtained by integration of the exothermal calorimetric peak employing Eq. (2.2). These plots displayed a typical sigmoidal profile characterized by a slow increase of α value at the beginning and the end of the reaction and a high increase of α at the intermediate stage. During the initial stage, although the curing rate is slow, there is a short time before the resin reaches the gel temperature. Along with the transformation into the gel state, the reaction rate increases rapidly, the maximum velocity corresponds to the peak heat flux. During intermediate time points, crosslinking degree of the network structure advances, and the resin transforms gradually into a glassy state. With the increased crosslinking degree, the curing rate decreases. In the last stage, when the curing degree reaches its maximum value, the curing rate decreases because of high viscosity.

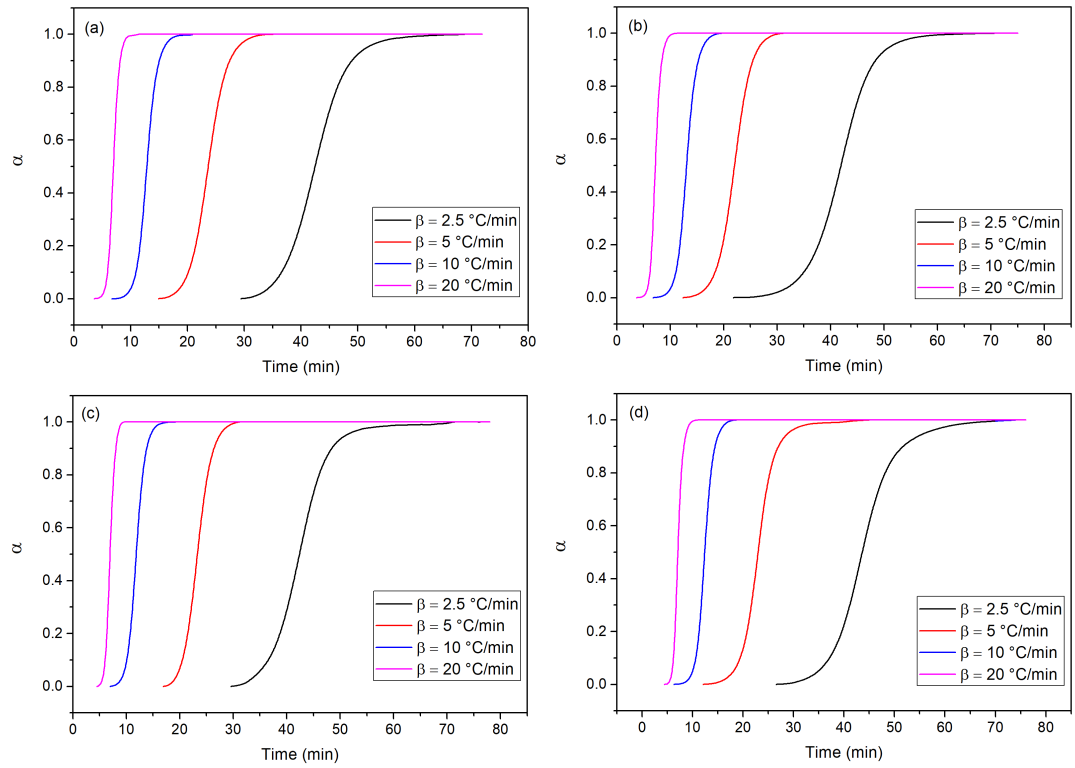

Figure 7.15. Time dependent degree of cure (conversion) for different prepreg systems, containing (a) 0.0 wt. % (neat) (b) 0.05 wt. % (c) 0.1 wt. % and (d) 0.2 wt. % F-SWCNTs at different heating rates.

Figure 7.15 presents the degree of conversion vs time plots at different heating rates for neat epoxy resin. At low heating rates, more time was available for the network to develop; hence, the peak temperature for the reaction conversion was the lowest. Dynamic DSC determination often leads to a sigmoidal form of conversion-temperature curves being observed indicating an autocatalytic kinetic in almost all studied systems. As illustrated in Figure 7.16, the addition of F-SWCNTs does not change the type for an autocatalytic cure reaction mechanism of the CF/epoxy prepreg system. It shows that the curing reaction becomes gentler, and the reaction rate is accelerated.

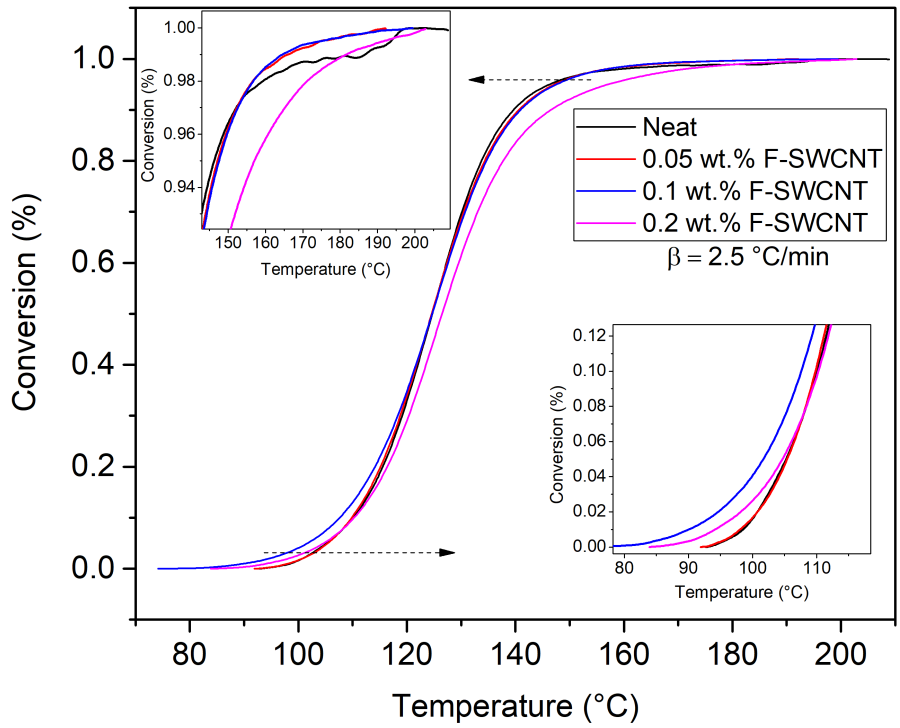

Figure 7.16. Temperature-dependent conversion for various F-SWCNTs content at 2.5 °C/min

According to the isoconversional principle, the conversion-dependent activation energy is determined using the temperature dependence of the curing process for different heating rates. The corresponding reciprocal temperatures are ascertained for defined values of conversion for the heating rates 2.5, 10, and 20 °C/min and displayed according to the Eqn. (4.7 - 9). Within the framework of this analysis, the evaluation and modeling of the reaction kinetics were carried out in the range of 0.1 to 0.95 with an interval of 0.05. ORIGIN PRO using the linear least square method was then developed to extract cure kinetic parameters according to the integral approaches; FWO, KAS, and Kissinger algorithms. The straight lines shown in Figure 7.17-19 represent these conversion values and are based on four points, which represent the applied heating rates.

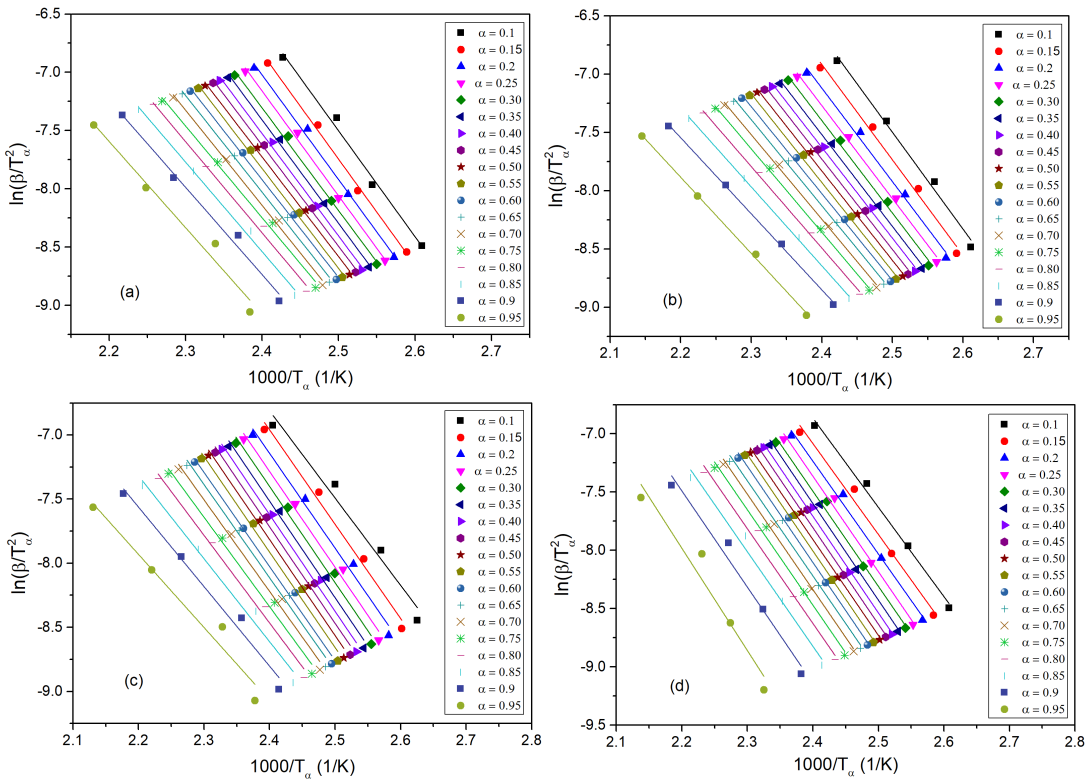

Figure 7.17. Performing KAS method for different prepreg systems, containing (a) 0.0 wt. % (neat) (b) 0.05 wt. % (c) 0.1 wt. % and (d) 0.2 wt. % F-SWCNTs

In Figure 7.17, the effective activation energy of the curing reaction for each prepreg system was determined utilizing the KAS method considering the slope of the linear plots of $\ln\left(\frac{\beta_i}{T_{\alpha,i}^2}\right)$ vs (1000/T) at different heating rates.

In Figure 7.18, the effective activation energy of the curing reaction for each prepreg system was determined using the FWO method considering the slope of the linear plots of $\ln(\beta_i)$ vs (1000/T) at different heating rates.

In Figure 7.19, the effective activation energy of the curing reaction for each prepreg system was determined employing the Kissinger method considering the slope of the linear plots of $\ln\left(\frac{\beta_i}{T_{p,i}^2}\right)$ vs (1000/T) at different heating rates.

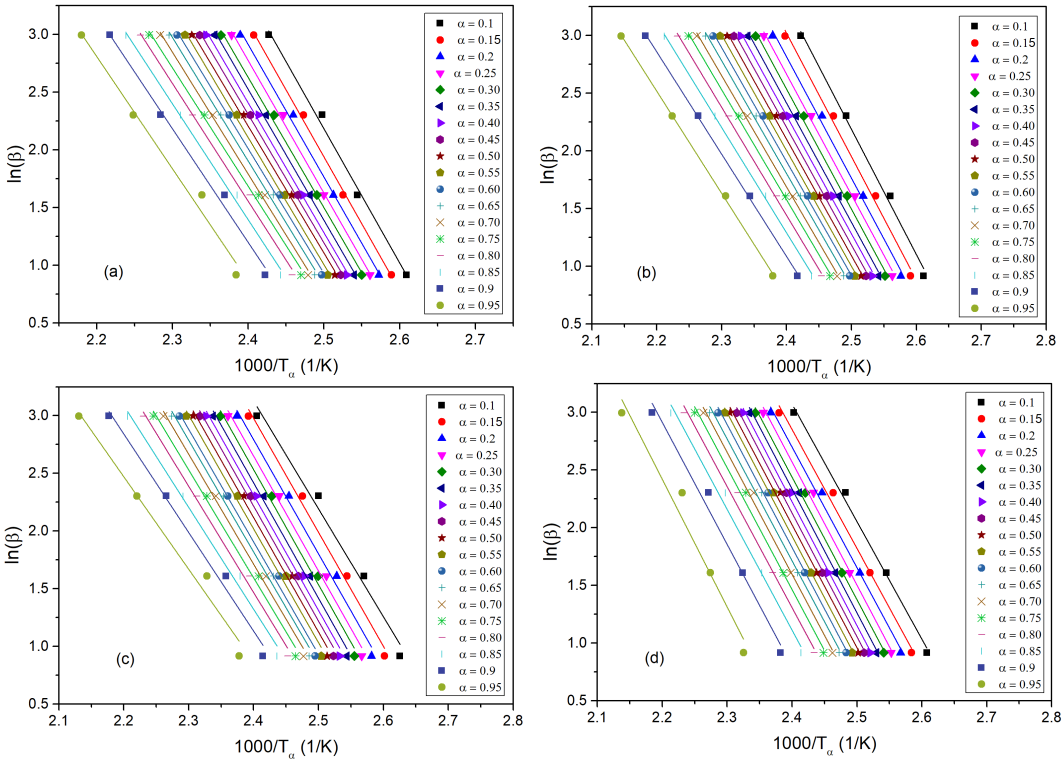

Figure 7.18. Performing FWO method for different prepreg systems, containing (a) 0.0 wt. % (neat) (b) 0.05 wt. % (c) 0.1 wt. % and (d) 0.2 wt. % F-SWCNTs

The dependence of E_α on a for curing reaction of various prepreg systems is presented in Figure 7.20. It indicates that the activation energy of the decomposition process is almost independent of the conversion degree for section 0.25–0.6 (a)-(b). It can be said that a good agreement among the E_α values determined by all considered isoconversional methods (FWO, KAS, and Kissinger) was obtained within the limits of inherent experimental errors. The activation energy curve determined by isoconversional FWO and KAS methods shows similar characteristics through the whole reaction process., However, the relative higher values of E_α computed by the FWO method could be explained by the worst approximation for temperature integral. Finally, it can be concluded that the more accurate method is KAS. The value of activation energy computed by the original Kissinger method is slightly lower than that obtained by KAS isoconversional method as well.

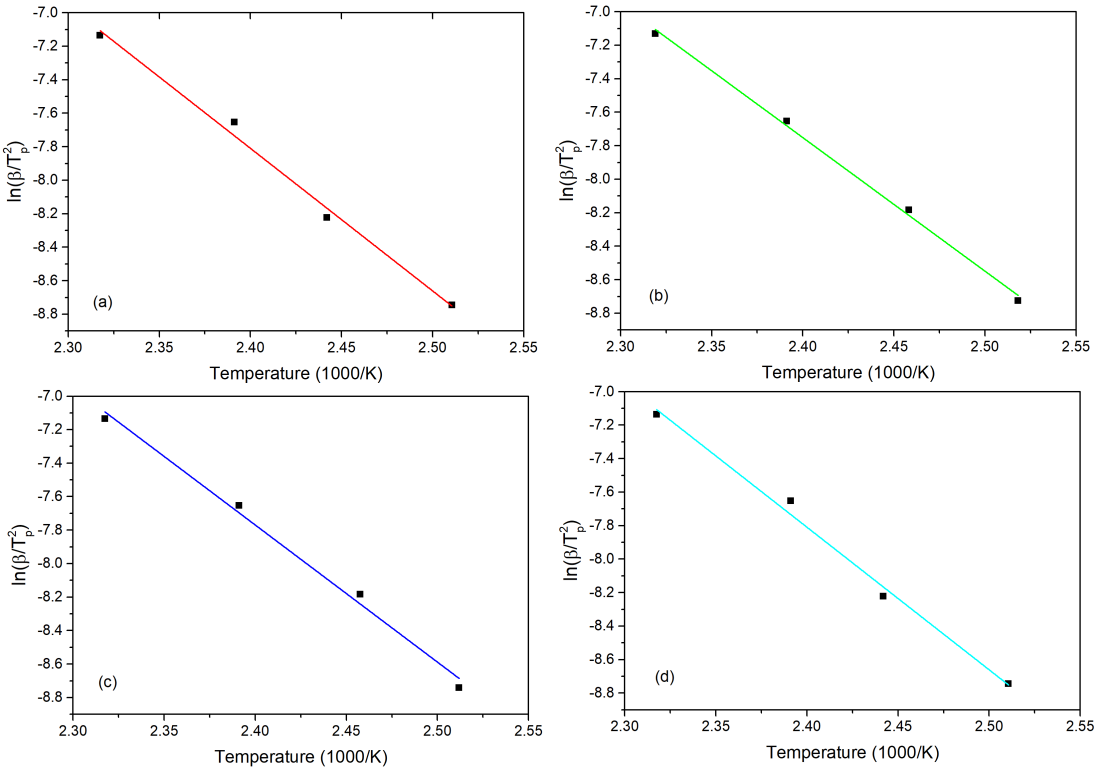

Figure 7.19. Performing Kissinger method for different prepreg systems, containing (a) 0.0 wt. % (neat) (b) 0.05 wt. % (c) 0.1 wt. % and (d) 0.2 wt. % F-SWCNTs

Table 7.2-5 gives the mean values of E_α obtained by the original Kissinger method as well as those obtained using isoconversional KAS and-FWO methods from prepregs containing various amounts of F-SWCNTs. For all investigated nanocomposites, the activation energy is lower for all conversion degrees in comparison to the prepreg containing neat epoxy resin. It means that the addition of F-SWCNTs increases the material's degradation efficiency. CNTs exhibit high thermal conductivity; they help to transport heat in composites, which reduces the activation energy. Thermal diffusivity increases with the increase of carbon nanotube's weight fraction because nanotubes exhibit very good thermal conductivity.

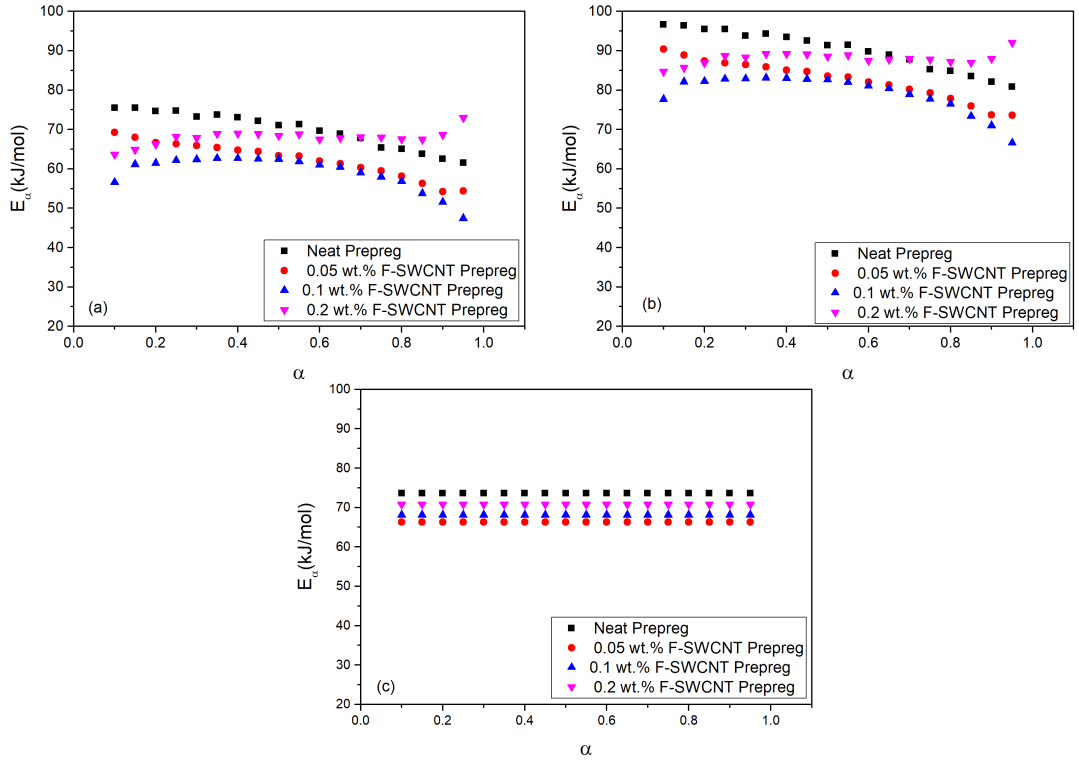

Figure 7.20. The dependence of E_a on a for curing reaction of various prepreg systems

Also, the presence of a high concentration of OH groups from the surface of the modified nanotubes in the sample containing 0.05 and 0.1 wt.% F-SWCNTs, increased the crosslinking effective activation energy of the crosslinking reaction. However, when the concentration was 0.2 wt.% of F-SWCNTs, the cure enthalpy of the prepreg was lower than the sample with 0.1 wt.% of F-SWCNTs. The difference was explained by the increase in viscosity caused by the addition of F-SWCNTs, due to the agglomeration degree of the hybrid prepreg system. The high homogeneity of the dispersion with single-wall carbon nanotubes creates percolated network much easier than agglomerated one.

Table 7.2. Activation Energy values for the conversion for prepreg systems, containing neat epoxy

α (%)	Eα-KAS (kJ/mol)	SD	R_2 KAS	Eα-FWO (kJ/mol)	SD	R_2 FWO	Eα-Kissinger (kJ/mol)	SD	R_2 Kissinger
0.1	75.5	0.61	0.98672	96.6	0.61	0.99169	73.6	0.25	0.99754
0.15	75.5	0.36	0.99529	96.4	0.36	0.99707			
0.2	74.6	0.42	0.99337	95.4	0.44	0.99564			
0.25	74.8	0.36	0.99519	95.5	0.37	0.99683			
0.3	73.2	0.37	0.9947	93.8	0.39	0.99645			
0.35	73.8	0.30	0.99652	94.3	0.32	0.9976			
0.4	73.0	0.33	0.99589	93.4	0.34	0.99719			
0.45	72.2	0.27	0.99707	92.5	0.29	0.99796			
0.5	71.1	0.30	0.99643	91.3	0.31	0.99755			
0.55	71.3	0.32	0.99594	91.5	0.33	0.99724			
0.6	69.7	0.36	0.99449	89.8	0.38	0.99636			
0.65	68.9	0.37	0.99407	89.0	0.38	0.99614			
0.7	67.8	0.34	0.99487	87.8	0.35	0.99664			
0.75	65.4	0.42	0.99147	85.3	0.44	0.99458			
0.8	65.0	0.42	0.99147	84.8	0.43	0.9947			
0.85	63.8	0.38	0.99256	83.5	0.40	0.99535			
0.9	62.2	0.56	0.98332	81.8	0.57	0.99006			
0.95	61.5	0.83	0.96303	80.8	0.84	0.97806			

Table 7.3. Activation Energy values for the conversion for prepreg systems, containing 0.05 wt. % F-SWCNTs

α (%)	Eα-KAS (kJ/mol)	SD	R_2 KAS	Eα-FWO (kJ/mol)	SD	R_2 FWO	Eα-Kissinger (kJ/mol)	SD	R_2 Kissinger
0.1	69.0	0.52	0.98843	90.2	0.54	0.99262	66.3	0.27	0.99633
0.15	68.0	0.53	0.98764	88.9	0.55	0.9921			
0.2	66.7	0.45	0.99064	87.4	0.47	0.99397			
0.25	66.3	0.38	0.99334	86.9	0.40	0.99566			
0.3	65.9	0.37	0.99346	86.5	0.39	0.99573			
0.35	65.4	0.31	0.99544	85.9	0.33	0.99697			
0.4	64.7	0.30	0.99545	85.1	0.32	0.997			
0.45	64.4	0.33	0.99443	84.7	0.36	0.99636			
0.5	63.7	0.27	0.99624	83.9	0.29	0.9975			
0.55	63.2	0.29	0.99572	83.3	0.31	0.99718			
0.6	62.0	0.26	0.99639	82.1	0.28	0.99761			
0.65	61.3	0.24	0.99693	81.3	0.25	0.99796			
0.7	60.3	0.21	0.99741	80.2	0.23	0.99827			
0.75	59.5	0.18	0.99811	79.3	0.20	0.9987			
0.8	58.1	0.19	0.99777	77.8	0.21	0.9985			
0.85	56.3	0.14	0.99869	75.9	0.16	0.9991			
0.9	54.2	0.14	0.99871	73.7	0.15	0.99912			
0.95	54.3	0.15	0.99837	73.6	0.16	0.99898			

Table 7.4. Activation Energy values for the conversion for prepreg systems, containing 0.1 wt. % F-SWCNTs

α (%)	Eα-KAS (kJ/mol)	SD	R_2 KAS	Eα-FWO (kJ/mol)	SD	R_2 FWO	Eα-Kissinger (kJ/mol)	SD	R_2 Kissinger
0.1	56.6	0.77	0.96235	77.7	0.80	0.97834	68.1	0.48	0.98954
0.15	61.1	0.55	0.98354	82.1	0.57	0.98996			
0.2	61.5	0.59	0.98125	82.2	0.61	0.98867			
0.25	62.2	0.55	0.98393	82.8	0.57	0.99018			
0.3	62.4	0.52	0.98554	82.9	0.54	0.9911			
0.35	62.7	0.49	0.98768	83.1	0.51	0.99235			
0.4	62.7	0.53	0.98537	83.0	0.55	0.99102			
0.45	62.5	0.56	0.98347	82.8	0.58	0.98989			
0.5	62.3	0.56	0.98347	82.5	0.58	0.98991			
0.55	61.9	0.56	0.98333	82.0	0.58	0.98985			
0.6	61.0	0.48	0.98719	81.1	0.50	0.99227			
0.65	60.4	0.54	0.98356	80.4	0.56	0.99008			
0.7	59.3	0.48	0.9863	79.2	0.50	0.99173			
0.75	58.0	0.53	0.98314	77.8	0.54	0.98999			
0.8	56.8	0.47	0.98584	76.5	0.49	0.99163			
0.85	53.8	0.57	0.97722	73.4	0.58	0.98706			
0.9	51.6	0.59	0.97345	71.0	0.60	0.98524			
0.95	47.4	0.77	0.94715	66.6	0.78	0.97214			

Table 7.5. Activation Energy values for the conversion for prepreg systems, containing 0.2 wt. % F-SWCNTs

α (%)	Eα-KAS (kJ/mol)	SD	R_2 KAS	Eα-FWO (kJ/mol)	SD	R_2 FWO	Eα-Kissinger (kJ/mol)	SD	R_2 Kissinger
0.1	63.6	0.42	0.99083	84.7	0.45	0.99419	70.8	0.51	0.98912
0.15	64.9	0.59	0.98303	85.7	0.61	0.98955			
0.2	66.2	0.66	0.98925	86.9	0.50	0.99322			
0.25	68.1	0.48	0.98992	88.7	0.49	0.99362			
0.3	67.9	0.63	0.98923	88.3	0.48	0.99389			
0.35	68.9	0.44	0.9904	89.2	0.48	0.99401			
0.4	68.9	0.41	0.99265	89.2	0.42	0.99533			
0.45	68.9	0.47	0.99038	89.1	0.48	0.9939			
0.5	68.4	0.50	0.98909	88.5	0.51	0.99309			
0.55	68.8	0.42	0.99239	88.8	0.43	0.99511			
0.6	68.5	0.53	0.99011	88.5	0.49	0.99371			
0.65	67.8	0.54	0.98675	87.7	0.56	0.99164			
0.7	68.1	0.47	0.99005	87.9	0.49	0.99369			
0.75	68.0	0.50	0.98873	87.7	0.52	0.99282			
0.8	67.5	0.64	0.98163	87.2	0.65	0.98847			
0.85	67.4	0.68	0.97922	87.0	0.69	0.98691			
0.9	68.6	0.86	0.968	88.0	0.87	0.97978			
0.95	73.0	1.43	0.92482	92.0	1.44	0.95115			

7.5.1. The Numerical Approach: Nonlinear Fitting

Convection function ($\alpha(T)$) was described as Eqn. (4.14). To start Newton's iterative method, an initial condition is needed. For convergent *A, B*, *C* values appropriate initial condition was chosen.

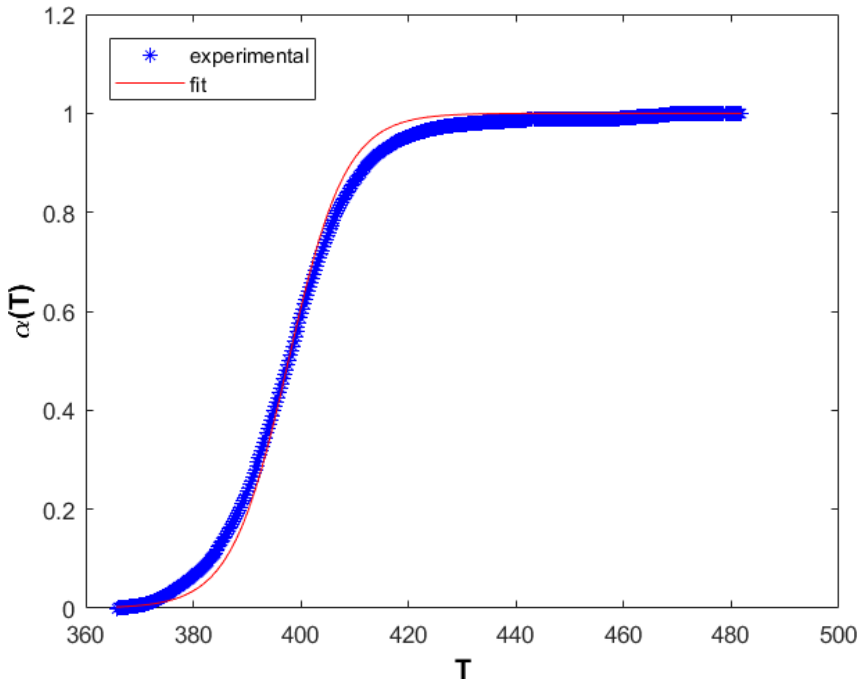

Figure 7.21. Temperature and conversion (α) values are plotted from experimental data and conversion function which is used fitting

$$z^0 = \begin{pmatrix} 0 \\ 0 \\ 0 \end{pmatrix}$$

For calculations, Matlab solver was used. Finally, unknowns were obtained as *A* = 0.5, *B* = 0.0765, *C* = 358.3126.

Figure 7.21 shows the experimental conversion $\alpha(T)$ values and least square approximation of $\alpha(T)$ the conversion function. T values are taken as Kelvin.

This section, it is seeking for values of pre-experimental factor A and activation energy E which are given in Eqn. (4.6). There are four unknowns as A, E, α, and $f(\alpha)$ in Eqn. (4.6). The function of $\alpha(T)$ is obtained and $f(\alpha)$.is chosen as described in Chapter 4. To calculate unknowns of the linearization, a linear fitting method is used. In Table 7.6, E and $\bar{A}$ values are given for different samples.

Table 7.6. A, B, C obtained from nonlinear fitting and Data Linearization Technique provide getting E, ln(A) for different β

Sample	β	A	B	C	E	ln(A)
Neat	2.5	0.5	0.0765	358.3126	89.8749	22.2212
	5	0.5	0.0767	367.8309	85.5814	20.9993
	10	0.5	0.0608	368.3936	73.3774	17.3604
	20	0.5	0.0564	377.0870	70.3343	16.4869
0.05 wt.% F-SWCNT	2.5	0.5	0.0732	356.5693	82.7869	20.0338
	5	0.5	0.0619	359.3702	71.0760	16.4988
	10	0.5	0.0558	365.7544	66.7037	15.3149
	20	0.5	0.0509	374.5726	69.8242	16.2947
0.1 wt.% F-SWCNT	2.5	0.5	0.0669	352.6327	73.1902	17.1211
	5	0.5	0.0627	358.7051	68.1392	15.6939
	10	0.5	0.0545	364.2501	63.2666	14.2895
	20	0.5	0.0515	375.6366	64.49896	14.6932
0.2 wt.% F-SWCNT	2.5	0.5	0.0651	353.4174	73.7206	17.7973
	5	0.5	0.0616	361.2695	76.1108	17.9529
	10	0.5	0.0596	369.6381	73.5011	17.3437
	20	0.5	0.0561	380.6521	73.1449	15.7400

Kinetic analysis was performed by a new mathematical approach based on the nonlinear least-square fitting a tanh function and lumbarization method. This new algorithm is called a GMN method. Experimentally determined differential scanning calorimetry (DSC) data sets for an epoxy resin functionalized by single-wall carbon

nanotubes are used for the verification of the GMN method. The results obtained from the GMN algorithm are also compared with the methods reported in the literature. Finally, the GMN algorithm was in good agreement with experimental data for the calculation of the kinetic parameters.

Table 7.7. Comparison of the optimum values of GMN method to with Kissinger and KAS* method

Sample	Kissinger		KAS*		GMN	
	E	ln(A)	E	ln (A)	E	ln (A)
Neat	73.6	13.6	75.5− 61.5	15.2−10.38	73.4	17.3
0.05 wt.% F-SWCNT	66.3	11.3	69.0 −54.3	13.3 − 8.2	66.7	15.3
0.1 wt.% F-SWCNT	68.1	11.8	61.1 −51.6	10.6 − 7.8	63.3	14.2
0.2 wt.% F-SWCNT	70.8	12.6	64.9 − 68.6	11.6 − 10.6	73.1	15.7

Kissinger's method gives an average of activation energy for the whole process containing all α values.

*The KAS method is an isoconversional method and changes depending on α. The range given in the table shows the values corresponding to the α value starting from 0.1 and reaching the value 0.9 with 0.05 increments.

7.6. The Effects of VBO Parameters on CFRP Laminates

Before starting prepreg production by modifying the filament winding machine by Prof. Tanoğlu Research Group, the effects of the VBO technique, which is explained in detail in the experimental chapter, were studied. One of the most important parameters, to obtain products with similar quality to parts produced by the autoclave technique, is air permeability. Studies have shown that the air pathways created in the in-plane

direction improve the surface quality of the final product. To observe influences of air permeability, the VBO technique was applied using KordSA's commercial woven type carbon fiber reinforced prepreg products.

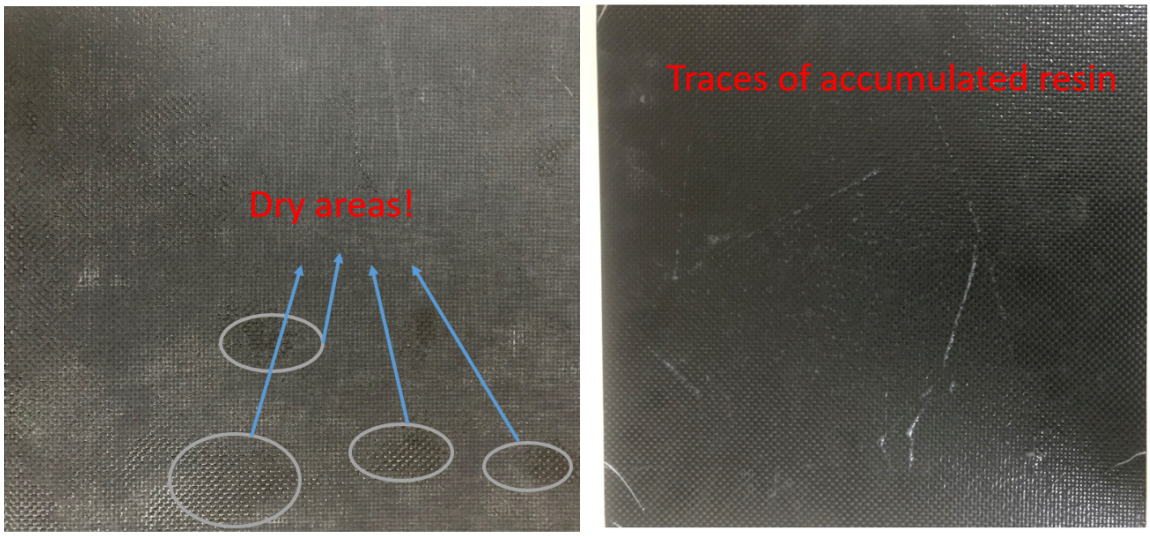

Figure 7.22. Images of laminations created by using KordSA's commercial woven type (200 g/m^2) carbon fiber reinforced prepreg. (left) Using perforating films without a dam, transverse air permeability (right) Using non-perforated film with E-glass dam, in-plane air permeability, not including caul plate

As seen in Figure 7.22 (left), the air permeability provided in the transverse direction (through-thickness) using perforating film (without using dams) created dry zones in the produced laminates. As seen in Figure 22 (right), resin-rich paths have been formed in laminates produced by using non-perforating film (including E-glass dams) in the in-plane direction where the air permeability is more dominant, due to the effect of the vacuum bag. However, dry areas were avoided in these laminates produced. With the air permeability provided in the in-plane direction, the caul plate placed on the prepregs has created laminates with very good surface quality without using any polishing process (Figure 7.23). Therefore, the same vacuum bagging lay-up technique has been used for all laminates that will be shown in the next section.

After determining the effect of vacuum bagging lay-up and curing behavior of the prepregs, the fabrication of prepreg-based hybrid composites process consisted of three main steps: pre-impregnation with resin system by incorporating F-SWCNT, hand lay-up of the prepreg and preparation of the VBO system and curing in the oven. While preparing the prepreg, a sponge was placed to apply pressure to the cylinder in the resin bath to ensure an even distribution of resin while avoiding resin-rich regions.

Figure 7.23. Achieving high surface quality by using non-perforating film (in-plane air permeability), E-glass dams, and caul plate

7.7. Preparing Prepregs with/without F-SWCNTs

For the perfect UD alignment of the carbon fiber tows, the feeding of materials in the rollers was used and the tension level was adjusted. Siddiqui et al. stated that the best impregnation was achieved for a fiber tension of 24.5 N and an exit die gap of 0.05 mm, where the fiber breakage was also negligible. In the presented study, the same combination of prepregging parameters was applied to the machine control system to control the prepreg thickness and resin content. High tension and more rollers could be caused not to impregnate well due to forming a rigid structure. Therefore, two rollers were used for all processes to guide the fiber tows through the mandrel.

The effects of these processing parameters on the thickness of the prepregs with/without F-SWCNT were measured and presented in Table 6. The thickness of the prepared prepregs varied between 0.5 and 0.7 mm. It should be noted that the thickness increased slightly after the prepregs were manufactured with 0.05 % wt. and a higher amount of SWCNTs. The slight increase observed in prepreg thickness is because of the increase in F-SWCNT amount on viscosity. To maintain the optimum resin viscosity required for the prepregging process, the solvent added to the mixture lost its effect after 0.025 % wt. and caused the resin to adhere more to the fibers.

Table 7.7. The average thickness of the prepreg and their composite samples

Resin Sample	Prepreg Thickness (mm)	Composite Thickness (mm)
0 (Neat)	0.538	3.02
0.025% wt. F-SWCNT	0.596	3.10
0.05% wt. F-SWCNT	0.647	3.30
0.1% wt. F-SWCNT	0.693	3.60
0.2% wt. F-SWCNT	0.762	3.80

7.8. Fabrication of CFRP Laminates

After hand lay-up of the prepreg on the tooling, a laminate 0°/90°/0°/90°/0°/90° was prepared with high tolerance on the orientation. During the placement of fabrics, air entrapment and wrinkling were avoided by applying debulking pressure after the vacuum bagging process. Then, the vacuum bag was prepared according to the following curing scheme as detailed in the previous section. T_{onset} values obtained as a result of DSC analysis were around 100 °C. A tolerance of ±5 C° was observed as a result of the test performed on the temperature control system of the oven used in the VBO process. Therefore, the onset temperature of the curing process was applied at 95 °C temperature for all laminates. Post-curing was applied at between 20 and 30 °C above the curing temperature under the recommendation given by the resin manufacturer. The vacuum bag was kept under vacuum until the internal pressure was between 0.8 and 1 bar during

temperature was increasing to the cure (95 °C for 1 h) and post-cure (120 °C for 2 h) sections. The representative samples of CFRP composites containing various amounts of F-SWCNTs as well as neat CFRP can be seen in Figure 7.25. The thickness of the prepregs-based hybrid composites is also given in Table 7.7. Fabricated hybrid composite laminates have an average thickness of 3 mm. The effect of the amount of resin in prepregs was also seen in the composites manufactured by the VBO method. It was observed that composite thicknesses were increased produced by adding more amount of F-SWCNT.

Figure 7.24. Fiber tensioner system for drum-type prepregging machine

Figure 7.25. Representative image of the manufactured laminates containing various amounts of F-SWCNTs

7.9. Characterization of CFRP Laminates

7.9.1 Microstructural Characterization

Microstructure characterization under the optical microscope was performed on the small chips of the samples were mounted in the resin. A fairly uniform distribution of carbon fibers in the prepreg is presented in Figure 7.26, a-d. The upper side shows the optical micrographs of the longitudinal distribution of carbon fibers in the prepreg, and the lower side shows cross-sectional uniform distribution of the carbon fiber in the prepreg, indicating the successful manufacturing process. Small gaps between fibers have been observed in some areas, which is one of the points that need to be improved in future studies.

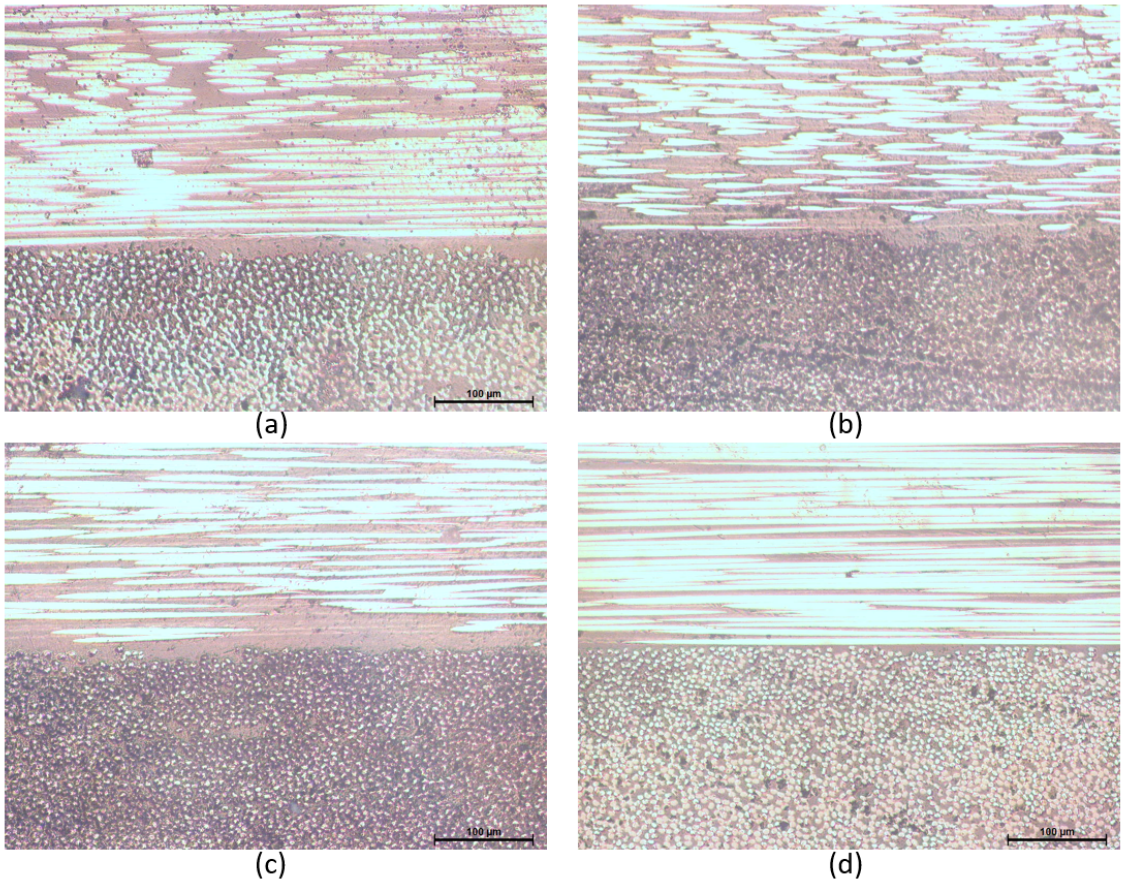

Figure 7.26. Optical Microscope images of hybrid composites at longitudinal and cross-sectional regions: a) 0 wt% F-SWCNT/CFRP, b) 0.05 wt% F-SWCNT/CFRP, c) 0.1 wt% F-SWCNT/CFRP, d) 0.2 wt% F-SWCNT/CFRP

7.9.2 Chemical Characterization

Matrix digestion and void content test were carried out to calculate the mass fractions of composite plates according to ASTM D3171-Procedure B standard. For the matrix digestion, sulfuric acid (H_2SO_4), and hydrogen peroxide (H_2O_2) was used. First, 1 g test specimens were prepared and weighted to the nearest 0.0001 g. Then each specimen was placed in 100 mL glass beakers. Minimum 20 mL sulfuric acid was added to a glass beaker and the beaker was placed on a hot plate and heated until the mixture starts to fume. After the solution was dark (with no appreciable change in color for 5 min), 50 or

30 % hydrogen peroxide was added down the side of the beaker to oxidize the matrix. The fibers floated to the top of the solution, and the solution appeared clear. After the solution appeared clear, the beaker was removed from the hot plate and allowed the solution to cool. The fibers were washed three times with distilled water and a final acetone wash was utilized after sulfuric acid and hydrogen peroxide was removed from the specimen. After washing, the specimens were dried in an oven for 1 hour and 100 °C. Finally, the dried specimens were weighted, and new values were recorded.

The density used for carbon fiber was 1.79 g/cm^3, and for the resin were 1.058 g/cm^3 as given in the experimental chapter. The density, void content, and fiber volume fraction of the CFRP with/without F-SWCNTs used in this research were calculated according to explained procedure and given in Table 7.8. The fiber volume fractions of the samples changed between 55.3% and 50.16%. The average density of the composite samples was calculated as 1.45 g/cm^3. The highest value of fiber volume fraction (V_f) belonged to the neat sample as 55.3%. A decrease in fiber volume fraction was observed with the addition of F-SWCNT. With the addition of 0.2% wt. F-SWCNT, fiber volume fraction was calculated to be 50.1%. The reason for the decline can be explained by the fact that adding more F-SWCNTs increases the resin viscosity, and they adhere more during impregnation. High fiber volume fractions undoubtedly improve the mechanical properties of the structure since the primary role of fibers in composite structures is to take place as a load-carrying component. However, as will be explained in the part of mechanical characterization, this small decrease is an underestimated situation besides its contribution to the mechanical properties of F-SWCNTs. In most applications, fiber volume fractions of CFRP laminates are generally expected to lie between 45% and 60%. Many studies are indicating that higher fiber volume fractions cause poor wettability and penetration of the matrix material into the fibers.

The average void content of all CFRP laminates was around 1%. While void content was 0.9% on average in samples without F-SWCNT, it started to increase gradually as shown in Table 7 with the addition of F-SWCNT. The void content did not increase significantly until the 0.1% wt. F-SWCNT addition, reaching a value of 1.2% at 0.5% wt. F-SWCNT. However, with the addition of 0.1% wt. F-SWCNT, void content was increased further, reaching a value of approximately 2% with the addition of 0.2% wt. F-SWCNT. The solvent applied during the preparation of prepregs has a significant effect on the void content in the composite structure. To minimize this effect, prepregs were subjected to heat treatment after impregnation, as described in the experimental

section. However, to maintain the optimum viscosity level, the amount of solvent was increased with the increase in the amount of F-SWCNT. At the end of this, the solvents that cannot be get rid of from prepregs during production created gaps in the structure during the VBO process and they likely influence the values.

Table 7.8. The average density, fiber-matrix volume fraction, and void content of the samples

F-SWCNT Content of Hybrid Composite (wt.%)	Density (kg/m^3)	Volume		
		Fiber, V_f (%)	Matrix, V_m (%)	Void Content (%)
0 (Neat)	1.43	55.32	43.75	0.90
0.025	1.44	54.12	42.78	1.10
0.05	1.44	53.96	44.79	1.23
0.1	1.45	52.38	46.11	1.50
0.2	1.48	50.16	47.92	1.92

7.9.3 Mechanical Characterization

7.9.3.1 Tensile Test

The representative tensile stress-strain curves of carbon fiber reinforced epoxy (CFRP) composites containing various amounts of F-SWCNTs as well as neat CFRP are given in Figure 7.27. The results revealed that the ultimate strength and strain at failure values were improved by the addition of low content of F-SWCNT as compared to the neat CFRP. Tensile strength, modulus of elasticity, and strain at failure values of composites are also given in Table 7.9. The average tensile strength of neat CFRP composites was measured to be around 770 MPa. It was found that due to the addition of

only 0.05wt % F-SWCNTs into the prepreg system, the tensile strength of the CFRP was significantly affected (the average tensile strength of 907 MPa was achieved, about 18% improvement). However, it was observed that the tendency for improving the tensile strength disappears as the content of F-SWCNTs is above 0.1 wt.%. This decay on the tensile strength values at relatively higher content of F-SWCNT may associate with the non-homogeneous dispersion and the formation of CNT agglomerations at high contents. The CNT agglomerations in the matrix system may act as micro defects and stress concentration points to reduce the mechanical properties.

It was also observed that the modulus values are reduced, on the other hand, failure strain values are increased with the increasing F-SWCNTs amount within the matrix. The average failure strain of neat CFRP was measured as 1.08%. The highest improvement in failure strain (i.e., approximately 4.74%) was achieved for the specimens containing 0.05 wt.% F-SWCNTs. Moreover, the increased amount of the F-SWCNTs resulted in a higher failure strain value of the CFRPs. This improvement observed in the failure strain value of the CFRP may be attributed to the higher compliance and toughness of the epoxy matrix due to the presence of carbon surfaces and preferential adsorption of the amine molecules in the hardener by CNT surfaces. These findings of failure strain are in conformance with the general trend in the literature related also to the better energy absorption behavior of CNTs within a matrix system. Soliman et al. reported that due to the addition of 1 wt.% of functionalized MWCNTs, failure strain and ultimate strength values of the CFRP composite were improved by 20 and 21%, respectively.

In our study, it was revealed that the fiber-dominant properties of CFRP composites may be improved by an innovative resin system containing F-SWCNTs. The fractured surface SEM images of CFRP laminate containing 0.2 wt. % of F-SWCNTs at various magnifications are shown in Figure 7.30. A random distribution of the F-SWCNTs inside the epoxy matrix was observed. The roughness of the surface indicates that F-SWCNTs or their agglomerates may act as a barrier to crack propagation, providing a relatively high amount of matrix plastic deformation.

As shown in Table 7.9, the modulus of elasticity of CFRP composites was presented with/without F-SWCNTs. The modulus of elasticity of composites fabricated with the developed prepregs containing neat epoxy was measured as 68.70 GPa. Due to the addition of F-SWCNTs, the modulus of elasticity was dropped up to 60.44 GPa. This decrease in the modulus of elasticity values is expected to be related to the higher compliance and toughness of the epoxy matrix due to the presence of carbon surfaces and

preferential adsorption of the amine molecules by CNT surfaces. It is known that the area under stress-strain graphs represents the toughness and the fracture energy absorbed during the loading of the material. So, it is revealed that the composites containing F-SWCNTs have higher toughness and energy absorption values. As shown in Figure 7.28, fiber breakage was predominantly experienced by the failure of samples with and without F-SWCNT after the tensile test. This shows that the interlaminar matrix delamination problem, which is the most common failure mode in composite materials today, has been successfully overcome thanks to the applied production method.

Table 7.9. Tensile properties of CFRP composites fabricated with/without F-SWCNTs. The values in the parentheses indicate the ± standard deviations

F-SWCNT Content of the Hybrid Composite (wt.%)	Average Tensile Strength (MPa)	Average Modulus of Elasticity (GPa)	Average Failure strain (%)
0 (Neat)	770.57 (26.78)	68.70 (1.08)	1.08 (0.42)
0.05	907.22 (31.24)	65.25 (1.22)	4.74 (0.74)
0.1	814.83 (40.30)	67.96 (1.54)	3.78 (0.88)
0.2	705.82 (35.74)	60.44 (1.38)	3.11 (0.78)

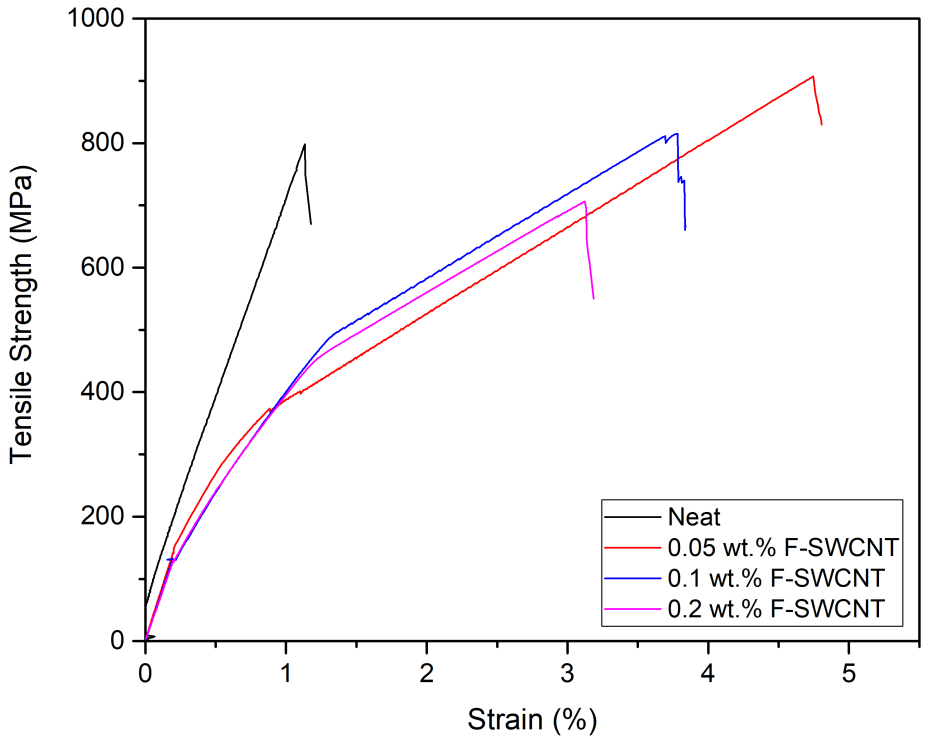

Figure 7.27. The tensile stress-strain curves of neat CFRP and CFRP containing various amounts of F-SWCNTs

The success of the production method detailed in the previous section is directly related to the applied vacuum level and air permeability. Failure modes in composites generally exist in three ways: formation of transverse matrix cracks (intra-ply cracking), interlaminar matrix delamination, and fiber breakage (fracture). It can be seen as the best example of this concept in Figure 7.29. Sample of the neat CFRP, which could not be compacted sufficiently due to the vacuum leakage applied during production, created resin-rich regions between the layers. Optical investigation for the cross-section regions of the samples with insufficient compaction showed that these resin-rich regions create interlaminar matrix delamination problems as a result of the tensile test. It was found that due to insufficient compaction, the tensile strength of the neat CFRP was significantly affected and calculated as 518.5 MPa. The main reason could be stiffness mismatch between the layers due to the resin-rich region, coming from the low compaction pressure.

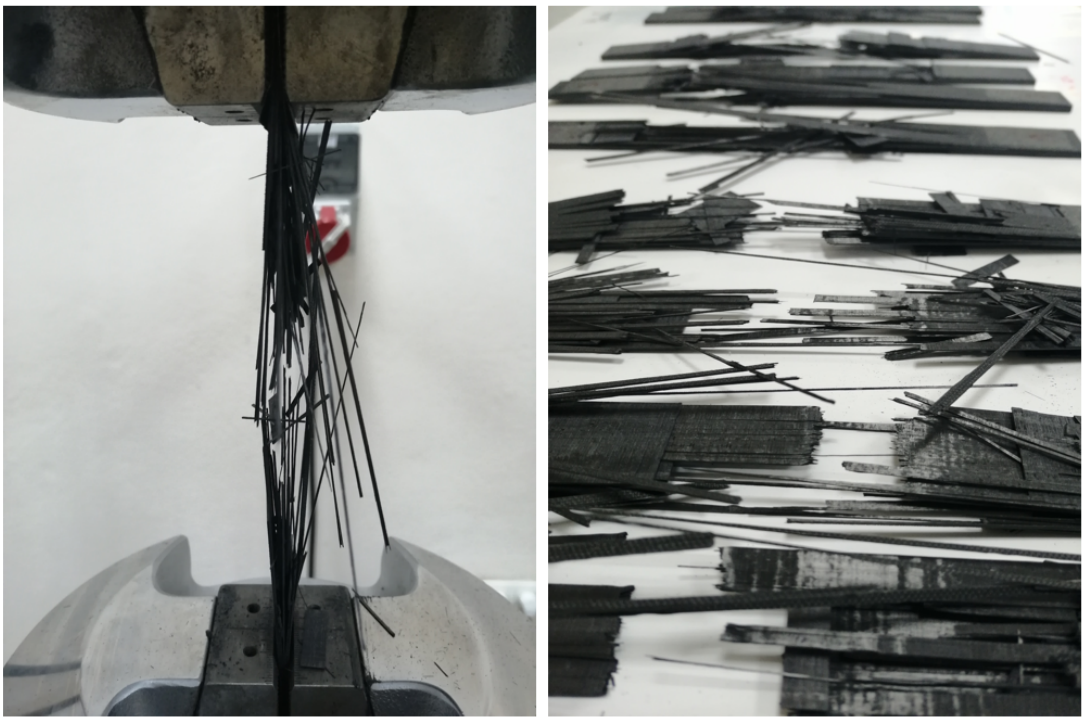

Figure 7.28. Fiber fracture failure mode in hybrid CFRP composites after tensile test

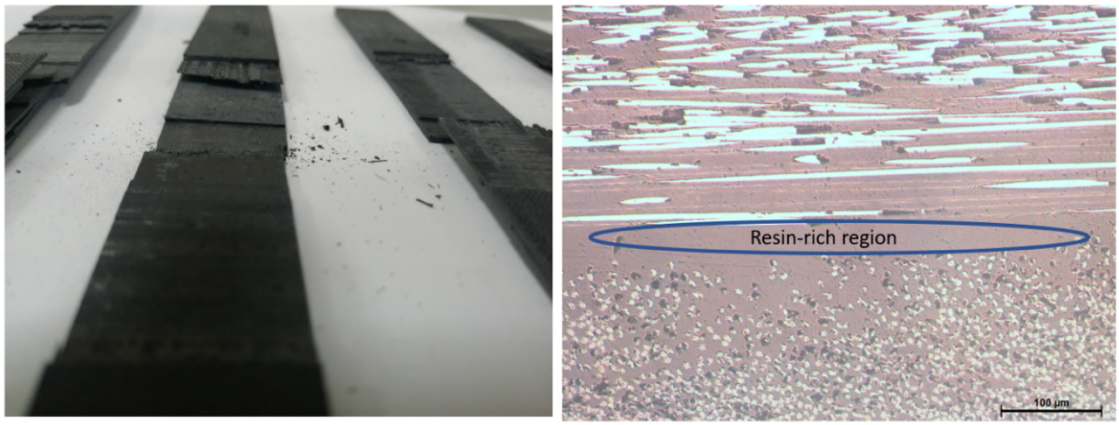

Figure 7.29. Interlaminar matrix delamination failure mode at between layers due to resin-rich region where the blue circle point out

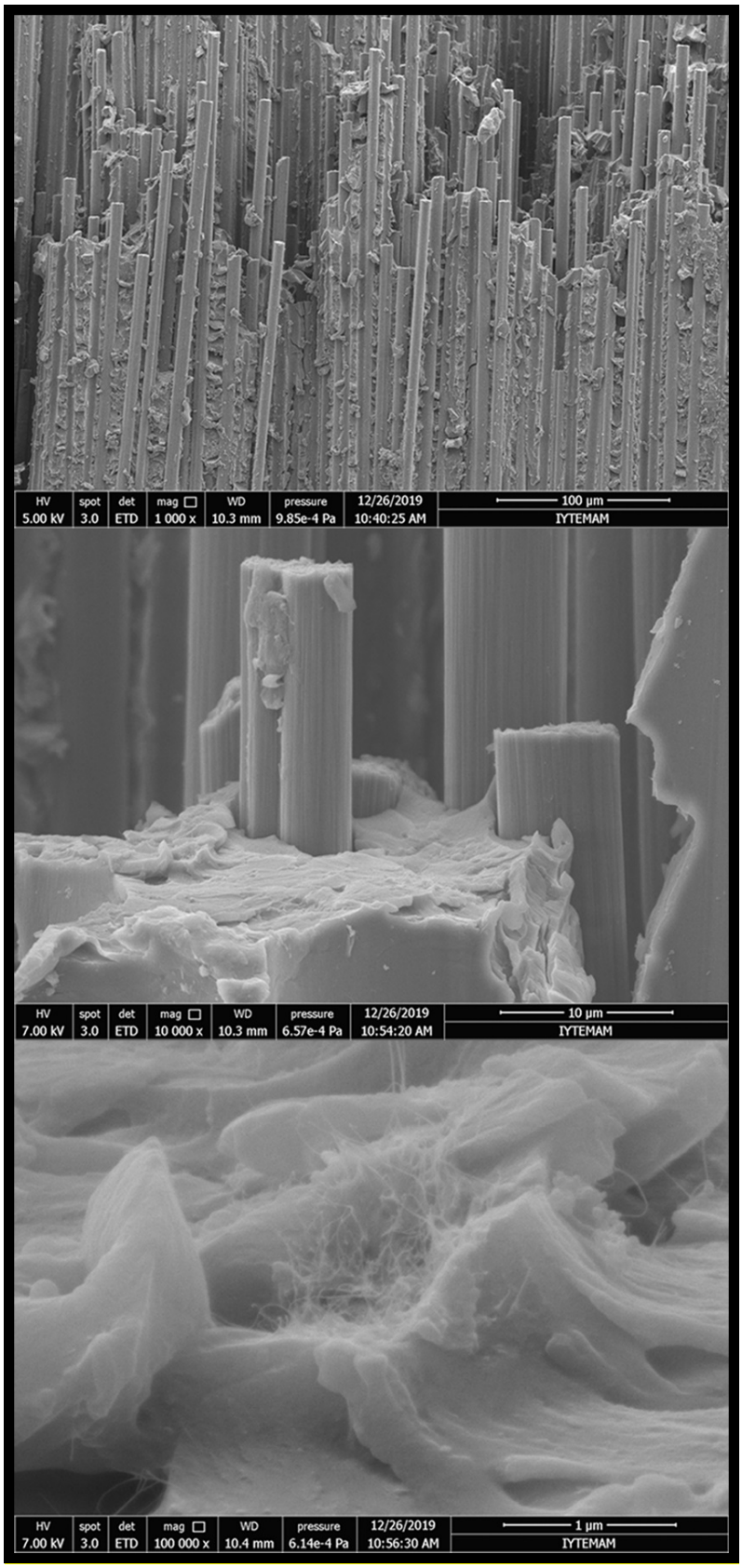

Figure 7.30. Fractured surface SEM images of CFRP laminate containing 0.2wt % of F-SWCNTs, at various magnifications

7.9.3.2 Charpy Impact Test

Impact fracture energy values of CFRP laminates containing various amounts of F-SWCNTs as well as neat CFRP are presented in Figure 7.31. The average impact strength of neat CFRP composites was measured as 87.28 J/m^2. The highest impact strength of 99.59 J/m^2 was achieved with a specimen containing 0.1 wt.% F-SWCNTs. This indicates about a 14% increase in impact strength due to the incorporation of SWCNTs with the neat CFRP microstructure. Similarly, the impact strength of the laminate was improved by 9% by the addition of 0.05 wt.% F-SWCNTs (94.78 J/m^2). However, it was seen that the further addition of F-SWCNTs to structure resulted in a decline in impact strength values. At 0.2 wt.% F-SWCNTs, average impact strength value of 85.88 J/m^2 which is 2% lower than for neat CFRP specimens as measured. The results imply that the incorporation of F-SWCNTs in prepreg-based CFRP laminates provides a significant effect on the impact behavior. In other words, the impact strength behavior of F-SWCNTs filled laminates exhibits a better performance by the addition of up to 0.2 wt.% F-SWCNTs.

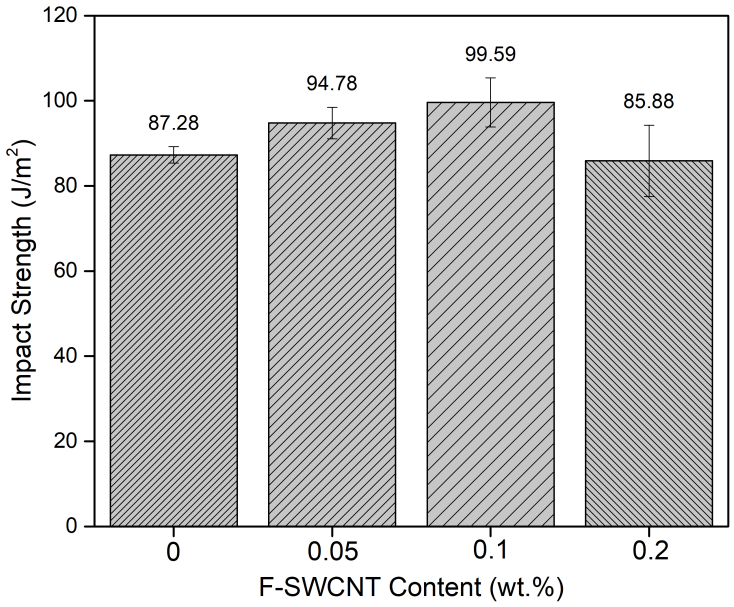

Figure 7.31. The impact strength values of CFRP composites fabricated with/without F-SWCNTs

F-SWCNTs act as a barrier during crack propagation, cause crack branching, and hence improve energy absorption during fracture. Similarly, Tehrani et al. indicated significant improvement for impact energy absorption (21.3%) due to the addition of 2.0 wt.% of MWCNTs into the composite systems. Also, Tehrani et al. revealed a 17% enhancement of the energy dissipation capacity by incorporating MWCNTs in CFRPs.

7.9.3.3 SBS Test

The results of the SBS tests are presented in Figure 7.32. It was found that the addition of the F-SWCNTs into the composite structure resulted in an improvement in the ILSS values. The average ILSS of neat CFRP composites was measured as 33.14 MPa. About 15% enhancement in ILSS was observed in samples containing 0.05 wt.% of F-SWCNTs. Similarly, an improvement of 21% (40.03 MPa) in ILSS was achieved with the addition of 0.1 wt.% F-SWCNTs to the composites. Notable enhancement of about 30% was measured with the addition of 0.2 wt.% F-SWCNTs (42.37 MPa). So, these findings indicate that F-SWCNTs have a positive effect on the interlaminar shear strength of the composites by reinforcing the matrix layers along the interlaminar region and enhance the interfacial bonding due to functionalized F-SWCNTs. Interlaminar shear strength is the matrix-dominant property and improved by the incorporation of F-SWCNTs in CFRP composites. Polarity groups such as carboxyl and hydroxyl activated by functionalization could react with epoxy resin during the curing of prepregs. This achievement in the resin system has led to a stronger bond between fibers and modified resin containing F-SWCNTs. The modified resin provides a more successful load transfer between fiber and resin. Sanchez et al. indicated that the ILSS values increase gradually with the addition of amino-functionalized CNTs added to the composites. The base value of shear strength (54 MPa) was increased by 10% (60 MPa) with 0.3 wt.% addition of the CNTs used. Similarly, Sharma et al. showed the effect of amino-functionalized CNTs (1.0 wt.%) in the resin on the increase of the interlaminar shear strength (improvement by 39%).

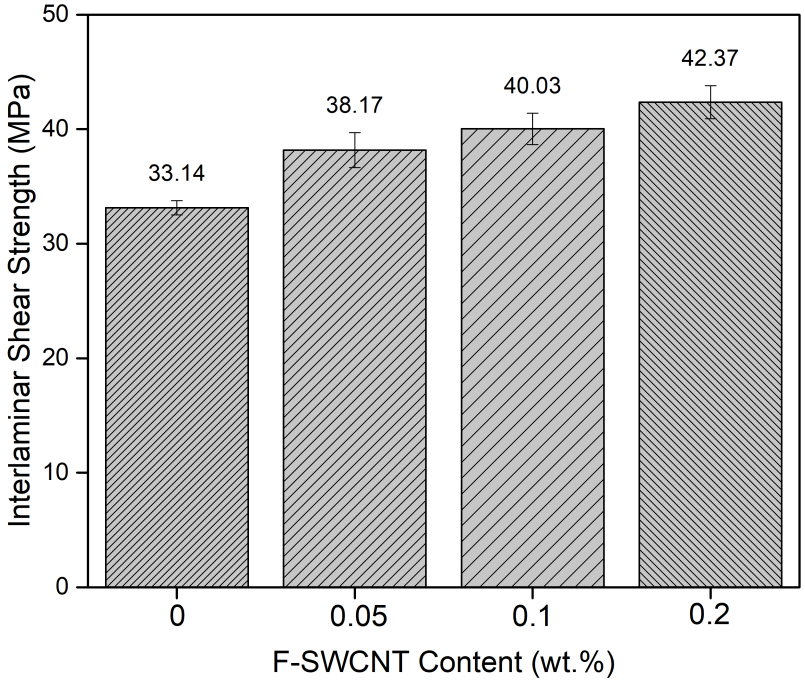

Figure 7.32. The average values of interlaminar shear of the composites fabricated with/without F-SWCNTs

7.9.3.4 TPB Test

Figure 7.33 also shows the effect of the incorporation of F-SWCNTs on the flexural strength of CFRP composites. The average flexural strength of neat CFRP composites was measured as about 770 MPa. An improvement was observed for the samples with 0.05 wt.% of F-SWCNTs. The peak strength value of 918MPa was achieved with a 23% increase in flexural strength. Similar studies reported that the flexural strength was improved by the incorporation of CNTs within the CFRP composites. Yokosuka et al. [24] showed that the flexural strength was reached 912 MPa (31% enhancement) with the addition of 5 wt.% cup-stacked carbon nanotubes (CSCNTs) in the CFRP. Sharma et al. [39] revealed an enhancement of 25% in flexural strength which was achieved by incorporation of 0.50 wt.% amino-functionalized MWCNTs in CFRP composites. Kim et al. presented an 18% increase in flexural strength (~740 MPa) due to the addition of 0.3 wt.% MWCNT in CF/epoxy composite. However, it was obvious that further addition

of F-SWCNTs causes a drop in flexural strength. The dropping trend in flexural strength values started with the addition of 0.1 wt.% F-SWCNTs. At this content, the flexural strength was 716.59 MPa, but it was 4% lower than those for the neat ones. Moreover, a remarkable drop of about 12% was recorded in specimens containing 0.2 wt.% F-SWCNTs (658.30 MPa). Agglomeration of CNTs at higher concentrations had a more pronounced effect on flexural strength.

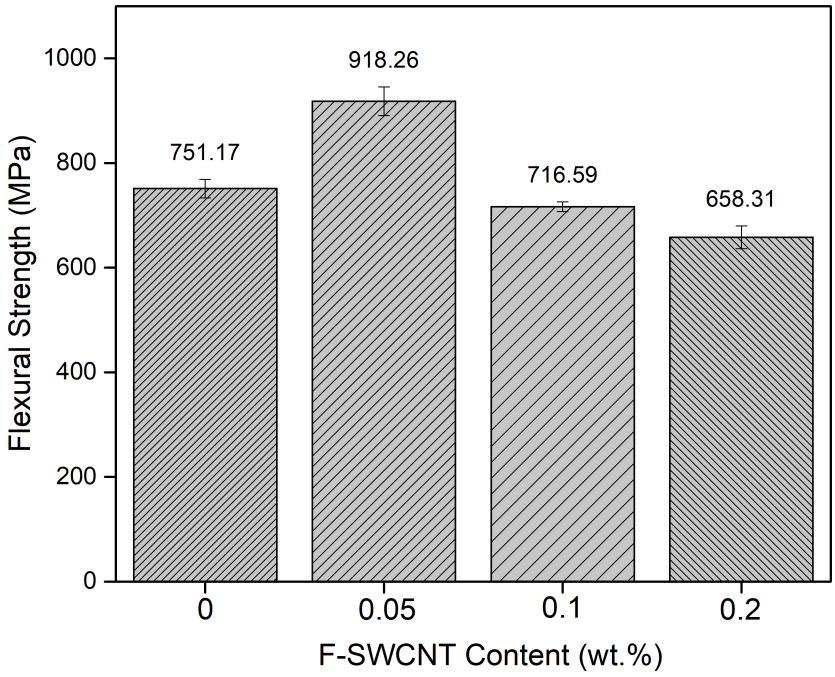

Figure 7.33. The average values of flexural strength of the composites fabricated with/without F-SWCNTs

7.9.3.5 DMA Test

The dynamic mechanical behavior of the composites fabricated with/without F-SWCNTs was investigated. Storage modulus (E'), loss modulus (E''), and tanδ values of the specimens are shown in Figures 15 and 16. At the low content of the F-SWCNTs, the addition of nanotubes resulted in lower storage modulus (E') values as compared to those with neat composites. However, it was observed that at relatively higher content of F-

SWCNTs, storage modulus values increased and reached the highest level at 0.2 wt.% F-SWCNTs compared to the neat ones. The storage modulus is affected by two competing parameters: the cross-linking density and the stiffening effect of the reinforcing. It is expected that the crosslinking density of the epoxy matrix is reduced due to the preferential adsorption and segregation of amine molecules towards F-SWCNT surfaces. On the other hand, the stiffening effect becomes effective due to the presence of a relatively high content of F-SWCNT. Figure 7.34 indicated that the loss modulus (E'') of the composites exhibits similar behavior with the storage modulus. A gradual increase was observed due to the addition of the F-SWCNTs. The increase may associate with the increasing compliance of the epoxy matrix due to the molecular segregations at F-SWCNTs/matrix interfaces, which cause higher viscous behavior. Glass transition temperature (T_g), which is the temperature at which the glassy to rubbery transition occurs. The ratio of the loss to the storage modulus value gives the tan δ. Glass transition temperature was assigned as the peak of the curves in Figure 7.35. No significant change in T_g was observed (change from128 to 134 °C). So, it was observed that the presence of F-SWCNTs has no significant effect on the T_g values.

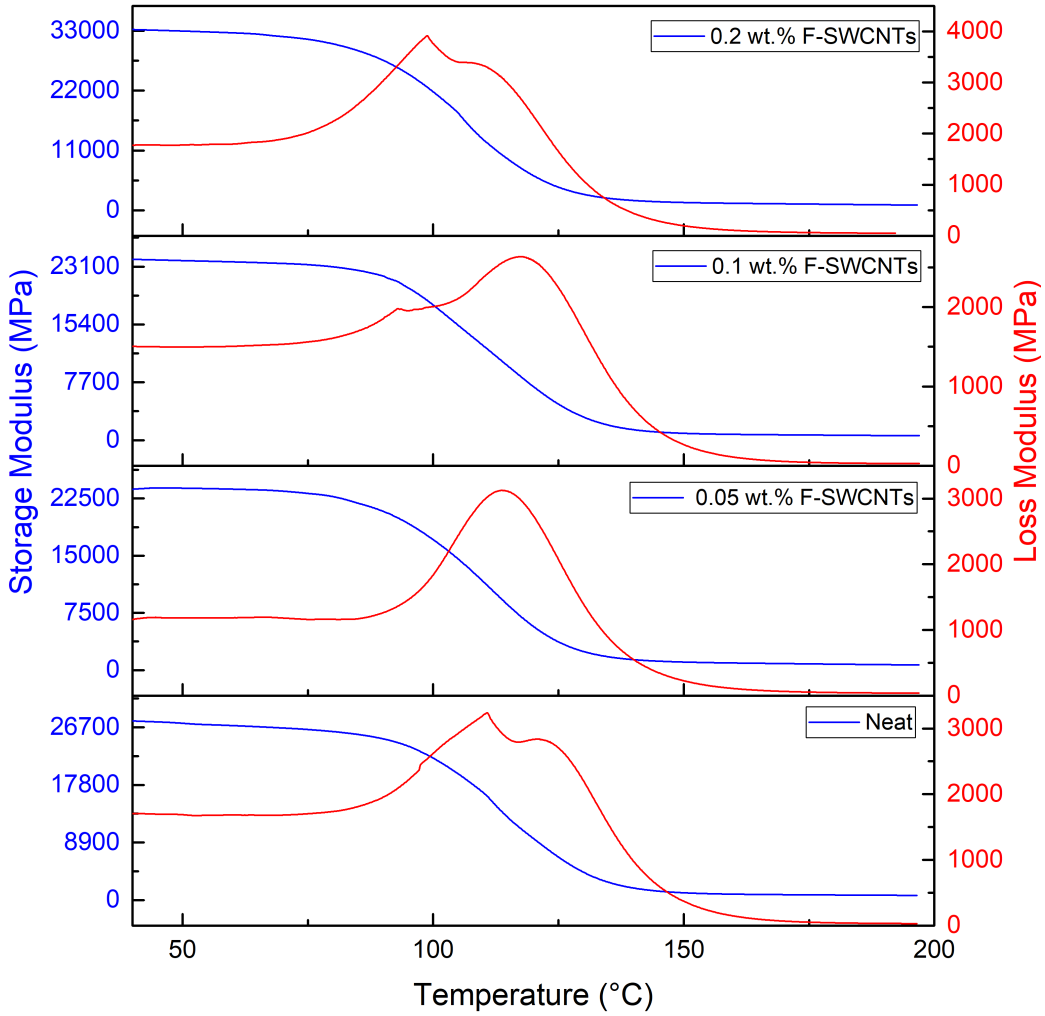

Figure 7.34. Storage modulus (E') and loss modulus (E'') of the composites with/without F-SWCNTs

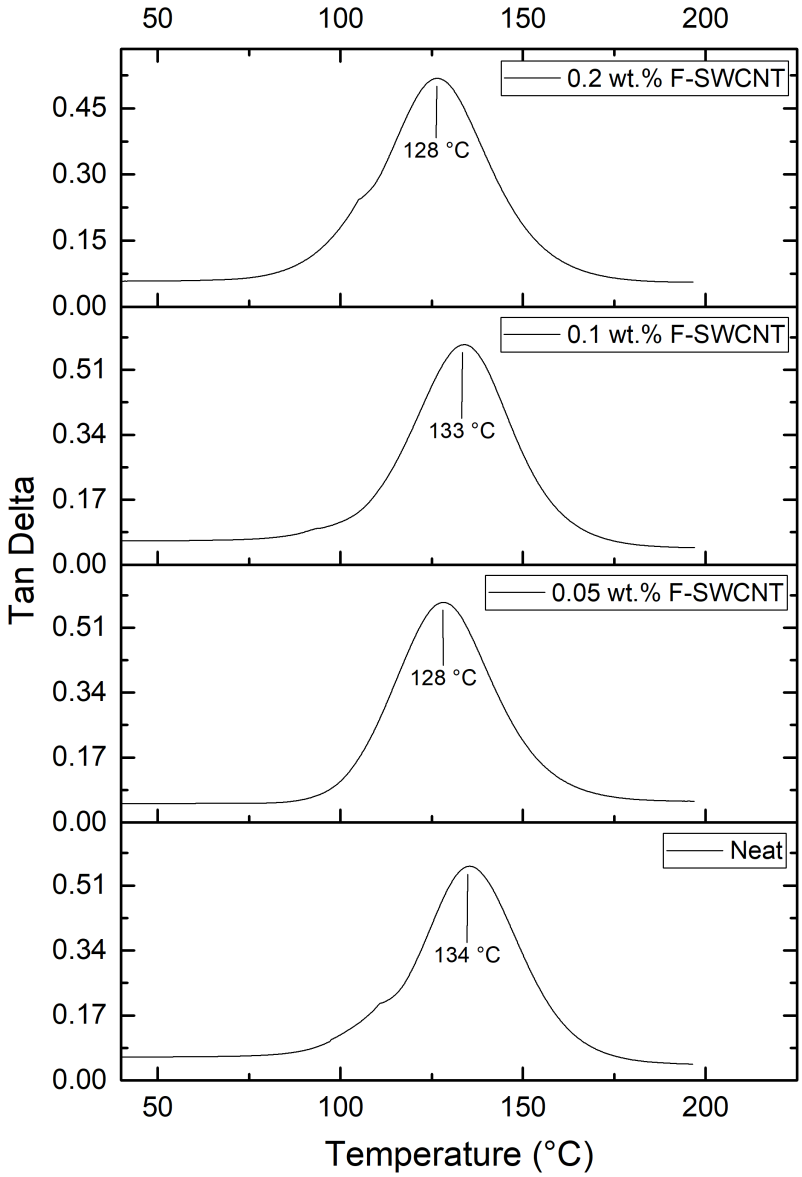

Figure 7.35. Tanδ values of the composites with/without F-SWCNTs

Table 7.10. Summary of average mechanical and thermomechanical properties of CFRP composites fabricated with/without F-SWCNTs. The value in the parentheses indicates the percentage enhancement in the corresponding properties

F-SWCNT Content of Hybrid Composite (wt.%)	Tensile Strength (MPa)	Modulus of Elasticity (GPa)	Flexural Strength (MPa)	Impact Strength (kJ/m2)	Interlaminar Shear Strength (MPa)	T_g Values (°C)
Neat	770.57	68.70	751.17	87.28	33.14	128
0.05	907.22 (18%)	65.25 (-5%)	918.26 (23%)	94.78 (9%)	38.17 (15%)	133
0.1	814.83 (6%)	67.96 (-1%)	716.59 (-4%)	99.59 (14%)	40.03 (21%)	128
0.2	705.82 (-8%)	60.44 (-12)	658.30 (-12%)	85.88 (-2%)	42.37 (30%)	134

Summary of average mechanical and thermomechanical properties of prepreg-based CFRP composites with/without F-SWCNTs was given in Table 7.10. The enhancement in the corresponding properties was shown in the parentheses. Optimum mechanical properties of F-SWCNTs filled CFRP composite was achieved at 0.05 wt.% of F-SWCNTs. However, mechanical properties were decreased due to the addition of higher content of F-SWCNTs, in comparison with neat CFRP. This may be attributed to the non-homogenous dispersion of CNTs and the formation of CNT agglomeration at relatively high contents. The thermomechanical characterization of the CFRP composites showed that there was no significant effect of CNT incorporation on the T_g values.

Improving the performance of fiber-reinforced polymer composites using nanotechnology will be possible by transferring the external load applied to the CNT/polymer composites to the CNTs and allowing them to take most of the load. The efficiency of charge transfer depends on the strength of the interfacial bond between the filler and the matrix material. A strong interfacial adhesion enables composites to achieve high mechanical properties through enhanced charge transfer from the matrix to the CNT.

CHAPTER 8

CONCLUDING REMARKS

Prepreg is materials obtained by the development of a reinforcing fabric pre-impregnated with a resin system. The resin system used already contains the appropriate curing agent. By impregnating the optimum amount of resin system into the reinforcing fabric, all the excess of manual placement during the curing process – resin pots, drips – is eliminated. Pressure and heat must be used together for the prepregs, which are readily placed on the mold, to cure and turn into a laminate. With a homogeneously pre-impregnated resin system, the laminate thickness will be uniform, and there is a theoretical possibility that each part coming out of the mold will be the same. Thus, it has superior properties in terms of part integrity and repeatability aspects. There are mainly four types of manufacturing methods for prepregs: solution dip, solution spray, holt melt, and film calendaring. Solvent dip and hot melt methods are widely used for practical applications. Both methods are based on the same principle, reducing the viscosity of the resin to impregnate properly the fiber bed. Thanks to the developed OoA prepregs, it has fewer curing times and minimizes operational costs. Laminates obtained after applied temperature and pressure have high fiber volume ratios and exhibit maximum strength properties.

Hybrid composites (also known as multiscale or hierarchical or nano-engineered composites) consist of at least two components with different size scales. The components usually consist of continuous fibers as in conventional composite structures and nanofillers that provide additional structural and functional properties. Nanofillers are expected to be incorporated homogeneously into the matrix component of the composite structure and add many features such as stronger bonding with continuous fibers. As in the presented study, the incorporation of CNTs as a nano-scale filler into a polymer matrix with continuous fiber reinforcements to produce hybrid composites attracts attention as one of the most well-seen subjects. The distribution of CNTs even in very small amounts into the polymer matrix has created great improvements, especially in the mechanical and thermal properties of the composite structure. The biggest challenge in the development of nanostructured composites by incorporating the outstanding properties of CNTs into

the polymer is to achieve a homogeneous and stable dispersion for improving strength properties. The performance of the CNT / polymer nanocomposite is improved by the functionalization process of CNTs. By changing the surface properties of CNTs with functionalization, the possibility of bonding with the medium in which it will be dispersed is increased. Strong bonds can be established with the polymer by forming defects in the sidewalls and open ends of CNTs by an oxidative process with strong acids such as HNO_3, H_2SO_4, or their mixture. As a result of the oxidation process, bonds with carboxylic acid (–COOH) or hydroxyl (–OH) groups are observed on the sidewalls of CNTs, and these bonds interact with polymers such as epoxy. The dispersion of CNTs into the polymer matrix in composite applications is generally performed mechanically. The most common mechanical methods are ultrasonication, calendaring, ball milling, stir, and extrusion, respectively. While the dispersion of CNTs can be carried out with only one of these techniques, it can also be done in a multi-step manner.

In this thesis, the aim is the preparation and characterization of laboratory-scale innovative CF/epoxy-based prepregs and their composites with/without carbon nanotubes. One of the novelties of the study relates to preparing modified epoxy resin and CF prepreg systems by incorporation of single-walled carbon nanotubes (SWCNTs) with multi-step dispersion techniques. To affect dispersion characteristics, SWCNTs were functionalized by oxidizing their surface with the carboxyl (-COOH) group using acid treatment. The modified resin system contained 0.05, 0.1, and 0.2 wt. % F-SWCNTs. FTIR spectroscopy was performed to identify new bonding groups formed after the F-SWCNTs. Unidirectional CF reinforced prepregs were prepared using the drum-type winding technique. For the fabrication of prepreg-based composite laminates, a vacuum bag-only method was performed.

Viscosity is the most important parameter for preparing prepregs to achieve good wetting of fibers. Siddiquie et al. noticed that viscosity must vary between 1.5 – 2.5 Pa.s for prepreg preparing. Rheological characterization was performed to take place in the desired range. Then, the drum-type prepreg process involves winding the filaments under tension on a rotating mandrel. As the mandrel rotates around the rotation axis, the pay-out eye on a carriage passes horizontally concerning the axis of the rotating mandrel, placing the filaments in the desired pattern or angle. The desired pattern per circuit is applied on the mandrel while impregnated in a bath with resin. The hoop pattern, in which the winding angle is 90°, creates UD products. The drum-type winding machine was modified by utilizing a solvent dip (solution impregnation) method using modified F-

SWCNTs dispersed within the epoxy resin system and carbon filaments. The prepreg system was controlled by the fiber feeding mechanism, and the rate of rotation of the mandrel in the control unit. After completion of the winding of the UD prepreg, the solvent was evaporated from the prepreg, and the resin reached B-stage using a drying oven according to the resin formulation. Prepregs had two different sides as a dry and resin-rich side. Dimensions of the manufactured prepreg were 600 mm x 1000 mm.

The thermal characterization of laboratory-scale was applied for carbon fiber/epoxy-based prepregs by incorporating F-SWCNTs. Investigation of the cure behavior of a prepreg system is crucial for the characterization and optimization of fiber-reinforced polymeric composites. The effect of F-SWCNTs on the curing process and kinetic parameters of the carbon fiber/epoxy-based prepregs were investigated using non-isothermal DSC. Analysis of curing behavior by DSC under linear heating presented thermograms indicating an exothermic peak. OriginPro was performed using the linear least square method to process DSC thermograms. Cure kinetic parameters the degree of cure, α, reaction rate, dα/dt can be extracted from thermograms. The activation energy of the curing reaction was calculated by the isoconversional methods as Kissinger-Akahira-Sunose (KAS), Flynn-Wall-Ozawa (FWO), and Kissinger method. However, the relative higher values of E_α computed by the FWO method could be explained by the worst approximation for temperature integral. It can be concluded that the more accurate method is KAS. The other novelty of the presented thesis is the new numerical approach for the determination activation energy of the thermosetting materials. It was proposed a new algorithm (GMN) for determining pre-exponential and activation energy of curing process by researchers of the presented thesis and Prof. Gamze Tanoğlu's Research Group (Murat Öz, Neslişah İmamoğlu). This method is based on the combination of the fitting for the measured conversion values via the least-squares minimization technique and linear fitting for the kinetic parameters.

Chemical, mechanical, and thermomechanical characterization was carryout out to investigate the effect of F-SWCNTs on prepreg-based CFRP composites. The fiber volume fractions of the samples changed between 55.3% and 50.16%. In most applications, fiber volume fractions of CFRP laminates are generally expected to lie between 45% and 60%. The mechanical results indicated that successful dispersion of the SWCNTs in the polymer matrix was achieved by the functionalization process, resulting in significant improvement for the mechanical behavior of the CFRP composites. Fiber-dominant properties (i.e., Tensile behavior) of CFRP composites could be improved by

an innovative resin system containing F-SWCNTs. It was revealed that the composites containing F-SWCNTs have higher toughness and energy absorption values. Moreover, the improvement of impact behavior was achieved by incorporating F-SWCNTs acting as a barrier to the branching effect of crack propagation. Matrix-dominant property (i.e., ILSS) was improved with the addition of F-SWCNTs in prepreg-based laminates, providing successful load transfer between F-SWCNTs and resin. No proper relationship existed between the variation of F-SWCNTs content and glass transition temperature in the presented thesis.

With the production and characterization studies, the performances of prepregs and their composites have been improved by the addition of nano-sized fillers. The presented thesis will be a guide for the development studies to be made in this field by examining the methodology and results used.

8.1. Future Works

The presented thesis is one of the most comprehensive studies on prepregs containing nano-sized fillers. Prepregs were prepared by dispersing functionalized nano-sized fillers in the matrix and impregnating carbon fiber reinforcement fabrics. Also, meter-level composites structures were fabricated and examined with microstructural investigations. Therefore, the feature of being comprehensive comes from analyzes in many different dimensions. The studies containing development, fabrication, and characterization topics have brought many important subjects that need to be improved. Some of these topics that are worth studying in the future are outlined below.

- Transmission Electron Microscopy (TEM) provides a much higher resolution than SEM to display dispersion of SWCNTs. TEM should be the preferred method to directly measure nanoparticle size, grain size, size distribution, and morphology at fracture areas.
- Dispersion of nanoparticles within the matrix increases the viscosity of the resin system. Therefore, the effect of adding SWCNTs on the rheological behavior of the resin system should be investigated to optimize the processing parameters for prepregging process.

- Covalent functionalization of the SWCNTs provides strong bonding between the nanoparticle and the matrix. However, there are some studies about the fragmentation of CNTs during the covalent functionalization that have been reported. The employment of strong acids combined with high power sonication cycles results in creating numerous defects on the CNTs sidewalls. Extensive damage to CNTs causes degradation of mechanical, electrical, and thermal properties. Further research could examine the effect of functionalization and dispersion on these properties.
- The investment cost of the solvent dip process used in the presented study is much lower than the hot-melt manufacturing process. However, it weakens the overall strength of the final composite material because of the solvent used in the process being trapped inside the prepreg sequence. Also, it may affect product quality as the solvent evaporates, changing the moisture content of the prepreg system. For further studies, this problem has to be minimized.
- Curing temperatures (T_{onset}, T_{offset}, etc.) of prepregs were determined from thermal characterization by DSC in non-isothermal measurements. However, much detailed thermal analysis of prepregs should be performed to achieve full information (time vs temperature) about the cure cycle.
- Optimization of prepregging parameters (fiber tension, mandrel rotational speed, winding angle) should be performed to improve the fabrication process.
- The effect of bagging arrangement on air permeability was investigated visually. It should be also calculated and discussed by designing a testing procedure for in-plane and transverse air permeability.
- Cure kinetics of nanoengineered thermosetting materials should be examined to establish mathematical relationships between the process rate, degree of cure, temperature, and CNTs. The effect of CNTs content on the reaction model could provide novel numerical approaches for determining curing mechanisms.
- The effect of the addition of SWCNTs on the interlaminar fracture toughness of prepreg-based CFRP should be studied to improve the interlaminar properties of the composites.

APPENDIX

PRODUCED MATLAB CODE FOR CURE KINETICS

```
%Matlab Code for the GMN method
T Vector of temperature
Y Convers ion from DSC
TT=T+273; %Kelvin
c1=0.0765;
c2=358.3126;
n=1.4;
m=0.6;
B=2.5; %C/min
BB=B/60; %K/ s e c
R=8.314;
y=@( x ) 0 . 5 * ( tanh( c1 *(x=c2 )=3)+1);
ee=max( abs ( y (TT)=Y) )
xx = linspace (TT( 1 ) ,TT(end ) ) ;
figure ( 1 )
plot (TT,Y, 'b* ' , xx , y ( xx ) , ' r=' )
legend( ' experimental ' , ' f i t ' , ' Location ' , ' northwest ' )
xlabel ( 'T' , ' FontSize ' , 1 2 , . . .
' FontWeight ' , ' bold ' , ' Color ' , ' k ' )
ylabel ( ' n alpha (T) ' , ' FontSize ' , 1 2 , . . .
' FontWeight ' , ' bold ' , ' Color ' , ' k ' )
dy=@( x ) 0.5* c1 *( sech( c1 *(x=c2 ) =3 ) . ^ 2 ) ;
f=@( x ) ( ( 0 . 5 * ( tanh( c1 *(x=c2 ) =3)+1) ) .^(m) ) . * ( 1 =0 . 5 * ( tanh( c1
*(x=c2 ) =3)+1) ) .^(n ) ;
G=dy (TT) . / f (TT) ;
X==1./(R*TT) ;
YY=log (BB*G) ;
```

```
p=polyf i t (X,YY, 1 ) ;
lnA=p ( 2 ) ;
E=p ( 1 ) ;
E1=E/10^3
A1=exp( lnA ) ; % linearfit
```

REFERENCES

[1] F. L. Matthews and R. D. Rawlings, Composite materials: engineering and science: Woodhead Publishing, 1999.

[2] P. Hubert and A. Poursartip, "A review of flow and compaction modeling relevant to thermoset matrix laminate processing," Journal of reinforced plastics and composites, vol. 17, pp. 286-318, 1998.

[3] B. D. Harper, G. H. Staab, and R. S. Chen, "A Note on the Effects of Voids Upon the Hygral and Mechanical Properties of AS4/3502 Graphite/Epoxy," Journal of Composite Materials, vol. 21, pp. 280-289, March 1, 1987.

[4] P. Olivier, J. Cottu, and B. Ferret, "Effects of cure cycle pressure and voids on some mechanical properties of carbon/epoxy laminates," Composites, vol. 26, pp. 509-515, 1995.

[5] L. K. Grunenfelder and S. R. Nutt, "Void formation in composite prepregs–Effect of dissolved moisture," Composites Science and Technology, vol. 70, pp. 2304-2309, 2010.

[6] Bianchi, I., Forcellese, A., Marconi, M., Simoncini, M., Vita, A., & Castorani, V. (2021). Environmental impact assessment of zero waste approach for carbon fiber prepreg scraps. Sustainable Materials and Technologies, e00308.

[7] Garofalo, J., & Walczyk, D. (2021). In situ impregnation of continuous thermoplastic composite prepreg for additive manufacturing and automated fiber placement. Composites Part A: Applied Science and Manufacturing, 147, 106446.

[8] C. Ridgard, "Out of autoclave composite technology for aerospace, defense and space structures," Proceedings of SAMPE 2009, Baltimore, MD, May 2009.

[9] Ridgard, C. (2010). Next generation out of autoclave systems. *Proc SAMPE*.

[10] van Grootel, A., Chang, J., Wardle, B. L., & Olivetti, E. (2020). Manufacturing variability drives significant environmental and economic impact: The case of carbon fiber reinforced polymer composites in the aerospace industry. Journal of Cleaner Production, 261, 121087.

[11] Song, Y. S., Youn, J. R., & Gutowski, T. G. (2009). Life cycle energy analysis of fiber-reinforced composites. *Composites Part A: Applied Science and Manufacturing*, *40*(8), 1257-1265.

[12] Hayes, B. S., & Seferis, J. C. (1997). The effect of fabric tension and the number of impregnation rollers on woven fabric prepreg quality and cured laminates. *Composites Part A: Applied Science and Manufacturing*, *28*(9-10), 791-799.

[13] Ahn, K. J., & Seferis, J. C. (1993). Prepreg processing science and engineering. *Polymer Engineering & Science*, *33*(18), 1177-1188.

[14] Romano, M., Eisenried, M., Jungbauer, B., Ehrlich, I., & Gebbeken, N. (2015). Influence of parameters of the production process on the material quality of unidirectionally reinforced prepregs. *Journal of Achievements in Materials and Manufacturing Engineering*, *68*(1), 32-44.

[15] Budelmann, D., Schmidt, C., & Meiners, D. (2020). Prepreg tack: A review of mechanisms, measurement, and manufacturing implication. Polymer Composites, 41(9), 3440-3458.

[16] Liu, L., Zhang, B. M., Wang, D. F., & Wu, Z. J. (2006). Effects of cure cycles on void content and mechanical properties of composite laminates. *Composite structures*, *73*(3), 303-309.

[17] Birt, E. A., & Smith, R. A. (2004). A review of NDE methods for porosity measurement in fibre-reinforced polymer composites. *Insight-Non-Destructive Testing and Condition Monitoring*, *46*(11), 681-686.

[18] Mehdikhani, M., Gorbatikh, L., Verpoest, I., & Lomov, S. V. (2019). Voids in fiber-reinforced polymer composites: A review on their formation, characteristics, and effects on mechanical performance. *Journal of Composite Materials*, *53*(12), 1579-1669.

[19] Lubin, G. (2013). *Handbook of composites*. Springer Science & Business Media.

[20] Rajaei, M., Beheshty, M. H., & Hayaty, M. (2011). Preparation and processing characterization of glass/phenolic prepregs. *Polymers and Polymer Composites*, *19*(9), 789-796.

[21] Cocchıerı Cotelho, E., Cerqueıra Rezende, M., & Scherbakoff, N. (2001). Rheological studies applied in the processing and characterization of carbon/carbon composites. *Journal of advanced materials*, *33*(4), 44-51.

[22] Botelho, E. C., Scherbakoff, N., & Rezende, M. C. (2000). Rheological analysis of the phenolic and furfuryl resins used in the carbon materials processing. *Materials Research*, *3*, 19-23

[23] Siddiqui, N. A., Khan, S. U., Ma, P. C., Li, C. Y., & Kim, J. K. (2011). Manufacturing and characterization of carbon fibre/epoxy composite prepregs containing carbon nanotubes. *Composites Part A: Applied Science and Manufacturing*, *42*(10), 1412-1420.

[24] Jang, B. Z. (1994). Advanced polymer composites: principles and applications. *ASM International, Materials Park, OH 44073-0002, USA, 1994. 305*.

[25] Peters, S. T. (Ed.). (2013). *Handbook of composites*. Springer Science & Business Media.

[26]. Shin, D. D., & Hahn, H. T. (2004). Compaction of thick composites: simulation and experiment. *Polymer Composites*, *25*(1), 49-59.

[27] Saad, M. T., Miller, S. G., & Marunda, T. (2014, November). Thermal characterization of IM7/8552-1 carbon-epoxy composites. In *ASME International mechanical engineering congress and exposition* (Vol. 46569, p. V08BT10A091). American Society of Mechanical Engineers.

[28] Shen, J., Huang, W., Wu, L., Hu, Y., & Ye, M. (2007). The reinforcement role of different amino-functionalized multi-walled carbon nanotubes in epoxy nanocomposites. *Composites Science and Technology*, *67*(15-16), 3041-3050.

[29] Hirose, S., Hatakeyama, T., & Hatakeyama, H. (2005, April). Curing and glass transition of epoxy resins from ester-carboxylic acid derivatives of mono-and disaccharides, and alcoholysis Lignin. In *Macromolecular Symposia* (Vol. 224, No. 1, pp. 343-354). Weinheim: WILEY-VCH Verlag.

[30] Francis, B., Thomas, S., Jose, J., Ramaswamy, R., & Rao, V. L. (2005). Hydroxyl terminated poly (ether ether ketone) with pendent methyl group toughened epoxy

resin: miscibility, morphology and mechanical properties. *Polymer*, *46*(26), 12372-12385.

[31] Ayadi, A., Nouri, H., Guessasma, S., & Roger, F. (2015). An original approach to assess elastic properties of a short glass fibre reinforced thermoplastic combining X-ray tomography and finite element computation. *Composite Structures*, *125*, 277-286.

[32] Ayadi, A., Nouri, H., Guessasma, S., & Roger, F. (2016). Large-scale X-ray microtomography analysis of fiber orientation in weld line of short glass fiber reinforced thermoplastic and related elasticity behavior. *Macromolecular Materials and Engineering*, *301*(8), 907-921.

[33] Ayadi, A., Nouri, H., Guessasma, S., & Roger, F. (2016). Determination of orthotropic properties of glass fibre reinforced thermoplastics using X-ray tomography and multiscale finite element computation. *Composite Structures*, *136*, 635-649.

[34] Nouri, H., Guessasma, S., Roger, F., Ayadi, A., & Maitournam, H. (2017). Exploring damage kinetics in short glass fibre reinforced thermoplastics. *Composite Structures*, *180*, 63-74.

[35] Gu, J., Dong, W., Xu, S., Tang, Y., Ye, L., & Kong, J. (2017). Development of wave-transparent, light-weight composites combined with superior dielectric performance and desirable thermal stabilities. *Composites Science and Technology*, *144*, 185-192.

[36] Jin, F. L., Ma, C. J., & Park, S. J. (2011). Thermal and mechanical interfacial properties of epoxy composites based on functionalized carbon nanotubes. *Materials Science and Engineering: A*, *528*(29-30), 8517-8522.

[37] Xie, X. L., Mai, Y. W., & Zhou, X. P. (2005). Dispersion and alignment of carbon nanotubes in polymer matrix: a review. *Materials science and engineering: R: Reports*, *49*(4), 89-112.

[38] Ajayan, P. M., Stephan, O., Colliex, C., & Trauth, D. (1994). Aligned carbon nanotube arrays formed by cutting a polymer resin—nanotube composite. *science*, *265*(5176), 1212-1214.

[39] Koo, J. H. (2019). *Polymer nanocomposites: processing, characterization, and applications*. McGraw-Hill Education.

[40] Ajayan, P. M., Schadler, L. S., & Braun, P. V. (2006). *Nanocomposite science and technology*. John Wiley & Sons.

[41] Yakobson, B. I., & Avouris, P. (2001). Mechanical properties of carbon nanotubes. *Carbon nanotubes*, 287-327.

[42] Qian, D., Wagner, and, G. J., Liu, W. K., Yu, M. F., & Ruoff, R. S. (2002). Mechanics of carbon nanotubes. *Appl. Mech. Rev.*, *55*(6), 495-533.

[43] Reich, S., Thomsen, C., & Maultzsch, J. (2008). *Carbon nanotubes: basic concepts and physical properties*. John Wiley & Sons.

[44]. Yu, M. F., Lourie, O., Dyer, M. J., Moloni, K., Kelly, T. F., & Ruoff, R. S. (2000). Strength and breaking mechanism of multiwalled carbon nanotubes under tensile load. *Science*, *287*(5453), 637-640.

[45] Wong, E. W., Sheehan, P. E., & Lieber, C. M. (1997). Nanobeam mechanics: elasticity, strength, and toughness of nanorods and nanotubes. *science*, *277*(5334), 1971-1975.

[46] Ajayan, P. M., Stephan, O., Colliex, C., & Trauth, D. (1994). Aligned carbon nanotube arrays formed by cutting a polymer resin—nanotube composite. *science*, *265*(5176), 1212-1214.

[47] Du, J., Bai, J., & Cheng, H. (2007). The present status and key problems of carbon nanotube based polymer composites. *Express Polymer Letters*, *1*(5), 253-273.

[48] Díez-Pascual, A. M., Naffakh, M., Marco, C., Ellis, G., & Gómez-Fatou, M. A. (2012). High-performance nanocomposites based on polyetherketones. *Progress in Materials Science*, *57*(7), 1106-1190.

[49] Bose, S., Bhattacharyya, A. R., Kulkarni, A. R., & Pötschke, P. (2009). Electrical, rheological and morphological studies in co-continuous blends of polyamide 6

and acrylonitrile–butadiene–styrene with multiwall carbon nanotubes prepared by melt blending. *Composites Science and Technology*, *69*(3-4), 365-372.

[50] Menzer, K., Krause, B., Boldt, R., Kretzschmar, B., Weidisch, R., & Pötschke, P. (2011). Percolation behaviour of multiwalled carbon nanotubes of altered length and primary agglomerate morphology in melt mixed isotactic polypropylene-based composites. *Composites Science and Technology*, *71*(16), 1936-1943.

[51] Thomas, S. P., Girei, S. A., Atieh, M. A., De, S. K., & Al-Juhani, A. (2012). Rheological behavior of polypropylene nanocomposites at low concentration of surface modified carbon nanotubes. *Polymer engineering & science*, *52*(9), 1868-1873.

[52] Zhou, K., Gu, S. Y., Zhang, Y. H., & Ren, J. (2012). Effect of dispersion on rheological and mechanical properties of polypropylene/carbon nanotubes nanocomposites. *Polymer Engineering & Science*, *52*(7), 1485-1494.

[53] Penu, C., Hu, G. H., Fernandez, A., Marchal, P., & Choplin, L. (2012). Rheological and electrical percolation thresholds of carbon nanotube/polymer nanocomposites. *Polymer Engineering & Science*, *52*(10), 2173-2181.

[54] Díez-Pascual, A. M., Naffakh, M., Marco, C., & Ellis, G. (2012). Mechanical and electrical properties of carbon nanotube/poly (phenylene sulphide) composites incorporating polyetherimide and inorganic fullerene-like nanoparticles. *Composites Part A: Applied Science and Manufacturing*, *43*(4), 603-612.

[55] Ribeiro, B. (2015). Obtenção e caracterização de compósitos nanoestruturados de poli (sulfeto de fenileno) reforçados com nanotubos de carbono.

[56] Botelho, E. C., Costa, M. L., Braga, C. I., Burkhart, T., & Lauke, B. (2013). Viscoelastic behavior of multiwalled carbon nanotubes into phenolic resin. *Materials Research*, *16*(4), 713-720.

[57] Xie, S., Li, W., Pan, Z., Chang, B., & Sun, L. (2000). Mechanical and physical properties on carbon nanotube. *Journal of Physics and Chemistry of solids*, *61*(7), 1153-1158.

[58] Falvo, M. R., Clary, G. J., Taylor, R. 2., Chi, V., Brooks, F. P., Washburn, S., & Superfine, R. (1997). Bending and buckling of carbon nanotubes under large strain. *Nature*, *389*(6651), 582-584.

[59] Bower, C., Rosen, R., Jin, L., Han, J., & Zhou, O. (1999). Deformation of carbon nanotubes in nanotube–polymer composites. *Applied physics letters*, *74*(22), 3317-3319.

[60] Overney, G., Zhong, W., & Tomanek, D. (1993). Structural rigidity and low frequency vibrational modes of long carbon tubules. *Zeitschrift für Physik D Atoms, Molecules and Clusters*, *27*(1), 93-96.

[61] Ma, P. C., Siddiqui, N. A., Marom, G., & Kim, J. K. (2010). Dispersion and functionalization of carbon nanotubes for polymer-based nanocomposites: A review. *Composites Part A: Applied Science and Manufacturing*, *41*(10), 1345-1367.

[62] Esumi, K., Ishigami, M., Nakajima, A., Sawada, K., & Honda, H. (1996). Chemical treatment of carbon nanotubes. *Carbon (New York, NY)*, *34*(2), 279-281.

[63] Bilalis, P., Katsigiannopoulos, D., Avgeropoulos, A., & Sakellariou, G. (2014). Non-covalent functionalization of carbon nanotubes with polymers. *RSC advances*, *4*(6), 2911-2934.

[64] Morishita, T., Matsushita, M., Katagiri, Y., & Fukumori, K. (2010). Noncovalent functionalization of carbon nanotubes with maleimide polymers applicable to high-melting polymer-based composites. *Carbon*, *48*(8), 2308-2316.

[65] Spitalsky, Z., Tasis, D., Papagelis, K., & Galiotis, C. (2010). Carbon nanotube–polymer composites: chemistry, processing, mechanical and electrical properties. *Progress in polymer science*, *35*(3), 357-401.

[66] Ma, P. C., Siddiqui, N. A., Cao, S. G., Tang, B. Z., & Kim, J. K. (2008). Effect of dispersion and functionalization of carbon nanotubes (CNTs) on the properties of CNT/epoxy nanocomposites. In *2nd International Conference on Advanced Materials and Structures (ICAMS-2)*.

[67] Gojny, F. H., Wichmann, M. H. G., Köpke, U., Fiedler, B., & Schulte, K. (2004). Carbon nanotube-reinforced epoxy-composites: enhanced stiffness and fracture toughness at low nanotube content. *Composites science and technology*, *64*(15), 2363-2371.

[68] Geng, Y., Liu, M. Y., Li, J., Shi, X. M., & Kim, J. K. (2008). Effects of surfactant treatment on mechanical and electrical properties of CNT/epoxy nanocomposites. *Composites Part A: Applied Science and Manufacturing*, *39*(12), 1876-1883.

[69] Ma, P. C., Kim, J. K., & Tang, B. Z. (2007). Effects of silane functionalization on the properties of carbon nanotube/epoxy nanocomposites. *Composites science and technology*, *67*(14), 2965-2972.

[70] Sahoo, N. G., Jung, Y. C., Yoo, H. J., & Cho, J. W. (2006). Effect of functionalized carbon nanotubes on molecular interaction and properties of polyurethane composites. *Macromolecular chemistry and physics*, *207*(19), 1773-1780.

[71] Sui, G., Zhong, W. H., Yang, X. P., & Yu, Y. H. (2008). Curing kinetics and mechanical behavior of natural rubber reinforced with pretreated carbon nanotubes. *Materials Science and Engineering: A*, *485*(1-2), 524-531.

[72] Sun, L., Warren, G. L., O'reilly, J. Y., Everett, W. N., Lee, S. M., Davis, D., ... & Sue, H. J. (2008). Mechanical properties of surface-functionalized SWCNT/epoxy composites. *Carbon*, *46*(2), 320-328.

[73] Bekyarova, E., Thostenson, E. T., Yu, A., Itkis, M. E., Fakhrutdinov, D., Chou, T. W., & Haddon, R. C. (2007). Functionalized single-walled carbon nanotubes for carbon fiber− epoxy composites. *The Journal of Physical Chemistry C*, *111*(48), 17865-17871.

[74] Siddiqui, N. A., Khan, S. U., Ma, P. C., Li, C. Y., & Kim, J. K. (2011). Manufacturing and characterization of carbon fibre/epoxy composite prepregs containing carbon nanotubes. *Composites Part A: Applied Science and Manufacturing*, *42*(10), 1412-1420.

[75] Garcia, E. J., Wardle, B. L., & Hart, A. J. (2008). Joining prepreg composite interfaces with aligned carbon nanotubes. *Composites Part A: Applied Science and Manufacturing*, *39*(6), 1065-1070.

[76] Chen, W. J., Li, Y. L., Chiang, C. L., Kuan, C. F., Kuan, H. C., Lin, T. T., & Yip, M. C. (2010). Preparation and characterization of carbon nanotubes/epoxy resin nano-prepreg for nanocomposites. *Journal of Physics and Chemistry of Solids*, *71*(4), 431-435.

[77] Tariq, F., Shifa, M., & Baloch, R. A. (2018). Mechanical and Thermal Properties of Multi-scale Carbon Nanotubes-Carbon Fiber-Epoxy Composite. *Arabian Journal for Science & Engineering (Springer Science & Business Media BV)*, *43*(11).

[78] You, Y.Z.; Hong, C.Y.; Pan, C.Y. Functionalization of carbon nanotubes with well-defined functional polymers via thiol-coupling reaction. Macromol. Rapid Commun. 2006, 27, 2001–2006. [CrossRef]

[79] Liu, C.; Cheng, H.M.; Zhao, H.; Yang, F.; Zhang, X. Surface modification of single-walled carbon nanotubes with polyethylene via in situ Ziegler–Natta polymerization. J. Appl. Polym. Sci. 2004, 92, 3697–3700.

[80] Zhang, Y.; Li, Q.; Wang, W.; Guo, A.; Li, J.; Li, H. Efficient and robust reactions for polyethylene covalently grafted carbon nanotubes. Macromol. Chem. Phys. 2017, 218, 1600449. [CrossRef]

[81] Baudot, C.; Volpe, M.V.; Kong, J.C.; Tan, C.M. Epoxy Functionalized Carbon Nanotubes and Methods of Forming the Same. U.S. Patent 299,082, 12 April 2009.

[82] Díez-Pascual, A.M.; Naffakh, M. Grafting of an aminated poly(phenylene sulphide) derivative to functionalized single-walled carbon nanotubes. Carbon 2012, 50, 857–868. [CrossRef]

[83] Wu, W.; Zhang, S.; Li, Y.; Li, J.; Liu, L.; Qin, Y.; Guo, Z.-X.; Dai, L.; Ye, C.; Zhu, D. PVK-modified single walled carbon nanotubes with effective photo induced electron transfer. Macromolecules 2003, 36, 6286–6288. [CrossRef]

[84] Blake, R.; Gun'ko, Y.K.; Coleman, J.; Cadek, M.; Fonseca, A.; Nagy, J.B.; Blau, W.J. A generic organometallic approach toward ultra-strong carbon nanotube polymer composites. J. Am. Chem. Soc. 2004, 126, 10226–10227. [CrossRef]

[85] Qin, S.; Qin, D.; Ford, W.T.; Resasco, D.E.; Herrera, J.E. Functionalization of single-walled carbon nanotubes with polystyrene via grafting to and grafting from methods. Macromolecules 2004, 37, 752–757. [CrossRef]

[86] Li, H.; Cheng, F.; Duft, A.M.; Adronov, A. Functionalization of single walled carbon nanotubes with well-defined polystyrene by “click” coupling. J. Am. Chem. Soc. 2005, 127, 14518–14524. [CrossRef]

[87] Li, Z.; Dong, Y.; Haussler, M.; Lam, J.W.Y.; Dong, Y.; Wu, L. Synthesis of, light emission from, and optical power limiting in soluble single-walled carbon nanotubes functionalized by disubstituted polyacetylenes. J. Phys. Chem. B 2006, 110, 2302–2309.

[88] Xu, L., Fu, J. H., & Schlup, J. R. (1994). In situ near-infrared spectroscopic investigation of epoxy resin-aromatic amine cure mechanisms. *Journal of the American Chemical Society*, *116*(7), 2821-2826.

[89] Hodgkin, J. H., Simon, G. P., & Varley, R. J. (1998). Thermoplastic toughening of epoxy resins: a critical review. *Polymers for advanced technologies*, *9*(1), 3-10.

[90] Ratna, D., & Banthia, A. K. (2004). Rubber toughened epoxy. *Macromolecular research*, *12*(1), 11-21.

[91] Chikhi, N., Fellahi, S., & Bakar, M. (2002). Modification of epoxy resin using reactive liquid (ATBN) rubber. *European Polymer Journal*, *38*(2), 251-264.

[92] Hsieh, T. H., Kinloch, A. J., Masania, K., Lee, J. S., Taylor, A. C., & Sprenger, S. (2010). The toughness of epoxy polymers and fibre composites modified with rubber microparticles and silica nanoparticles. *Journal of materials science*, *45*(5), 1193-1210.

[93] Qiu, J., Zhang, C., Wang, B., & Liang, R. (2007). Carbon nanotube integrated multifunctional multiscale composites. *Nanotechnology*, *18*(27), 275708.

[94] Bekyarova, E., Thostenson, E. T., Yu, A., Kim, H., Gao, J., Tang, J., ... & Haddon, R. C. (2007). Multiscale carbon nanotube− carbon fiber reinforcement for advanced epoxy composites. *Langmuir*, *23*(7), 3970-3974

[95] Chen, W. J., Li, Y. L., Chiang, C. L., Kuan, C. F., Kuan, H. C., Lin, T. T., & Yip, M. C. (2010). Preparation and characterization of carbon nanotubes/epoxy resin

nano-prepreg for nanocomposites. *Journal of Physics and Chemistry of Solids*, *71*(4), 431-435.

[96] Ma, P. C., Kim, J. K., & Tang, B. Z. (2007). Effects of silane functionalization on the properties of carbon nanotube/epoxy nanocomposites. *Composites science and technology*, *67*(14), 2965-2972.

[97] Ma, P. C., Mo, S. Y., Tang, B. Z., & Kim, J. K. (2010). Dispersion, interfacial interaction and re-agglomeration of functionalized carbon nanotubes in epoxy composites. *Carbon*, *48*(6), 1824-1834.

[98] Shen, J., Huang, W., Wu, L., Hu, Y., & Ye, M. (2007). The reinforcement role of different amino-functionalized multi-walled carbon nanotubes in epoxy nanocomposites. *Composites Science and Technology*, *67*(15-16), 3041-3050.

[99] Hirose, S., Hatakeyama, T., & Hatakeyama, H. (2005, April). Curing and glass transition of epoxy resins from ester-carboxylic acid derivatives of mono-and disaccharides, and alcoholysis Lignin. In *Macromolecular Symposia* (Vol. 224, No. 1, pp. 343-354). Weinheim: WILEY-VCH Verlag.

[100] Francis, B., Thomas, S., Jose, J., Ramaswamy, R., & Rao, V. L. (2005). Hydroxyl terminated poly (ether ether ketone) with pendent methyl group toughened epoxy resin: miscibility, morphology and mechanical properties. *Polymer*, *46*(26), 12372-12385.

[101] Pizzutto, C. E., Suave, J., Bertholdi, J., Pezzin, S. H., Coelho, L. A. F., & Amico, S. C. (2010). Mechanical and dilatometric properties of carboxylated swcnt/epoxy composites: effects of the dispersion in the resin and in the hardener. *Journal of Reinforced Plastics and Composites*, *29*(4), 524-530.

[102] Callister Jr, W. D. (2002). Ciência e Engenharia de Materiais: Uma introdução, 5ª edição. *Rio de Janeiro: LTC*.

[103] Oriakhi, C. O. (2000). Polymer nanocomposition approach to advanced materials. *Journal of Chemical Education*, *77*(9), 1138.

[104] Tao, K., Yang, S., Grunlan, J. C., Kim, Y. S., Dang, B., Deng, Y., ... & Wei, X. (2006). Effects of carbon nanotube fillers on the curing processes of epoxy resin-based composites. *Journal of Applied Polymer Science*, *102*(6), 5248-5254.

[105] Zhou, T., Wang, X., Liu, X., & Xiong, D. (2009). Influence of multi-walled carbon nanotubes on the cure behavior of epoxy-imidazole system. *Carbon*, *47*(4), 1112-1118.

[106] Hakiki, F., Salam, D. D., Akbari, A., Nuraeni, N., Aditya, W., & Siregar, S. (2015, October). Is epoxy-based polymer suitable for water shut-off application?. In *SPE/IATMI Asia Pacific Oil & Gas Conference and Exhibition*. OnePetro.

[107] Hamerton, I. (1996). *Recent developments in epoxy resins*(Vol. 91). iSmithers Rapra Publishing.

[108] Xu, L., & Schlup, J. R. (1998). Etherification versus amine addition during epoxy resin/amine cure: An in situ study using near-infrared spectroscopy. *Journal of applied polymer science*, *67*(5), 895-901.

[109] Stark, W., & Bohmeyer, W. (2013). Non-destructive evaluation (NDE) of composites: Using ultrasound to monitor the curing of composites. In *Non-Destructive Evaluation (NDE) of Polymer Matrix Composites* (pp. 136-181). Woodhead Publishing.

[110] Hamerton, I. (1996). *Recent developments in epoxy resins*(Vol. 91). iSmithers Rapra Publishing.

[111] Cai, H., Li, P., Sui, G., Yu, Y., Li, G., Yang, X., & Ryu, S. (2008). Curing kinetics study of epoxy resin/flexible amine toughness systems by dynamic and isothermal DSC. *Thermochimica Acta*, *473*(1-2), 101-105.

[112] Sbirrazzuoli, N., Girault, Y., & Elégant, L. (1997). Simulations for evaluation of kinetic methods in differential scanning calorimetry. Part 3—Peak maximum evolution methods and isoconversional methods. *Thermochimica Acta*, *293*(1-2), 25-37.

[113] Mahadevan, S., Giridhar, A., & Singh, A. K. (1986). Calorimetric measurements on as-sb-se glasses. *Journal of non-crystalline solids*, *88*(1), 11-34.

[114] Šesták, J., & Berggren, G. (1971). Study of the kinetics of the mechanism of solid-state reactions at increasing temperatures. *Thermochimica Acta*, *3*(1), 1-12.

[115] Vyazovkin, S., Burnham, A. K., Criado, J. M., Pérez-Maqueda, L. A., Popescu, C., & Sbirrazzuoli, N. (2011). ICTAC Kinetics Committee recommendations for

performing kinetic computations on thermal analysis data. *Thermochimica acta*, *520*(1-2), 1-19.

[116] Mahadevan, S., Giridhar, A., & Singh, A. K. (1986). Calorimetric measurements on as-sb-se glasses. *Journal of non-crystalline solids*, *88*(1), 11-34.

[117] Akahira, T., & Sunose, T. (1971). Method of determining activation deterioration constant of electrical insulating materials. *Res Rep Chiba Inst Technol (Sci Technol)*, *16*(1971), 22-31.

[118] Flynn, J. H., & Wall, L. A. (1966). General treatment of the thermogravimetry of polymers. *Journal of research of the National Bureau of Standards. Section A, Physics and chemistry*, *70*(6), 487.

[119] Kissinger, H. E. (1957). Reaction kinetics in differential thermal analysis. *Analytical chemistry*, *29*(11), 1702-1706.

[120] Saeb, M. R., Nonahal, M., Rastin, H., Shabanian, M., Ghaffari, M., Bahlakeh, G., ... & Puglia, D. (2017). Calorimetric analysis and molecular dynamics simulation of cure kinetics of epoxy/chitosan-modified Fe3O4 nanocomposites. *Progress in Organic Coatings*, *112*, 176-186.

[121] Zheng, X., Li, D., Feng, C., & Chen, X. (2015). Thermal properties and non-isothermal curing kinetics of carbon nanotubes/ionic liquid/epoxy resin systems. *Thermochimica Acta*, *618*, 18-25.

[122] Hardis, R., Jessop, J. L., Peters, F. E., & Kessler, M. R. (2013). Cure kinetics characterization and monitoring of an epoxy resin using DSC, Raman spectroscopy, and DEA. *Composites Part A: Applied Science and Manufacturing*, *49*, 100-108.

[123] Xie, H., Liu, B., Yuan, Z., Shen, J., & Cheng, R. (2004). Cure kinetics of carbon nanotube/tetrafunctional epoxy nanocomposites by isothermal differential scanning calorimetry. *Journal of Polymer Science Part B: Polymer Physics*, *42*(20), 3701-3712.

[124] Ryu, S. H., Sin, J. H., & Shanmugharaj, A. M. (2014). Study on the effect of hexamethylene diamine functionalized graphene oxide on the curing kinetics of epoxy nanocomposites. *European polymer journal*, *52*, 88-97.

[125] Borchardt, H. J., & Daniels, F. (1957). The application of differential thermal analysis to the study of reaction kinetics1. *Journal of the American Chemical Society*, *79*(1), 41-46.

[126] Ozawa, T. (1970). Kinetic analysis of derivative curves in thermal analysis. *Journal of thermal analysis*, *2*(3), 301-324.

[127] Flynn, J. H., & Wall, L. A. (1966). A quick, direct method for the determination of activation energy from thermogravimetric data. *Journal of Polymer Science Part B: Polymer Letters*, *4*(5), 323-328.

[128] Akahira, T., & Sunose, T. (1971). Method of determining activation deterioration constant of electrical insulating materials. *Res Rep Chiba Inst Technol (Sci Technol)*, *16*(1971), 22-31.

[129] Siddiqui, N. A., Khan, S. U., Ma, P. C., Li, C. Y., & Kim, J. K. (2011). Manufacturing and characterization of carbon fibre/epoxy composite prepregs containing carbon nanotubes. *Composites Part A: Applied Science and Manufacturing*, *42*(10), 1412-1420.

[130] Wu, X., Zhan, L., Li, S., & Li, W. (2017). Study on the Cure Kinetics of Epoxy Resin Prepreg in Fiber Metal Laminates. In *MATEC Web of Conferences* (Vol. 88, p. 02004). EDP Sciences.

[131] Kumar, A. A., & Sundaram, R. (2016). Cure cycle optimization for the resin infusion technique using carbon nanotube additives. *Carbon*, *96*, 1043-1052.

[132] Abdalla, M., Dean, D., Robinson, P., & Nyairo, E. (2008). Cure behavior of epoxy/MWCNT nanocomposites: the effect of nanotube surface modification. *Polymer*, *49*(15), 3310-3317.

[133] Fang, Z., Wang, J., Gu, A., & Tong, L. (2007). Curing behavior and kinetic analysis of epoxy resin/multi-walled carbon nanotubes composites. *Frontiers of Materials Science in China*, *1*(4), 415-422.

[134] Cividanes, L. S., Simonetti, E. A., Moraes, M. B., Fernandes, F. W., & Thim, G. P. (2014). Influence of carbon nanotubes on epoxy resin cure reaction using different techniques: a comprehensive review. *Polymer Engineering & Science*, *54*(11), 2461-2469.

[135] Roberts, T. (2007). Rapid growth forecast for carbon fibre market. *Reinforced Plastics*, *51*(2), 10-13.

[136] Dirk, H. J. L., Ward, C., & Potter, K. D. (2012). The engineering aspects of automated prepreg layup: History, present and future. *Composites Part B: Engineering*, *43*(3), 997-1009.

[137] Mills, A. (2001). Automation of carbon fibre preform manufacture for affordable aerospace applications. *Composites Part A: Applied science and manufacturing*, *32*(7), 955-962.

[138] Campbell Jr, F. C. (2011). *Manufacturing technology for aerospace structural materials*. Elsevier.

[139] Thorfinnson, B., & Biermann, T. F. (1986, April). Production of void free composite parts without debulking. In *31st International SAMPE symposium* (pp. 480-490).

[140] Davé, R. S., & Loos, A. C. (2000). *Processing of composites*(p. 320). Munich: Hanser Publishers.

[141]. Thorfinnson, B., & Biermann, T. F. (1987). Degree of Impregnation of Prepregs--Effects on Porosity. *Advanced Materials Technology'87*, 1500-1509.

[142] Palardy-Sim, M. (2016). *Evaluation and Impact of the Degree of Impregnation of Uncured Out-of-Autoclave Prepreg*. McGill University (Canada).

[143] Ridgard, C. (2000). Advances in low temperature curing prepregs for aerospace structures. In *SAMPE 2000: 45 th International SAMPE Symposium and Exhibition* (pp. 1353-1367).

[144] Ridgard, C. (2009). Out of autoclave composite technology for aerospace, defense and space structures. *Proc SAMPE*.

[145] Boyd, J., & Maskell, R. K. (2001). Product design for low cost manufacturing of composites for aerospace applications. *IN: 2001: A materials and processes odyssey*, 898-907.

[146] Matthews, F. L., & Rawlings, R. D. (1999). *Composite materials: engineering and science*. Elsevier.

[147] Hubert, P., & Poursartip, A. (1998). A review of flow and compaction modelling relevant to thermoset matrix laminate processing. *Journal of Reinforced Plastics and Composites*, *17*(4), 286-318.

[148] Harper, B. D., Staab, G. H., & Chen, R. S. (1987). A note on the effects of voids upon the hygral and mechanical properties of AS4/3502 graphite/epoxy. *Journal of composite materials*, *21*(3), 280-289.

[149] Grunenfelder, L. K., & Nutt, S. R. (2010). Void formation in composite prepregs–effect of dissolved moisture. *Composites Science and Technology*, *70*(16), 2304-2309.

[150] Peltonen, P., & Järvelä, P. (1992). Methodology for determining the degree of impregnation from continuous glass fibre prepreg. *Polymer testing*, *11*(3), 215-224.

[151] Hsiao, K., Kay, J., & Fernlund, G. (2011, September). Gas transport and water evaporation in out-of-autoclave prepregs. In *The 26th annual technical conference of the American Society for Composites/The 2nd Joint US-Canada conference on composites*.

[152] Kay, J., & Fernlund, G. (2012, May). Processing conditions and voids in out of autoclave prepregs. In *Proceedings of the SAMPE 2012 conference of the society for the advancement of materials and process engineering* (pp. 1-12).

[153] Arafath, A. R. A., Fernlund, G., & Poursartip, A. (2009, July). Gas transport in prepregs: model and permeability experiments. In *Proceedings of International Conference on Composite Materials*.

[154] Louis, B. M. (2010). *Gas transport in out-of-autoclave prepreg laminates* (Doctoral dissertation, University of British Columbia).

[155] Grunenfelder, L. K., & Nutt, S. R. (2010). Void formation in composite prepregs–effect of dissolved moisture. *Composites Science and Technology*, *70*(16), 2304-2309.

[156] Grunenfelder, L. K., & Nutt, S. R. (2011). Out-Time Effects on VBO(Vacuum Bag Only) Prepreg and Laminate Properties. *SAMPE Journal*, *47*(5), 6-12.

[157] Ridgard, C. (2009). Out of autoclave composite technology for aerospace, defense and space structures. *Proc SAMPE*.

[158] Hu, W., Centea, T., & Nutt, S. (2020). Effects of material and process parameters on void evolution in unidirectional prepreg during vacuum bag-only cure. Journal of Composite Materials, 54(5), 633-645.

[159] Farhang, L., Mohseni, M., Zobeiry, N., & Fernlund, G. (2020). Experimental study of void evolution in partially impregnated prepregs. Journal of Composite Materials, 54(11), 1511-1523.

[160] Hu, W., & Nutt, S. (2020). Effects of debulk temperature on air evacuation during vacuum bag-only prepreg processing. Advanced Manufacturing: Polymer & Composites Science, 6(1), 38-47.

[161] Andrew, J. J., Arumugam, V., & Santulli, C. (2016). Effect of post-cure temperature and different reinforcements in adhesive bonded repair for damaged glass/epoxy composites under multiple quasi-static indentation loading. Composite Structures, 143, 63-74.

VITA

Yusuf Can UZ

EDUCATION

- ***Ph.D.*** in English, 2021, Mechanical Engineering, İzmir Institute of Technology.
- ***M.Sc.*** in English, 2014, Mechanical Engineering, İzmir Institute of Technology.
- ***B.Sc.*** in English, 2011, Mechanical Engineering, İzmir Institute of Technology.

SELECTED CONFERENCES AND PUBLICATIONS

ONEN, Onursal; **UZ, Yusuf Can**. Investigation of Scholte and Stoneley waves in multi-layered systems. *Physics Procedia*, 2015, 70: 217-221.

Y. Can, O. Bostan, G. Çağrı, and O. Önen, "An ultrasonic waveguide sensor for monitoring alcohol concentration in water-alcohol mixtures An ultrasonic waveguide sensor for monitoring alcohol concentration in water-alcohol mixtures," 2016.

Uz, Y.C., Kartav, O., Tanoğlu, M. "Fabrication and Characterization of Carbon Fiber Reinforced Prepregs and their Composites Containing Carbon Nanotubes", PPM 2017, Marmaris, Muğla, Turkey.

M. Oz , G. Tanoğlu, N. Imamoğlu, **Y.C. Uz**, M. Tanoğlu "A New Mathematical Approach for Determining Kinetic Parameters of Curing Process", NTMSCI 9 Special Issue, No. 1, 136-142 (2021).